Master's thesis

NTNU
Norwegian University of Science and Technology
Faculty of Engineering
Department of Mechanical and Industrial Engineering

Frode Berglid

Development of a Stewart Platform for Testing of Vision-Based Tracking of Ship Motions

Master's thesis in Robotics and Automation
Supervisor: Olav Egeland
July 2020

NTNU
Norwegian University of
Science and Technology

Abstract

This master thesis aims to develop a mechanism to simulate ship motions, which will be used to test and validate a vision-based system for tracking the motion of a target ship for use in crane operations. The purpose behind the tracking system is to coordinate the motion of the crane load with the wave-induced motion of the target ship to have a safe landing when moving a load from one ship to another. The work will include the design and production of the platform's mechanical parts—selection and implementation of a mechatronic system and development of a graphical user interface with a visualization of the platform where the inverse kinematics is calculated. A SBCE approach will be utilized to explore the solutions space for a potential mechanism, and a functioning prototype will be made. After a minimum viable prototype is achieved, the focus will shift to a pre-study, allowing more time to be allocated to explore potential improvements that can later be implemented. The final prototype was capable of simulating ship motions and could be used for testing of the vision-based tracking software. Nevertheless, it is desirable to get more accurate ground truth data for the pose of the platform. Two alternatives to achieve this are discussed in the thesis, which either requires more precise actuators, components, tolerance for machining and calibration, or an IMU to measure the platform's pose. Since it is concluded that entirely accurate motion is not necessary to test and validate the tracking software, an IMU is recommended since it will be an order of magnitudes cheaper than developing or purchasing a precise platform. An IMU is also already partly implemented by the end-user.

Sammendrag

Målet for denne avhandlingen er å utvikle en Stewart Platform til å simulere skipsbevegelser som vil bli brukt til å teste og validere et vision-basert system for sporing av skipsbevegelser til bruk i kranoperasjoner. Målet bak sporingssystemet er å koordinere bevegelser av kranlasta med de bølgeinduserte bevegelsene på destinasjonsskipet, for å oppnå en trygg landing ved flytting av last fra et skip til et annet. Arbeidet vil omfatte produksjon og design av plattformens mekaniske deler, seleksjon og implementasjon av et mekatronikk system og utvikling av et grafisk brukergrensesnitt med visualisering av plattformen, der invers kinematikken må kalkuleres. En "SBCE" metodikk vil bli benytta gjennom produktutviklingsfasen. Dette vil tillate mange potensielle løsninger å bli utforsket. Etter en plattform, som har oppnådd de nødvendige krava for det gitte bruksområde, vil fokuset bli endra til et slags for studie, noe som vil gi mer tid til å utforske potensielle forbedringer og nye funksjonaliteter som senere kan bli implementert.

Den ferdigstilte plattformen var i stand til å simulere skipsbevegelser, og var tilstrekkelig til det gitte formål ved å teste det vision-baserte sporings programmet. Likevel var det ønskelig å oppnå mer nøyaktig data av de simulerte skipsbevegelsene. To alternativer for å oppnå dette er diskutert gjennom avhandlinga, og vil enten kreve mer presise aktuatorer, toleranser og kalibrering eller implementasjon av en IMU. Det er konkludert at det ikke er nødvendig å simulere helt nøyaktige båtbevegelser, og det er dermed anbefalt å implementer en IMU. Dette vil være et mye billigere alternativ og kan gi presise data for å ppnå bedre testing og validering av det vision-baserte sporingsprogrammet. Denne løsningen har delvis blitt implementer av plattformens sluttbruker.

Acknowledgement

I would like to thank my supervisor, Professor Olav Egeland, for enabling this project and being there when I needed guidance. I would also like to thank the workshop members for the help with the production of the Platform.

Contents

List of Tables

List of Figures

Abbreviations

PD	=	Product development
SBCE	=	Set-Based Concurrent Engineering
PDM	=	2 Product data management
DOF	=	degree of freedom
IMU	=	Inertial measurement unit
PCB	=	printed circuit board
CMM	=	Coordinate-Measuring Machine

Chapter 1

Introduction

1.1 Motivation

When moving a payload from one ship to another, the unintended movements induced by the waves, and relative motion between the ships is both a constant challenge and a potential hazard. For a crane to perform its various tasks, such as gripping, lifting, and transporting, it is paramount that the payload stays in an easily controllable position.[1].

Several solutions have been explored to combat unintended movements. One solution is a stabilized platform which provides a leveled loading area. Another solution found is having the crane attached to a stabilized platform, canceling out any unintended movements. In this thesis, a crane will be responsible for compensating for the induced motion on its parent ship, and the relative motion of the target ship to coordinate the transfer of the payload. For input, the crane needs information about the relative orientation of the ship. A vision-based tracking system is currently under development, which will provide part of the information needed to compensate for the induced wave motion. This thesis aims to produce a setup that will be used to develop and test a vision-based tracking system. For the setup, a Stewart platform with an attached downscaled ship model was selected. This method will be easily accessible and can be stationed next to the crane, and with 6DOF, it is possible to simulate ship motions accurately.

1.2 Objective

The objective of this thesis is to build a Stewart Platform, which was selected as the test setup. The decision was made to make instead of buying a Stewart Platform, to reduce costs. It will also allow for a more informed decision, as more research can be done before a higher investment is made. Furthermore, it gives full control and access to the source code, where it can be integrated with other software and could potentially be used as a wrapper for the software of a later bought platform. In addition to work as a test setup, a pleasing and presentable finalized design was desirable, such that it could be showcased to visitors. The work can be broken down into four main categories: Design, mechatronics, graphical user interface, and manufacturing. Most focus has been directed towards the Platform's design, which is beneficial since it is easier to improve and iterate on the software and user-interface than with the hardware. A high-level breakdown is presented in the list below.

- Selection of parts for the Stewart Platform. The main parts are the actuators, microcontroller, motor controller, joints and power supply
- Designing a 3D model of the platform and production drawings of the relevant parts
- Implementation of a mechatronics system to control the actuators
- Designing a Graphical user interface, which will include making visualization and solving the inverse kinematics of the Platform
- Implementing a method for loading and playing back prerecorded motions
- Production of the designed Platform

Once a minimum viable Platform is achieved for the test setup, the focus will be directed towards a pre-study, which will allow more concepts and ideas to be explored, which later can be implemented.

1.3 Technology challenge

With a project that integrates solutions from multiple engineering disciplines, the project's main challenges were integrating them into a functioning prototype within the given timeframe. The work presented in this thesis was performed in the first half of 2020, and a project thesis has not been conducted on this topic.

The disciplines include robotics, mechatronics, electronics, mechanical, computer science, UI/UX design, industrial design, and manufacturing. Although the finalized platform would be useful for the given use case of testing the tracking system, developing a finalized product would require far more time to complete.

1.4 Thesis structure

The thesis starts by presenting the motive and objectives in Chapter 1. Chapter 2 describes the necessary theory and kinematics needed for the platform's simulation, while Chapter 3 will give insight into the product development methodology used in this thesis. Chapter 4 will present and discuss the design of the overall platform and its various parts. Chapter 5 will present the mechatronic system for controlling the actuators. Chapter 6 will present and discuss the software and the graphical user interface. Chapter 5-7 will also include discussion of the choices, where the second half of each chapter is more of a pre-study containing improvements and future work. Chapter 7 will present the finalized platform and the calibration procedure performed and planned. Chapter 8 gives a short discussion of the project, while chapter 9 contains a conclusion, final remarks, and future work.

Chapter 2

Preliminaries

This chapter will present the necessary theory for simulating the Stewart Platform, and deriving its inverse kinematics. The following information is collected from lecture notes and the book Modern Robotics[2].

2.1 Kinematics

A robot mechanism is constructed by connecting a chain of rigid bodies, called links, together. The point where the links are connected is called joints, which allows relative motion between adjacent links. The start of the chain of links is called the base, while the end is called the end-effector. The kinematics for a robot mechanism is divided into two categories: The forward kinematics is to find the pose of the end-effector given a set of joint values. The inverse kinematics is to determine the set of joint values that gives the desired pose for the end-effector.

2.1.1 Rotation matrix

The rotation matrix will be introduced to mathematically describe the motion of a rigid body moving in three-dimensional physical space. By attaching a reference frame to the rigid bodies, the relative orientation between the frames can be described. A rotation about a fixed axis is called a simple rotation. The following equations can be used to describe the simple rotation about the x, y and z axis.

$$\boldsymbol{R}_x(\phi) = \begin{bmatrix} 1 & 0 & 0 \\ 0 & \cos\phi & -\sin\phi \\ 0 & \sin\phi & \cos\phi \end{bmatrix} \tag{2.1}$$

$$\boldsymbol{R}_y(\theta) = \begin{bmatrix} \cos\theta & 0 & \sin\theta \\ 0 & 1 & 0 \\ -\sin\theta & 0 & \cos\theta \end{bmatrix} \tag{2.2}$$

$$\boldsymbol{R}_z(\psi) = \begin{bmatrix} \cos\psi & -\sin\psi & 0 \\ \sin\psi & \cos\psi & 0 \\ 0 & 0 & 1 \end{bmatrix} \tag{2.3}$$

2.1.2 Composite rotations

Composite rotations can be made up by combining rotations. The rotation from frame a to frame c can be divided in a rotation from a to b, followed by a rotation from b to c

$$\boldsymbol{R}_c^a = \boldsymbol{R}_b^a \boldsymbol{R}_c^b \tag{2.4}$$

This can be extended for three or more rotations,

$$\boldsymbol{R}_d^a = \boldsymbol{R}_b^a \boldsymbol{R}_c^b \boldsymbol{R}_d^c \tag{2.5}$$

2.1.3 Euler angles

it can be shown that three composite elemental rotations are sufficient to reach any target frame. The Euler angles are the three angles used in these rotations, which describe the orientation of a rigid body relative to a fixed reference frame.

ZYZ Euler angles

A common Euler angle convention represents the composite rotation using the following combinations, where the rotations are done about the current axis, and with the following sequence.

$$\boldsymbol{R}_{ZYZ} = \boldsymbol{R}_z(\psi)\boldsymbol{R}_y(\theta)\boldsymbol{R}_z(\phi) \tag{2.6}$$

Roll-pitch-yaw Euler angles

Other conventions exist, such as the roll-pitch-yaw Euler angles. Here, rotation about all the axis in the cartesian coordinate system is used to represent the rotation, which is beneficial for representing ships' orientation and is defined in the following equation.

$$\boldsymbol{R}_{ZYX} = \boldsymbol{R}_z(\psi)\boldsymbol{R}_y(\theta)\boldsymbol{R}_x(\phi) \tag{2.7}$$

This convention also applies to rotations about its current axis. A rotation $\boldsymbol{R}_2^1 = \boldsymbol{R}_{ZYZ}$ from frame 1 to 2, is then described by the following sequence of rotations. Frame 1 to frame $1'$, by an angle ψ about the current z-axis. Next, a rotation by an angle of θ from frame $1'$ to $1''$ about the current y-axis. The last rotation is from frame $1''$ to frame 2 by an angle ϕ about the current z-axis. An illustration of this is seen in the Figure below.

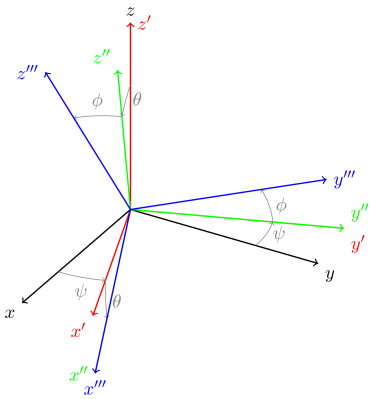

Figure 2.1: XYZ Euler angles

The resulting rotation matrix for these composite rotations is described by the following matrix.

$$\boldsymbol{R}_{ZYX} = \begin{bmatrix} c_\psi c_\theta & c_\psi s_\theta s_\phi - s_\psi c_\phi & c_\psi s_\theta c_\phi + s_\psi s_\phi \\ s_\psi c_\theta & s_\psi s_\theta s_\phi - c_\psi c_\phi & s_\psi s_\theta c_\phi - c_\psi s_\phi \\ -s_\theta & c_\theta s_\phi & c_\theta c_\phi \end{bmatrix} \tag{2.8}$$

Euler angles about fixed axis

When describing ship orientation, it is also beneficial to have the rotations about a fixed axis, as opposed to the previously mentioned convention, where the sequence is for rotations about its current axis.

It can be shown that a rotation matrix for a sequence of Euler angles about fixed axes is the same as the rotation matrix for equal Euler angles about the current axes, but with the rotations done in reverse order.

$$\boldsymbol{R}_{XYZ,fixed} = \boldsymbol{R}_{ZYX} = \boldsymbol{R}_z(\psi)\boldsymbol{R}_y(\theta)\boldsymbol{R}_x(\phi) \tag{2.9}$$

2.1.4 Quaternions

Quaternions are an alternative method to represent rotations, which can be written in terms of rational expressions in the Euler parameters. 4 parameters are used to describe the rotation, and it has no singularities. This makes it well suited for use in 3D computer graphics, as it does not suffer from what is known as gimbal lock. Moreover, quaternions consume less memory and are faster to compute than matrices. The quaternion is usually represented as a complex number with one real part and three imaginary parts, which is written as

$$q = q_s + q_1 i + q_2 j + q_3 k \tag{2.10}$$

It can be helpful to rewrite it as in the equation below, to get an intuitive feel of what the quaternions represent. Here, i, j, and k represent a normalized unit vector, and the angle θ is the amount the rigid body is rotated about this unit vector. The reader is referred to an interactive video[3], where this can be further explored and visualized.

$$q = \cos\theta/2 + \sin\theta/2(i, j, k) \tag{2.11}$$

If either a rotation matrix or quaternion is known, the other can be found through the following relation, where $\boldsymbol{k}^\times$ is the skew-symmetric representation of the unit vector.

$$\boldsymbol{R}_k(\theta) = \cos\theta \boldsymbol{I} + \sin\theta \boldsymbol{k}^\times + (1 - \cos\theta)\boldsymbol{k}\boldsymbol{k}^T \tag{2.12}$$

2.1.5 Composite quaternions

Similarly to rotation matrices, the composite rotation matrix

$$\boldsymbol{R} = \boldsymbol{R}_1 \boldsymbol{R}_2 \tag{2.13}$$

Can be described as the following composite quaternions.

$$\boldsymbol{q} = \boldsymbol{q}_1 \circ \boldsymbol{q}_2 \tag{2.14}$$

2.1.6 Homogeneous transformation matrices

In addition to describing the relative orientation between coordinate frames, it is necessary to describe the translational position of a frame relative to another. The concept of a homogeneous transformation matrix is introduced, which both describes the relative position and orientation between the frames. Here $\boldsymbol{R}_b^a$ is the rotation matrix from a to b, and $\boldsymbol{r}_{ab}^a$ is a three-dimensional vector describing the position of the origin of frame b relative to the origin of frame a in a coordinates, which is also referred to as the displacement from a to b.

$$\boldsymbol{T}_b^a = \begin{bmatrix} \boldsymbol{R}_b^a & \boldsymbol{r}_{ab}^a \\ \boldsymbol{0}^T & 1 \end{bmatrix} \tag{2.15}$$

The inverse of of $\boldsymbol{T}_b^a$ is found to be $\boldsymbol{T}_a^b$

$$(\boldsymbol{T}_b^a)^{-1} = \begin{bmatrix} (\boldsymbol{R}_b^a)^T & -(\boldsymbol{R}_b^a)^{\boldsymbol{T}} \boldsymbol{r}_{ab}^a \\ \boldsymbol{0}^T & 1 \end{bmatrix} = \begin{bmatrix} \boldsymbol{R}_a^b & \boldsymbol{r}_{ba}^b \\ \boldsymbol{0}^T & 1 \end{bmatrix} = \boldsymbol{T}_a^b \tag{2.16}$$

Similarly to rotation matrices, the homogenous transformation matrices can be combined to describe a composite displacement.

$$\boldsymbol{T}_c^a = \boldsymbol{T}_b^a \boldsymbol{T}_c^b \tag{2.17}$$

This can also be extended to three or more transformations.

$$\boldsymbol{T}_d^a = \boldsymbol{T}_b^a \boldsymbol{T}_c^b \boldsymbol{T}_d^c \tag{2.18}$$

2.1.7 The Homogeneous transformation matrix of a translation

The homogeneous transformation which only involves a translation along a fixed axis is described by

$$\mathbf{Trans}_k(h) = \begin{bmatrix} \boldsymbol{I} & h\boldsymbol{k} \\ \boldsymbol{0}^T & 1 \end{bmatrix} \tag{2.19}$$

The following homogeneous transformation matrices respectively describe a translation along the x and z axes

$$\mathbf{Trans}_x(a) = \begin{bmatrix} 1 & 0 & 0 & a \\ 0 & 1 & 0 & 0 \\ 0 & 0 & 1 & 0 \\ 0 & 0 & 0 & 1 \end{bmatrix}, \quad \mathbf{Trans}_z(d) = \begin{bmatrix} 1 & 0 & 0 & 0 \\ 0 & 1 & 0 & 0 \\ 0 & 0 & 1 & d \\ 0 & 0 & 0 & 1 \end{bmatrix} \tag{2.20}$$

2.1.8 The displacement of the end effector

The displacement of the end-effector relative to the base can be described by a homogeneous transformation matrix and is obtained through the composite displacements of the n links. The relative displacement between link frame $i-1$ and i is denoted as $\boldsymbol{T}_i^{i-1}$ for $i = 1, 2, ..., n$. With the fixed base frame denoted as frame 0. Frame 1 fixed in link 1, Frame 2 in link 2, and so on up to the final frame n.

$$\boldsymbol{T}_n^0 = \boldsymbol{T}_1^0 \boldsymbol{T}_2^1 ... \boldsymbol{T}_n^{n-1} \tag{2.21}$$

2.2 Robot joints

Figure 2.2 illustrates basic joints found in typical robot applications. A **revolute joint** (R), also called a hinge joint, allows rotational motion about the joint axis. The **prismatic joint** (P), also called a sliding or linear joint, allows translational motion along the direction of the joint axis. The **spherical joint** (S), also called a ball-and-socket joint, has three DOF and functions similar to our shoulder joint. The **universal joint** (U), has two DOF, and consist of a pair of revolute joints

arranged with the joint axes orthogonal. The other joints will not be used in this project.

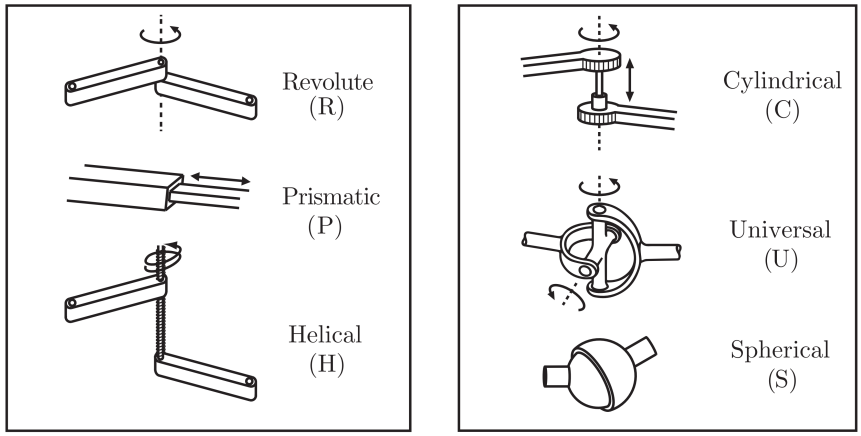

Figure 2.2: Typical robot joints [2]

2.3 Kinematics of closed chains

A closed chain is any kinematic chain containing one or more loops. These consist of a moving platform connected to a fixed base by a set of "legs" and is typically referred to as parallel mechanisms. These mechanisms exist with varying amounts of DOF, with several configurations among them, including redundant axes for avoiding singularity. One of these parallel mechanisms is the Stewart-Gouch platform, which will be discussed further in the next section.

Whereas in open chains, the forward kinematics can be more or less considered trivial, the opposite can be said for closed chain systems. For the general base case Stewart platform, the forward kinematics have 40 independent solutions. Nevertheless, this is reduced by exploiting symmetries or other special features. For this thesis, the forward kinematics will not be required; instead, the inverse kinematics is used.

2.3.1 Stewart Platform inverse kinematics

Several configurations are possible for the Stewart Platform, where some of the variations can be seen in Section 4.1. Here the inverse kinematics for a 6×SPS Stewart-Gough platform will be examined. This configuration has passive spherical joints attached to both the base and the moving platform, with an actuated prismatic joint in between.

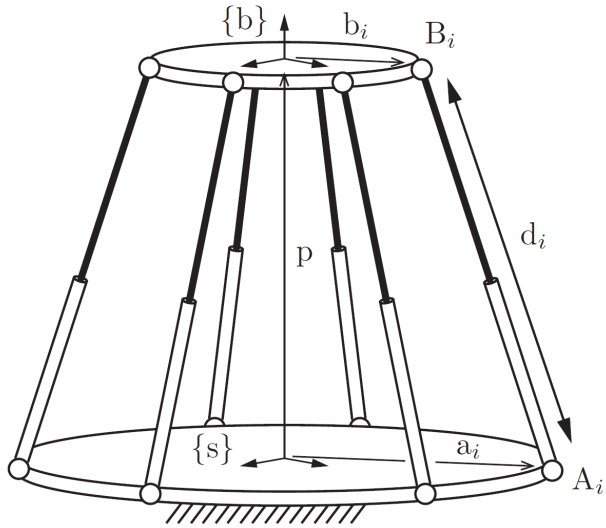

Figure 2.3: Stewart-Gough platform[2]

Let {s} and {b} denote the fixed and body frames, respectivly. $\boldsymbol{d}_i$ is the vector directed from joint $\boldsymbol{a}_i$ to joint $\boldsymbol{b}_i$, $i = 1, 2, ..., 6$. Reffering to Figure 2.3, the following definitions are made:

$\boldsymbol{p} \in \mathbb{R}^3 = \boldsymbol{p}$ in {s}-frame coordinates,

$\boldsymbol{a}_i \in \mathbb{R}^3 = \boldsymbol{a}_i$ in {s}-frame coordinates,

$\boldsymbol{b}_i \in \mathbb{R}^3 = \boldsymbol{b}_i$ in {b}-frame coordinates,

$\boldsymbol{d}_i \in \mathbb{R}^3 = \boldsymbol{d}_i$ in {s}-frame coordinates,

$\boldsymbol{R} \in SO(3)$: The orientation of {b} as seen from {s}.

To derive the kinematics constraint equations, it is noted that, vectorially,

$$\boldsymbol{d}_i = \boldsymbol{p} + \boldsymbol{b}_i - \boldsymbol{a}_i, \quad i = 1, 2, ..., 6 \tag{2.22}$$

writing Equation 2.22 in s-coordinate frames yields the following equation

$$\boldsymbol{d}_i = \boldsymbol{p} + \boldsymbol{R}\boldsymbol{b}_i - \boldsymbol{a}_i, \quad i = 1, 2, ..., 6 \tag{2.23}$$

With this information, the length of leg i denoted as s_i can be calculated from the following equation

$$s_i^2 = \boldsymbol{d}_i^T \boldsymbol{d}_i = (\boldsymbol{R}\boldsymbol{b}_i - \boldsymbol{a}_i)^T((\boldsymbol{R}\boldsymbol{b}_i - \boldsymbol{a}_i)) \quad i = 1, 2, ..., 6 \tag{2.24}$$

The vector a_i and b_i are known constant vectors, which can be found in the appendix in Figure 9.10 for the designed platform. Thus, given the translation vector $\boldsymbol{p}$ and rotation matrix $\boldsymbol{R}$, solving the lengths for the six legs s_i becomes straightforward and can be determined directly from Equation 2.24.

2.4 Ships coordinate frame

Figure 2.4, shows how the 6 DOF of a boat is defined. The reference frame is placed in the ships centre of gravity, which is calculated from its mass moments about its three axes; x, y, z.

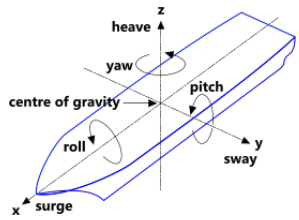

Figure 2.4: Ships coordinate frame[4]

Chapter 3

Product development methodology

This chapter will give insight into the purpose behind a prototype and what it is. It will also present SBCE and the reasoning behind the PD methodology used in the project.

3.1 Prototypes

Most people probably have some formulation for what a prototype is, but what is it really, and what is prototyping? This question was asked to fellow students, and the typical answers were along the line that a prototype is a physical artifact with the purpose of testing if something works. Although a small sample size, this is an indication that prototypes are mainly seen as a physical artifact used for verification and validation. Nevertheless, there exist numerous formulation for what a prototype is. According to Oxford dictionaries [5], a prototype is "A first or preliminary version of a device or vehicle from which other forms are developed." Another definition by Ulrich and Eppinger [6] defines a prototype as "An approximation of the product along one or more dimensions of interest. " The last definition would involve both physical and non-physical models, and include everything from sketches to fully functioning products [7]. On the other hand, there exist stricter definitions, such as [8] "We define a prototype as a concrete representation of part or all of an interactive system. A prototype is a tangible artifact, not an abstract description that requires interpretation."

3.1.1 Prototypes characteristics

The characteristics, resolution and fidelity, can be used to describe the level of detail present in a prototype [7]. Researchers often interchange the terms, and to

better differentiate the two, the following definition will be used. Fidelity will be used to describe the level of richness of the data and functionality. And resolution will refer to the look and feel of the prototype [9].

Another way to distinguish prototypes is trough the terms horizontal and vertical prototypes. In a horizontal prototype, the function is not implemented in full detail, but the prototype can still be used for demonstration purposes. On the other hand, vertical prototypes show functions in their intended final form, but here only a few selected functions are implemented [7].

3.2 Set-Based Concurrent Engineering

The following information about Set-Based Concurrent Engineering is gathered from [10]. To get a clearer picture of what SBCE is and its advantages, Point-Based Serial/Concurrent Engineering is first presented.

Traditional serial engineering can be represented as a series of functions, as shown in Figure 3.1. Here each function is doing a specific job based on certain criteria, and when finished, it is "thrown over the wall" to the next function. This method will typically result in rework since different functions do their job without knowing limitations and restrictions for later functions. This is somewhat of a simplification, as there are feedback from other functions, but these are often delayed and come after a function has committed to a particular solution.

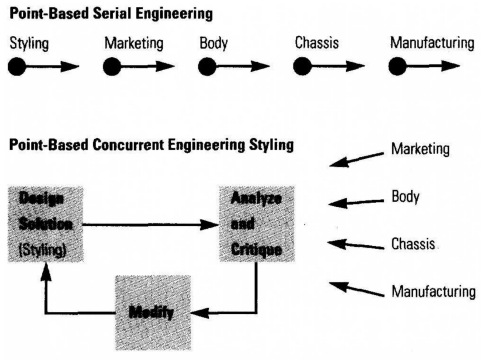

Figure 3.1: Traditional Point-Based approaches to product development [10]

The other method, Point-Based Concurrent Engineering, shown in Figure 3.1, shift away from the mentality of "throwing it over the wall." Instead, each function work in parallel with the different functions. An example would be that styling has come up with a design, which is shown to the following functions and is modified based on their input. Although an improvement over serial engineering, the basic idea remains the same, pick a solution and iterate it until it meets the requirements. This results in increased rework and additional communication demands. And since

the development teams never get a clear picture of the possibilities, the resulting design is typically far from optimal. It might not even converge to an acceptable solution; instead, the team just stops working on the project when it runs out of time. Despite the drawbacks, many companies have been successful with an iterative point-based approach. In these scenarios, it is typical that the cost of rework is low, iterations and feedback cycles are fast and the quality of the initial starting point, "the first guess," is high.

Toyota's Set-Based Concurrent Engineering (SBCE), on the other hand, differs significantly. Instead of iterating on one particular solution, the team works relatively independently to develop and communicate a set of different solutions concurrently. A safe solution is selected but is subjected to change as the project progresses. The sets of ideas are gradually narrowed down, based on information from development, testing, the customer and the other sets. This process is illustrated in Figure 3.2. The advantage of this approach is that instead of reworking and iterating the design when a function conflicts with something discovered later, a different set can be chosen, while the weaker ones are gradually eliminated. This approach may take more time in the initial stages to define possible solutions, which might seem like doing unnecessary work, in addition to requiring more resources early in the project. Nevertheless, it gives the possibility to more quickly move towards convergence and production compared to its point-based counterparts.

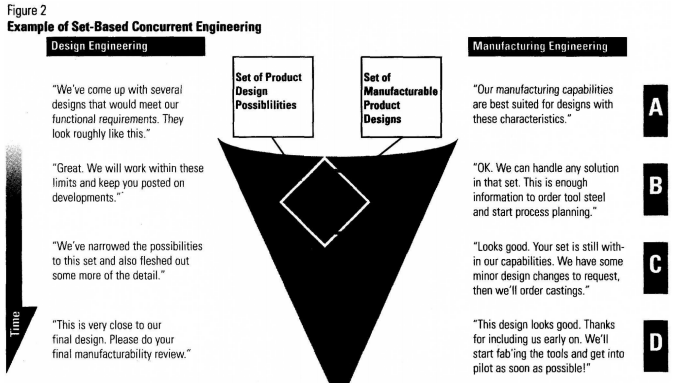

Figure 3.2: Example of Set-Based Concurrent Engineering [10]

3.3 Methodology

Browning [11] states that "lack of value stems less from doing unnecessary activities and more from doing necessary activities with the wrong information (and then having to redo them)." To reduce waste, A SBCE approach has been utilized to explore multiple concepts and sub-functions of the design. Moreover, it has been observed that a small team and individuals often tend to focus quickly on one solution [10]. This will typically result in many iterations and rework as

new information is found. Furthermore, this allows for greater freedom to explore multiple solutions, as it is always possible to fall back to a previous design. Besides, multiple designs might have a higher chance of finding a good starting point, as Floyd [12] argues that prototypes may serve as a catalyst for eliciting good ideas.

Nevertheless, some activities that can be seen as wasteful have been performed, since it does not add much value, and might require rework as it has been done at a to early stage. For instance, a high fidelity rendering of the Platform was completed, and modeling of details such as cables was performed. It provided some useful information on the vision and appearance of the Platform but was also done as it was uncertain if it was possible to produce the Platform. However, visual communication is essential to create understanding, involvement, and commitment of people [13].

Other examples are that the parts have been sanded and painted to achieve a higher fidelity prototype, even though improvements and new parts have been found and considered implemented. During the early stages, a high-fidelity prototype is not necessarily beneficial as high-fidelity prototypes tend to result in superficial feedback, often related to the appearance and detail rather than basic functionality [14]. Besides, for this project, it was more desirable to have feedback related to the software and mechatronics portion of the project, rather than the design. A high fidelity prototype is also made such that people will not get hung up in details that are deliberately left out or not looked at. And since the prototype is meant to be useable for the given use case without further work, extensive work has been performed to give the Platform a finished appearance. Nevertheless, a much grander timeframe would have been needed to perform these activities without having them be seen as wasteful.

With a SBCE approach, decisions are inferred as long as possible. However, due to the pandemic, this approach could not be utilized to a full extent, where all the different aspects could not be worked at simultaneously. Moreover, inferring decisions, which is typically is good and result in less rework, resulted in design changes as alternative parts had to be ordered.

Since a separate prototype will not be made for testing of the various parts of the project, the design was at a certain point locked in when drawings were sent to production and parts were 3D printed. While the Platform was under production, many new ideas were found and collected, which can later be implemented in a new version. New ideas might also be found as the prototype is finished, as prototypes are commonly seen as a means for verification and validation. For example, the four prototypes: proof-of-concept, proof-of-product, proof-of-process, and proof-of-production. Here all the different prototypes serve the function to either verify or validate assumptions, expectations, and calculations made at an earlier stage [7], [15].

3.4 SolidWorks modeling methodology

There are some modeling techniques used in the SolidWorks model that should be made aware of when overtaking the project. The following sections will briefly explain some of these techniques and some tips that were not taught in the modeling courses, which can be helpful for future work. Further information and tutorials can easily be found on Google and YouTube.

3.4.1 Equations

To reduce work for remodeling if parts are changed, the equation feature within SolidWorks was first utilized. With it, it is possible to define variables that other dimensions can be derived from or linked to through equations. It is also possible to use simple programming features such as if statements. A more in-depth look can be seen in this webinar[16], which gives a good idea of what is possible to achieve.

With equations, it could be possible to define all the parts used in the models, with only the top and base radii for intersection with the brackets, the angle between the two joints in the bracket, the stroke length of the actuators, and the weight/load on the top plate. An equation for the thickness for the plates can be expressed through the selected material with a load as a variable. A minimum size for the components must be specified to fit the components in the enclosure, which can be implemented with if statements. Thus, different behavior for the dimensioning occurs, where the plate stays at the minimum diameter, while the brackets are moved further in on the plate. All parts can then be linked to a single text file containing the bare minimum of variables/dimensions needed. When changing the variables in the text file, an entirely new platform with different dimensions would be rebuilt within minutes. However, it would only be useful for a certain range in dimensions, as a smaller or bigger platform should have a different overall structure.

Nevertheless, most of the equations used in the models have been removed to make it easier to modify when someone else takes over the project. This was done since it can be intricate to get an overview of the models, even if one is familiar with the feature. Additionally, it can be more beneficial to implement after a finalized design is achieved.

3.4.2 Top-down vs bottom-up

In bottom-up modeling, the parts are first designed and then placed into the assembly trough mates, which is the method most commonly used. This is a preferred technique when the parts are standardized, have known dimensions, or not dependent on other features. In top-down modeling, the parts are modeled in the assembly itself. This has, for instance, been used in the 3D printed board where the PCBs for Arduino and motor controllers are connected. Here the PCBs are placed in an assembly and can be moved around freely. The board is then modeled in context to the PCBs, such that when they are moved, the entire board and

hole locations are automatically updated. This approach is beneficial as it requires much less rework if changes are made, but can require more time to setup. One can also combine these two methods in an approach referred to as middle-out.

Another similar technique has been used, where the assemblies are modeled as a multibody part. This has, for example, been used in the electronic enclosure, which contains several parts that are dependent on each other. This provides the same benefits as a top-down modeling technique but can be much faster to set up depending on the part/assembly. Additionally, features can be shared. For instance, a single extrude feature can be applied to all the different bodies within the multibody part. After the multibody part is completed, the different bodies can be saved out as individual parts and to an assembly. All parts can then later be modified trough changing the parent part. Furthermore, the individually saved out parts can have features added and be further modified. This has, for instance, been used on the back portion of the electronics enclosure, where the part was later converted to a sheet metal, where radius and bends are added to match the dies used for manufacturing. In all assemblies and sub-assemblies where this approach has been used, both the parent multibody and the saved out assembly is added. The parent parts are suppressed and hidden and can found in a separate folder in the design tree to make it easy to find and modify.

3.4.3 Syncrounous modelling

When modeling parts, the intent behind the part is reflected in how they are dimensioned, and the relationship added, such as equal length, concentricity, perpendicularity symmetry, etc. With models containing many such relations, unwanted behavior can occur when the part is changed in a way that goes against the original design intent, requiring extensive work to alter the relations used. If the change is only minor, and will likely not require further changes, a faster option to change the part can be achieved with synchronous modeling. An example of this is the move face command, which was used when test printing several parts to get a press fit tolerance. Another feature that has been used is the delete face command. If these features have been used, they will typically be found at the bottom of the design tree.

Synchronous modeling is most practical for parts where the model three is not available, such as in cases were a STEP file is imported. Since this technique can be confusing as changes are made to the driving feature, it has not been used extensively.

3.4.4 Configuration and design table

Configurations allow multiple variations of a part or assembly to be created within a single document. The different configurations can be created manually by adding and suppressing features. A design table can also be used, which is essentially an excel file containing different values for dimensions used in the different configurations. Multiple configurations exist for several of the parts in the created model.

For example, the top plate can be toggled between a circular shape, hexagonal, and the topology optimized shape. The main assembly also contains some configurations, among them, an exploded view. The exploded view can also be animated, which can help determine the platform's assembly procedure.

3.4.5 Solidworks PDM and naming

SolidWorks PDM is a helpful tool for version control and general data management. It is beneficial to keep all the parts of a project within the same folder, and with the PDM, a hidden folder structure can be obtained for easy management. This was not used for the projects, as it is neither available for students nor taught through courses. Instead, some helpful tips for data management are presented here.

Firstly, it can be beneficial to use a name generator for naming parts and assembly files. The names can be just a simple set of numbers that increments every time a new part is generated such that conflicts do not occur when everything is in the same folder. This is also beneficial since descriptive names often can be nearly identical for several parts, and it will not break the flow by having to wait to find a suitable name. Since a free generator was not easily found, and the previously used could not be accessed when connected to NTNU through VPN, the filename used the first descriptive name found. With numbers as filenames, it can be time-consuming to navigate to the correct file without a PDM, or opening the main assembly and navigating in the design three. A quick tip is to customize the folder that contains the SolidWorks file to be optimized for videos. It is then possible to extract the description from the SolidWorks part's properties, such that it is displayed in the folder. A better option is to download SolidWorks file utilities, formerly known as SolidWorks explorer, a free standalone program that makes navigation and management of the files much easier.

Chapter 4

Design

This chapter will present and discuss the design and concept explored for the platform. The design alternative was mainly evaluated based on ease of manufacturing and aesthetics, which is subjected to the author's experience as a CNC-operator and personal preference. Strength analysis and material choices are also presented for the relevant parts. Lastly, a price offer by Stryvo AS for manufacturing the relevant parts can be found in the appendix, which will give good estimation for the cost, although prices will vary depending on the manufacturer.

Figure 4.1: Keyshot render of developed Platform

4.1 Selection of robot mechanism

a mechanism with 6DOF is required to simulate ship motions accurately, which can be achieved by either an open or closed chain mechanism.

Open-loop serial chain robot manipulators work similarly to a human arm, and have advantages with large workspaces and dexterous maneuverability, but have a rather poor load carrying capabilities due to its cantilever structure. Consequently, the links are bulky on the base, and the end-effector tends to bend under heavy load and vibrate at high speeds. Thus, their precision and positional capabilities are reduced trough possessing a large workspace. Closed chain mechanisms, often referred to as parallel mechanisms, possess far greater load-carrying capacity, dynamic performance, and precise positioning. This can be observed by using the biological world for reference, where one would observe that humans use both arms in cooperation to handle heavy loads, or for more precise work like writing, uses three fingers in parrallell[17].

For simulations of ship motions, the higher load carrying capacity and precision is desired, and with 6DOF needed, the choice is narrowed down to what typically called a Stewart Platform.

4.1.1 Parallel mechanism configurations

A 6-DOF parallel mechanism can be constructed in several ways, with different benefits. These configurations will not be explored in-depth; instead, a few of the interesting takes are shown in the following figures with references to additional information.

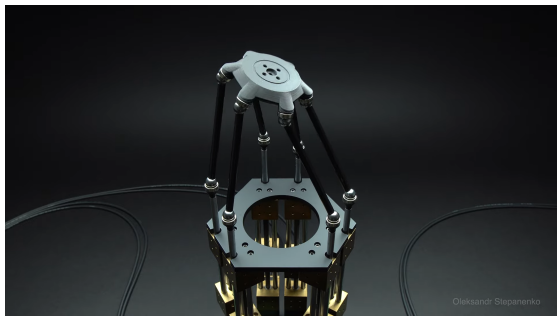

(a)[18]

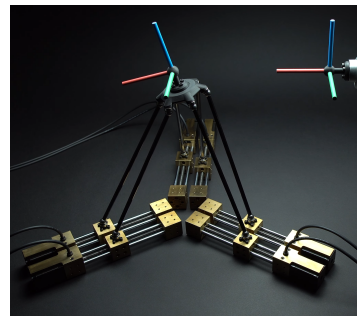

(b)[19]

Figure 4.2: Stewart platforms with vertical and horizontal slides

In the two configurations seen in Figure 4.2, the legs themself are not actuated and are of a fixed size. This enables the platform to reach very high speeds and acceleration, since all the heavy parts, such as motor, gearboxes, and slides are mounted at the base. Furthermore, the configuration, seen in Figure 4.2 (a), can

theoretically have unlimited vertical travel. These configurations are suitable for highly dynamic motion, jitter, and vibration study.

The circular base mechanism, seen in Figure 4.3(a), is an interesting take on the mechanism. It achieves motion in 6DOF, but sacrifices workspace, since the legs cannot vary in size and is not for practical use as the author states himself. On the other hand, the cable driven configuration, seen in Figure 4.3(b), can have a workspace only limited by the size of the room it is installed in. Furthermore, it can reach remarkably high speed and accelerations, making it suitable for racing simulations, helicopter flights, or other scientific experiments.

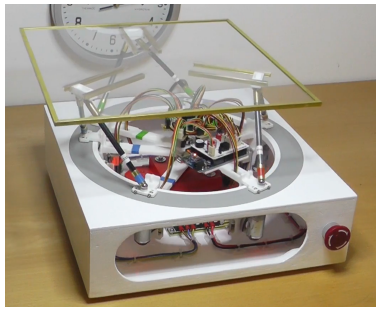

(a)[20]

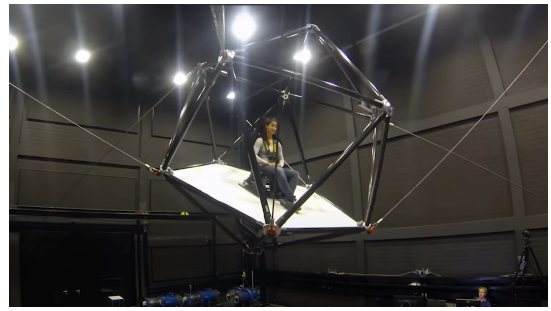

(b)[21]

Figure 4.3: Circular Base and cable driven 6-DOF mechanisms

The most commonly created configurations are the two variations seen in Figure 4.4, where one is actuated with servo motor with fixed leg lengths, while the other has linear actuators. The version with the servo motors can be produced at a low cost. Additionally, with many open-source projects available, it could be quick to develop and was considered in the early stages of the thesis. However, it would only be suitable for small scale ship models and with limited workspace. After further clarification of the budget, and desires for use with the crane, this idea was quickly dismissed.

The most typical configuration is with a linear actuator, which can be made suitable for a wide range of tasks, depending upon the selected components and parameters. An open-source project by progressive automation was available, seen in Figure 4.4(b). This gave confidence that a platform could be completed within the given timeframe. The mechatronic system and PID controller for the actuators could be kept while improving the graphical user interface, implementing needed features, and making a new design that would be presentable for demo and showcases.

(a)[22]

(b)[23]

Figure 4.4: Servo and linear actuator Stewart Platforms

4.1.2 Selection of actuators

A quick estimation of the actuators' needed speed was achieved by looking at videos of ships at sea. An estimation for the period from going to max roll and back again was counted to 9 seconds. With a stroke length of 150mm and 50.8mm/s actuator speed, the design platform should be capable of a full period in approximately 6 seconds. This is reduced to 8.6 seconds at full load, as the actuators would be moving at 1.38 inches or 35mm/s. Using these simple calculations allowed for a prototype and Platform to be produced quickly, even though it is quite rudimentary. This method only considers the rotation speed about the ship's roll axis, as defined in Figure 2.4. It does not consider the size of the model ship, which, at the time, was not selected.

Several actuators were explored for this project. It was narrowed down to the two cheapest options with feedback and approximately 50mm/s speeds, namely the P16-P by Actuonix[24] and PA-14P[25] by Progressive Automations. An early prototype of Platform with these actuators can be seen in Figure 9.1 in the appendix, where items to show scale was added. Both of these have previously been used on other platforms, the P16-P in the Platform by Acrome[26], and the PA-14P by Progressive Automations Platform[23], which gave an estimation of performance to be expected. The PA-14P was selected for its higher force and larger resulting Platform, which would enable other future use cases.

4.1.3 Parameters and workspace

Different characteristics are obtained depending on the size difference for the top and bottom joint connections, as seen in Figure 4.5. With a smaller base than the top, a higher tilt angle can be achieved with the same stroke length. Doing the opposite will result in a lower tilt angle, but a more stable platform. The latter also has the side benefit of less weight due to the smaller resulting plate. Since

crane operations are performed under normal weather conditions and vision-based tracking software can "extrapolate" results, little requirements were set. To quickly estimate the workspace of the robot, the 3D model made in SolidWorks was used. By adding a limit mate to the actuators, and mating the spherical joint, the 3D model could be moved freely to test the theoretical single-axis range of motion. The size for the bottom plate was set such that there would be enough space in the electronics enclosure for the components. The top plate was made smaller to increase stability, and dimensions were set at even round numbers for ease of manufacturing. A quick check with the 3D model showed a roll of up to 38 degrees when the platform was in the height that allows maximum rotation. This would be more than sufficient since roll angles in extremely rough weather conditions are at 35-45 degrees. Moreover, it exceeded the capability of the selected spherical joint, although this can be increased with universal joints, which will be discussed later. Furthermore, the characteristics can be easily changed later if new requirements, restrictions, or knowledge are gained by replacing the top plate.

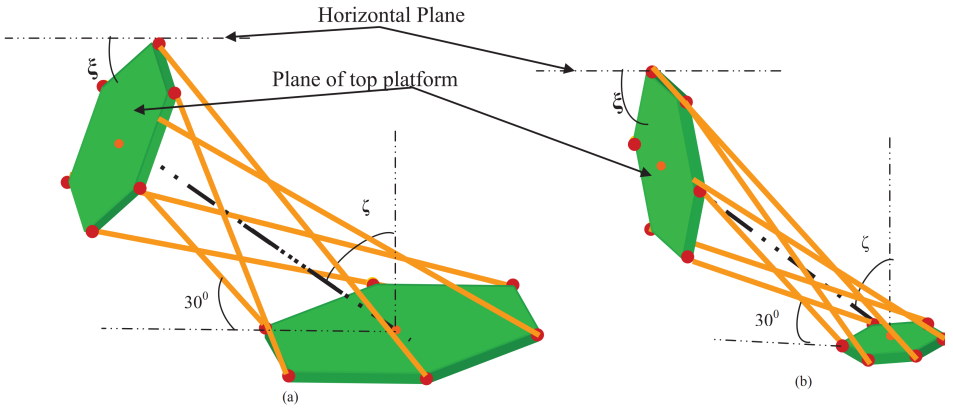

Figure 4.5: Tilt angle of top plate for different base and platform radii[27]

Reconfigurable parameters

Something else that can be considered is adding a slider where the angled bracket is attached, which allows adjusting the base and top joint positions relative to the manufactured plates. This could be highly beneficial in the prototyping stage since a single prototype can be made to test different parameters. However, simulations can be performed to determine the platform's workspace with different parameters without a physical platform. If calculations or specifications and restrictions are unknown, such a design will allow for the mechanical prototype to be manufactured before the parameters are set. It could also be a useful feature for a finalized platform since that capabilities and range of motion can be altered for different use cases, particularly for an expensive platform.

One could also motorize the sliders, such that the base can be controller from

the software. This will make the reconfiguration faster and could even allow for real-time adjustments such that higher tilt angles could be achieved. Existing implementations of motorized sliders have not been found, but it should be said that minimal investigation has been performed, as the adjustable feature is not intended to be implemented. Nevertheless, it could be worth exploring further and how real-time adjustments can be leveraged if no existing implementation is found.

4.2 Overall design

Having selected the actuators for the platform, the driving element for the design were the joints and the placement of the enclosure for the mechatronic components. There were three main ideas for the placement: hidden away on the floor, mounted to the side, or mounted underneath. Placing it on a separate box would make the platform's design easier, but was discarded as it could leave a mess with the cables, and the platform would preferably be self-contained with a single power cable connected to it. The next option was to place the electronics on the side, as seen in the figures in the appendix. A quick hand sketch was made of a drafted trapezoidal shape for the side-mounted enclosure where a screen was intended to be mounted. The pictured shape was not possible to obtain with the sizes of the components, where a simple rectangular replacement shape can be seen in the appendix in Figure 9.4-9.8. Furthermore, the design was pivoted away from containing a screen and microcomputer for controlling the platform, discussed in section 5.6, which was one of the motivations behind the placement.

Thus, several designs where the electronics are placed underneath were explored, where the driving design element is the shape of the top and bottom plate. These can be shaped almost entirely arbitrarily since as long as the actuators' connections are evenly spaced in a circular pattern, the functionality would be the same. Most typical shapes are circular, triangular, and hexagonal, but other more lucrative shapes can be implemented. The circular shape was chosen, as it was found the most ascetically, although this is subjected to personal opinions. It is also less typically used, which would set it apart from most other Stewart platforms. Furthermore, the circular shape would offer more room for the electronics and would have no sharp edges that could reduce the potential for injuries if the platform were to hit a bystander. The downsides are that a circular shape would have excess material and weight compared to, for example, triangular and hexagonal shapes, for the same diameter spacing for the actuators connections. A topology study has been run with a given load scenario, which will result in a shape that gives the best strength to weight ratio. This will be further discussed and explained in Section 4.12.3, and the different top plate designs can be seen in Figure 4.25.

4.3 Selection of joints

A Stewart platform is typically configured with universal joints at the base and spherical joints to the platform. Spherical joints will allow for an extra degree of

freedom along the linear actuator axis, which would be useful for the actuator's assembly and orientation. Downsides with spherical joints are that they typically have a lower range of motion. A universal joint can also be combined with a bearing, as seen in this demo[28] by Actuonix Motion Devices, which will add another DOF along the linear actuator axis while keeping the universal joint's increased range of motion.

A low cost, compact, and inline spherical joint were desired, and much time has been invested searching for suitable joints. The spherical joint from IGUS seen in Figure 4.6b was found. This was a great option priced at 38 NOK for joint and house assembly, although something more compact and a little higher quality solution was desired. Igus offered a flange variant seen in Figure 4.6a, this was more compact, but it had an extended lead time due to the pandemic. Search for a similar option lead to the one seen in Figure 4.6d, which would be a superb joint. However, this is also reflected in the significantly higher price of 324$. Nevertheless, it would be an excellent option for a more expensive and higher quality Stewart Platform. Lastly, the two different clip bearings, seen in Figure 4.6c and e, were considered. Clip bearings would be the optimal solution for compactness, as this will allow for full flexibility over the joint connection design, and the corresponding part would be easy to manufacture.

(a)[29]

(b)[30]

(c)[31]

(d)[32]

(e)[33]

(f)[34]

Figure 4.6: Selection of joints considered for the platform

As for the universal joint, a compact solution with strict tolerances was desired. The strict tolerance would center the joint on the actuators, and for the top part of the actuator, an Ø20 H7 tolerance would be suited. However, the universal joints are typically placed on the bottom, where the dimension needed would be in the range of Ø19.60 to Ø19.75, and each joint would have to be tailored to each specific

actuator, or larger errors would have to be accepted. So for a universal joint for the base connection, an unbored universal joint that could be customized would be ideal, but here the prices started at 400 NOK and would require extra machining time.

The selected joint used for the platform is the ball and socket joint seen in figure 4.6b. This was both the cheapest option, and the range of motion would be sufficient for the current use case. The clip bearings, as seen in Figure 4.6e, would be better suited, more compact, and easier to implement, but not available. The other clip bearings were possible to get delivered, but as only a few were in stock, some of them had to be 3D printed, which would have questionable quality. Also, it was more than six times as expensive as the selected joint. An idea to achieve a more compact solution with the selected joint was found, as presented in the next section.

4.4 Angled brackets

With the joint's housing assembled perpendicular to the plate, the usable range of motion for the joints would be decreased, since they will be at a certain angle. A typical solution is to mount the joints to an angled bracket. This will increase the usable range of motion for the spherical joints since the brackets set the angle to its neutral position given a certain home position. The platform in the SolidWorks model was set to its middle height position, and a 3D sketch was made to calculate the two angles for the bracket.

Figure 4.7: Rendering of the angled brackets

4.4.1 Joint distance

In the initial design which can be seen in the appendix in Figures 9.4-9.8. The distance from the spherical joints rotation point to the top and bottom plates were fairly large. Although not directly a problem, a fair amount of effort was made to move the rotation point closer to the top plate. The best option would be to either cast mold or machine the brackets, such that the joint could be directly attached to it, but was discarded due to price. Next in line is the clip bearings previously discussed. This would be both suitable for a 3D printed and machined brackets, as the bearings could be snapped directly in. Nevertheless, other options were explored due to availability and price.

Since the brackets are intended to be 3D printed, the used option of modifying the selected joint housing would be an acceptable solution for a one of production. This would bring the joint closer to the plate, although not as close as the previously mentioned options. A cutout that matched the spherical and hexagonal shape was made in the bracket, and after inserting the housing to the bracket, the two ends could be cut off. This shape would be tricky and expensive to manufacture if the brackets were to be milled to achieve a tighter tolerance and higher quality, where a simple hole for the clip bearing should be used instead. Nevertheless, the 3D printed brackets work excellently for the intended use case. However, they will require more effort to account for the variable height caused by the 3D print quality when calibrating the platform.

The cutout for the joint housing in the currently used bracket was made to a press-fit that will be sufficiently strong to hold them together based on a quick experiment and the fact that the force acting upon the house would press them together. Nevertheless, the parts were glued together to ensure that the housing would not drift. Furthermore, The height of the bracket was made such that when cutting the bearings, only the part that previously contained the threaded hole would be cut off. This will leave the same wall thickness as the unmodified version, and the specification and weight limit for the modified version should more or less be intact. To further reduce the height, the joints housing can be made even shorter since the joints are rated for a much higher load than what the actuators are capable of. However, to be on the safe side, this was not tested as enough spare parts were not ordered. Large chamfers were added for aesthetical reasons, which gave the illusion of a more compact bracket, although this can be removed if it is manufactured to reduce complexity.

4.4.2 Static study

Assessing the brackets' strength can be tricky to accomplish in a static study since the 3D printed part is not isotropic. However, a destruction test has been performed by applying 80kg to a single joint connection, which showed no signs of damage when printed at 20% infill. This indicated that the 3D printed brackets would handle at least five times the maximum force of the actuators, and even higher loads are possible with a higher infill. Thus further test was not necessary.

4.5 Top plate

Both the top and bottom plate would have the angled brackets mounted to them, and needed a method for securing them to the plate such that they would be perfectly aligned relative to each other. Additionally, it was uncertain whether a single fastener was enough to secure it from rotating and shifting under operation, particularly when the part is 3D printed and directly threaded. The three most feasible methods identified for orientating and mounting the brackets were; using two fasteners for each bracket, making a separate guide for aligning the brackets, and lastly, milling slots for the bracket.

4.5.1 Orienting the brackets

By using two fasteners, the potential rotation would be minimized. Nevertheless, the disadvantage with this method is that the orientation and location of the brackets relative to each other would not be very precise due to the tolerance of the clearance holes that the fasteners pass trough. The tolerance could be made smaller, but this would require machining and not just water cutting. And once the plate is set up on a machining center, other options would be worth exploring. Additionally, the angled brackets would either have to be wider or taller since two screws would interfere with the joint housing cutout.

The next option is to make a guide to orient and locate the brackets on top of the plate. This could be a template laser cut from a piece of wood, a printed piece of paper containing the brackets' location, or a 3D printed part with a cutout for the bracket that can be pushed against the side of the plate. All of these methods would not be so precise because of the rough edges on the plate due to the water cutting procedure, and the inherent inaccuracies caused when making the guides. In order to make the guides more accurate, they would have to be machined, which would be just as costly as the proposed slots. Additionally, if the platform were to be disassembled, the guide would be needed again and would be a large downgrade for ease of assembly. Lastly, this option does not provide any added methods to secure the brackets against rotation. Thus the option of milling slots became the best option with these requirements in mind, even though the slots would more than double the manufacturing time.

A more cost-efficient solution can be achieved if the slots are cutoff entirely with the water cutter. This will eliminate the milling procedure and significantly improve cost and manufacturing time. The brackets could be attached to the plates the same way as in Figure 4.21, but without a cut out for the flange. However, this would result in the brackets slightly extruding on the top, and middle-ground option when it comes to tolerances.

4.5.2 Material

For the material, a lightweight option was desired to maximize the useful workload of the actuators. Plastic or wood could be considered if a thicker top plate is

desired since it would have to be thicker to match the strength. If the price was not an issue, titanium could be considered, which would result in a thinner plate with the same strength. Nevertheless, aluminum was the obvious choice. From the strength analysis, a safety factor of 1.5 was achieved with a thickness of 7mm. This enabled sufficient depth for the pockets of 2-3mm, and room for countersunk screws. Additionally, a nice brushed aluminum finish can be achieved.

4.5.3 Static study

A static study of both the top and bottom plate were performed to verify that the selected thickness would be sufficient. Fixtures were placed on the milled slot, and an evenly distributed load was placed on the plate. The load was set to 930N, which is the max force produced when all the actuators are moved simultaneously. A 7mm thick 1060 aluminum alloy was used for this simulation, which resulted in a factor of safety of 2.1. Figure 4.8 shows the exaggerated deformation that would occur from this load condition.

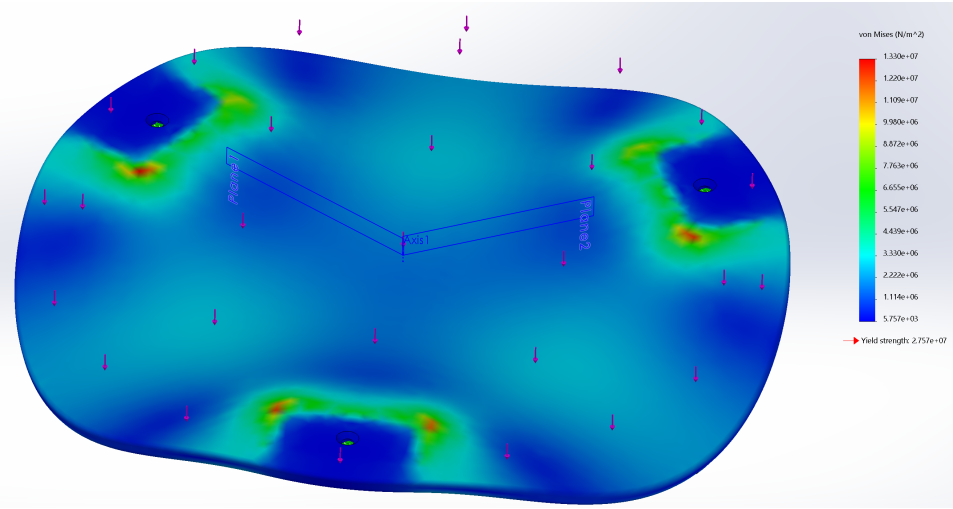

Figure 4.8: Visualisation of stress on the top plate

Since the load was evenly distributed on the plate, lower FOS is possible depending on the load placement. However, with the model ship weighing in under 10kg, the resulting FOS gave confidence that the selected thickness would be more than sufficient. Furthermore, it is never intended to run the Stewart Platform at full capacity, as this will result in a slower speed, and it would stop moving above the set load. One could consider reducing the thickness, but this was not desired due to the needed size for the slot and countersunk holes.

4.6 Bottom plate

The same choices and alternatives for the top plate can be applied for the bottom plate. However, since the bottom plate's loading condition differs from the top plate, where the bottom plate is larger and supported with three small feets, a different thickness would be required to achieve the same FOS. With only a single part manufactured from another sheet thickness, potential cost savings from utilizing another material would be lost due to the change over time. Thus both the top and the bottom plate are designed to use the same material and thicknesses, which enables the appearances to be matched if the intended brushed finish is used.

4.6.1 Static study

For the bottom plate's static study, the fixtures were placed on the circular faces where the platform feet connect, and a load of 930N was distributed on the three slots. With the same 7mm thickness and 1060 alloy material, a FOS of 1.3 was obtained.

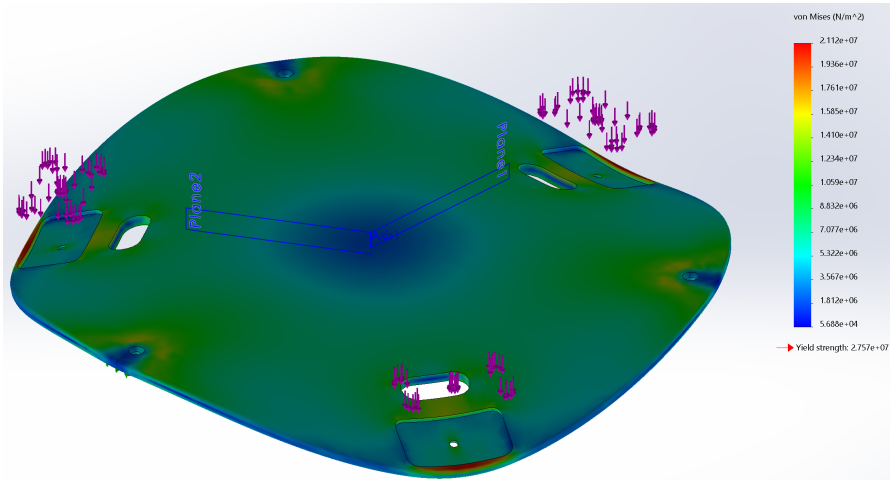

Figure 4.9: Visualisation of stress on the bottom plate

From the static study, it is observed that the main problem areas with stress concentration are at the edge next to the slot and where the platform feet are attached. Some modification to the shape of the slot, and increasing the diameter of the feet can improve this. However, for the best result, the feet should be placed directly underneath the slots. This would require changes that would increase manufacturing cost, which will be explored and discussed in Section 4.12.4. One should also compare the cost of the design change with the cost of increasing the plate thickness. Since it is more certain how the load will be disturbed on the bottom plate and higher load would render the platform useless, the lower FOS was accepted.

4.7 Electronics enclosure

The electronics enclosure was split into two parts, the back, which is bent from a single piece of metal, and the front, which will be 3D printed. This was done for several reasons. Firstly, to match the appearance of the front with the cover that goes around the base. To enable ordering the back portion of the electronics enclosure before the final dimensions for the front were ready. Lastly, with a printed part, the front of the box can easily be reconfigured by printing a new part in the future without remanufacturing the back portion of the box.

Figure 4.10: Rendering of electronics enclosure, isometric view

Figure 4.11: Rendering of electronics enclosure, front view

The back portion could either be manufactured by welding four sheets of metal together or bent to shape from a single part. If a CNC hydraulic press brake is available, then the obvious choice would be to manufacture it from a single piece, as setup time for a single bend is in the range of 1-3 minutes. If several parts were to be made, then the difference in manufacturing time between would become more substantially in favor of using a single sheet.

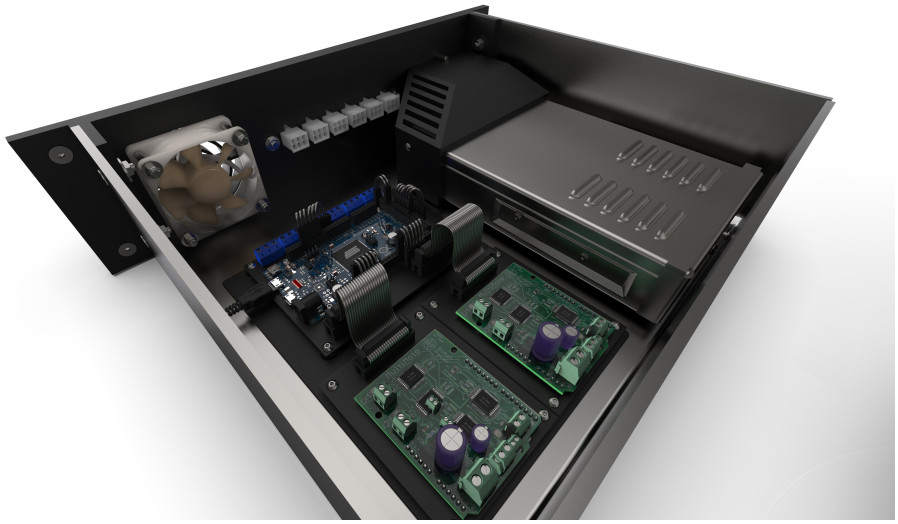

Figure 4.12: Rendering of electronics enclosure

4.7.1 Molex Hub

The Molex hub, seen in Figure 4.13, was separated into a single entity for the same reasons that the electronics are split into two parts, namely, making it easier to test different parameters without remanufacturing the front part of the electronics enclosure. With everything tested, and suitable dimensions found, this portion can be incorporated into the electronics enclosure, such that the front is in one piece. Moreover, the screws used for attaching the Molex hub could have been removed if left unchanged since the part was printed with press-fit tolerances.

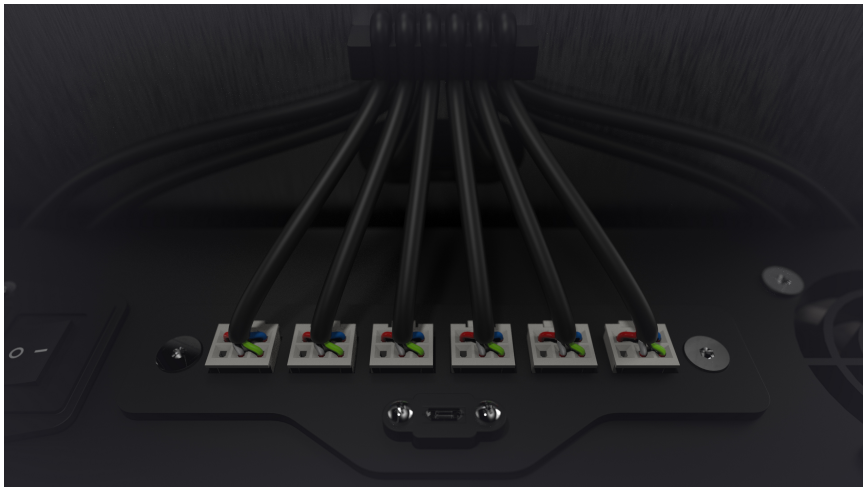

Figure 4.13: Rendering of designed Molex hub

4.8 Bushings

Three options were explored for mounting the spherical joints to the actuators. Firstly, the actuator producer was contacted and asked whether it was possible to have the actuators delivered with other tip options, which is an option seen in similar actuators. As this was not possible, two options were left; drilling holes in the actuators or the bushings used.

Drilling and tapping holes reduce weight and total length by eliminating the bushings, which could be a viable option. When drilling, particular care would have to be taken to avoid leaving marks on the soft aluminum. Moreover, twisting action caused by drilling can harm the actuators, and leaving marks on the shaft can interfere with the actuators' extensions. However, softer material can be placed in between, and potential marks can be grounded away. Furthermore, it is uncertain how modifying the actuators would interfere with its integrity, but based on the platform by progressive automation, it seems to work fine with lighter loads. Nevertheless, the tools would have to be centered 12 times to get it as centered as the bushings, which would be time-consuming and might lead to worse accuracy depending on the equipment available.

The option of bushing and pins was used, as seen in Figure 4.14. It will be faster and more practical to prototype, since the bushing can be 3D printed, and the bushings can be reused to test different actuators. The bushings are attached with a pin, which has a threaded part that locks it in place

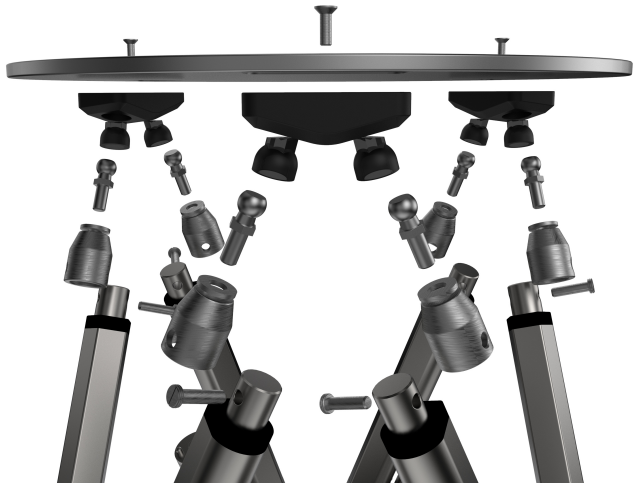

Figure 4.14: Rendering of bushing and pins, exploded view

An H7/H6 tolerance could easily be achieved for an experienced CNC-operator on the mating surfaces for the pin and the shaft, leaving little deviation when assembled. To achieve the highest possible accuracy, each bushing should be tailored to each actuator. This will add some time to manufacture, but as only two values would have to be changed in the G-codes, it will not nearly be as time-consuming as centering each actuator when drilling directly into them.

A cone is added on the end of the bushing for aesthetical purposes. This will add complexity for machining, but with A CNC-machine, v-style insert, and a cutoff tool, the whole part could be made from one clamp. It will require a 2.5 axis or higher CNC lathe, for the hole for the pin, and some extra setup time. The threads for the spherical joint could be tapped in either direction. Thus after parting it off, it will only require manual chamfering of the tapped hole, which can be done while the CNC machine is running.

4.8.1 Power supply cover

For safety reasons, a cover for the power supply was 3D printed to avoid contact with the 230V cables. For the enclosure's visible portions to have a symmetric design, the Molex connectors cut into space for the power supply. The power inlet was also placed vertically centered on the front cover, and in line with the Molex hub and fan. These factors resulted in the designed shape. Cutouts were added to the part to enable sight of the connections and are small enough such that it is not possible to get shocked. The cover is secured with a single fastener directly screwed to the power supply, which will enable fast disassembly. Flat faces were added to the inside of the cover, such that double-sided tape could be added to keep it better secured.

Design for 3D printing

Although it is said that complexity is free for 3D printing, some effort was made to optimize the shape to avoid support material, since this will leave a worse finish. On the final part, Two faces were removed such that the cover does not encapsulate the power supply as the one in the early design was seen in Figure 9.6 and 9.8. It would still leave adequate protection when combined with the enclosure walls. The sliced part for 3D printing, seen in Figure 4.15, have support generated for the cutouts that enable sight, and the cutout for the wires. Both of which can be eliminated, since it is not necessary to have a vision of the connectors, and the cutout for the cables could be slightly altered to avoid the support material. These modifications were not performed since it was later decided that the parts should be sanded and painted, enabling a perfect finish to be achieved. Additionally, the generated support was in barely visible areas, and thus the motivation to remove them was gone. Design for 3D printing was also kept in mind for all the other parts. An example is for the threaded hole for the angled brackets, where the hole has an angle to avoid support material for the overhang. However, the challenges for the other parts were more straightforward to overcome.

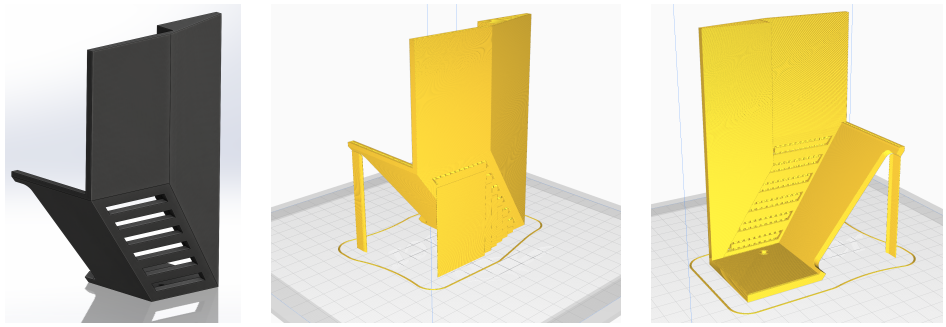

(a) (b) (c)

Figure 4.15: SolidWorks and sliced model of the power supply cover

4.9 Grommet

A cutout in the bottom plate was added for a grommet for passing through the cables. It was first intended to buy a plastic grommet, but due to the pandemic, the type and shape envisioned for the design were not possible to deliver to Norway. Instead of spending more time searching for one, it was faster to just design and 3D print one, enabling full control of the design. Moreover, the part could be sanded and painted to match the rest of the parts.

Figure 4.16: Rendering of grommet

The grommet was split into three parts, such that it could be secured around the cables without removing the Molex connector at the end. The two top parts wrap around the cables, while the bottom part is inserted to lock it into a single unit. Four cutouts are also added to the part, such that a screwdriver can be used for easy disassembly.

Figure 4.17: Rendering grommet and bracket, exploded view

4.10 Platform feet

Three aluminum rods were machined with attached vibration dampening feet, which can be adjusted to level the platform.

Figure 4.18: Rendering platform feets, exploded view

As seen in the strength analysis result for the bottom plate in Section 4.6.1, the feet should ideally be placed directly underneath the angled brackets. This will reduce the stress on the plate, and allow for a thinner plate to be used. However, this would require a redesign of the brackets, feet, or both. Alternative options are presented in Section 4.12.4.

4.11 Prototype versions

Producing parts from wood with a laser cutter can be considered one of the fastest ways of prototyping. For this project, the electronics enclosure and top/bottom plate could be designed with this manufacturing method in mind. All of the other parts used in the Platform could also be prototyped by 3D printing. Thus, small alterations to the design can be made to avoid machining and reduce cost, but with reduced max load and lower obtainable precision. For the simulation of ship motions, this could be acceptable since the model is fairly light, and there is less demand for the precision of the movement, as discussed in Section 6.5.1.

4.11.1 Top/bottom plates

A prototype version for the top and bottom plates can be laser cut from the same file sent for water cutting. However, the slots would not be ideal for prototyping. These can be removed for the prototype version as a precise assembly is not required for verification of the Platform's functionality. Furthermore, it is possible to engrave/burn the wood with the laser cutter, which can be used as guides for the brackets. On the other hand, the enclosure would require a redesign with tabs and slots such that the different sides can be glued together.

4.11.2 Electronics enclosure

The prototype version was produced from medium density fiberboard. With a laser cutter, the different plates are cut out in a couple of minutes. This prototype version could be acceptable for a final platform since the box itself would seldom be visible, and the reduced strength does not matter. Precise manufacturing is also less of an importance for the enclosure. Moreover, compared with the manual bending machine available in the workshop, the laser cut part achieved much better tolerance. This is the version currently used on the Platform. However, only 6mm plates were available, compared to the 4mm designed. This left 2mm less clearance for the actuator cables, which was enough to interfere with the cables, such that the enclosure could not be slid out freely.

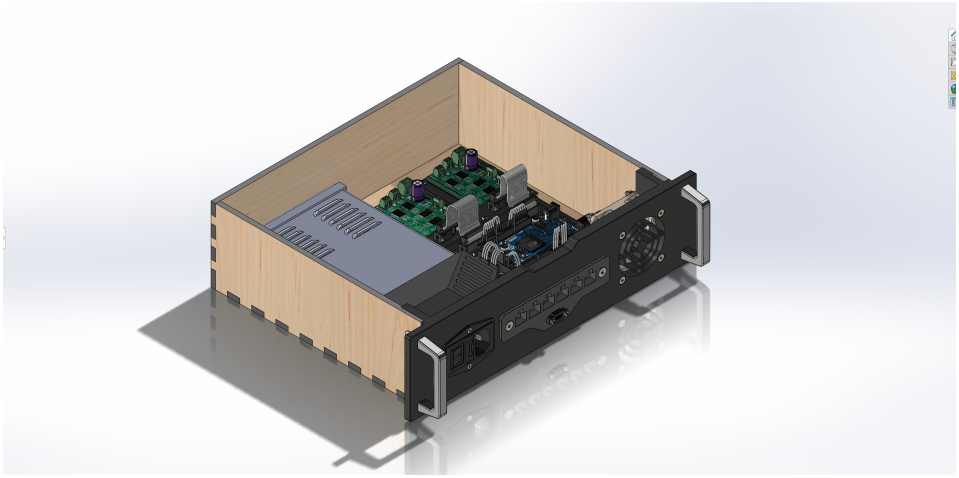

Figure 4.19: Prototype version of the electronics enclosure

4.11.3 Surface finish

The 3D printed parts can achieve an excellent surface by sanding, spray filling, and painting [35]. This process was done to most of the 3D printed parts used for the final Platform, which enabled the Platform to look more like the renderings.

Another approach is to use a vinyl wrap. Here the parts should be spray filled and sanded to achieve a smooth surface, but instead of painting, a vinyl wrap is applied. This has the advantage that any appearance can be achieved and generally results in a better finish when a DIY approach is used. Brushed aluminum wraps were considered for the 3D printed parts to match the top/bottom plates and the 3D mouse's appearance. The parts were instead painted, as it required little effort after sanding, but it does not exclude the wrap as it is not a problem to apply this over the painted parts later.

4.12 Improvements and ideas

The following sections will present and discuss some of the ideas and improvements gathered troughout the process. For the specific use case of simulating ship-motions, many of these suggestions will be redundant. However, for future applications these suggestions could be considered.

4.12.1 Quick release mechanism

The produced platform currently has no options for attachment of loads. Fasteners were intended to be implemented into the design when the model ship arrived. However, it was held up in customs, and after final assembly, the model had yet to arrive. Nevertheless, several options have been explored, and the top plate can be disassembled such that additional fasteners can be introduced later.

The first and most obvious choice would be a pattern of tapped holes to secure a load to the platform. Moreover, an assortment of plates with similar patterns can be manufactured, that different loads can be attached to. Having an intermediate plate would be beneficial for calibration reasons since the intermediate plate itself would be manufactured to fit precisely to the top plate of the platform. Then if different models or loads are to be simulated, the models can be calibrated according to the intermediate plate and not the platform itself. However, the precision of using fasteners is questionable because of the tolerance of the clearance hole, as previously discussed in the angled brackets' design.

It is desired to remove or minimalize all sources of errors such that the physical platform is true to the theoretical one. Furthermore, a quick changeover time for different loads would be preferable, if future or multiple use cases are considered.

To improve the accuracy, locating pins can be added, where more precisely machined holes are made in the top plate, and similarly machined pins are fastened to the intermediate plates. This would drastically improve the positional capabilities. Nevertheless, securing the load with fasteners would still be time-consuming.

Magnets were explored to address the changeover time, with the intent of drilling holes were magnets that could be glued to the top plate, and the intermediate plate would have pins that would be attracted. This would result in quick changeover time, and locating pins can be added to improve positional accuracy. However,

it would only be suitable for lighter loads, since many or strong magnets would be needed to secure the heaviest loads the platform is capable of, particularly if safety factors are added to minimize the risk of injury. This would also remove its practicality, as it then would be too heavy to separate them quickly

(a)[36] (b)[37] (c)[38]

Figure 4.20: Quick release mechanism; magnet, quater turn and flex locators

Preexisting solutions for quick attachments were explored for easier implementation and drive down the cost. IMAO corporation was found that produces a range of different quick attachments suitable for the platform. Figure 4.20 shows three potential candidates for the quick release mechanisms. The flex locator, shown in figure 4.20c, has the highest repeatability of 0.01mm and a clamping force of 600N, with variants with up to 0.008mm repeatability and 4500N clamping force. However, the flex locator was discarded as it requires more than double the current plate thickness. This leaves the quarter-turn fastener seen in Figure 4.20(b). This option has a repeatability of 0.01mm and is strong enough to secure any load the platform is capable of moving. The magnet option can be quite useful for lighter loads and quick change over. Thus, a final design for the top plate can be arranged for both types of quick fasteners.

Intermediate plates

The plates should have two flat faces in the x and z direction and the top face in y direction for reference. Furthermore, The quick-release mechanism's position would be machined relative to these faces, which would make the intermediate plate accurate relative to the top plate coordinate frame, and loads can be calibrated relative to the intermediate plate. This will enable a much faster and accurate calibration of new loads since the entire platform does not have to be calibrated.

4.12.2 Angled brackets

Several test print was made such that the housing was flush with the 3D printed part. However, the final printed bracket was made with a different filament, which resulted in a gap of about 0.2mm. So if new parts are printed, the depth of the

cutout might have to be slightly altered, or some sanding will be required to get an exact fit. Additionally, after sanding, the part will naturally get smaller. To achieve a good tolerance in relation to the slot, this must be accounted for, which also has limits in precision. Achieving a tight tolerance this way will be difficult, time-consuming, and less precise than to mill the part and redesigning it for use with a clip bearing. Alternatively, reverse-engineering the shape of the ball and directly attaching the joint to the brackets. Because of the brackets' angle, the machining process can be challenging, since the clip bearings require a flat side on the back to hold it in place. However, it can be achieved with many different tools, for example, a groove milling tool.

Joint distance reduction

Further reduction in the distance can be achieved by making the slot a trough hole, such that the bottom part of the bracket is flush with the top plate, as seen in Figure 4.21. This, combined with a bracket with a machined spherical cutout for the ball joint, will give the solution where joints are as close as possible to the top plate without extending beyond it. With this concept, the bracket will be visible from the top. By welding the brackets to the plate, the parts can be milled or ground to hide the bracket after painting altogether. It is also possible to machine the holes in the top plate directly, but this will require much material to be removed.

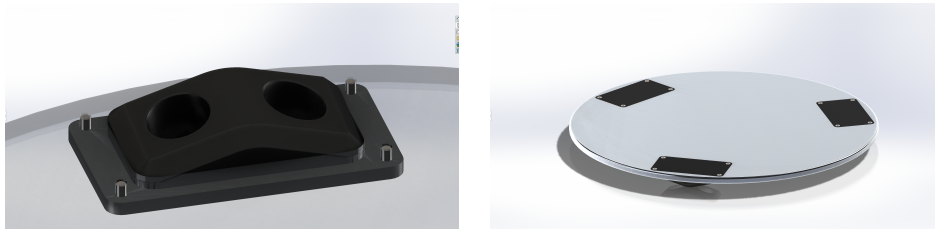

(a) (b)

Figure 4.21: Concept for new design for the angled brackets

Threaded inserts

Several methods were explored to improve the strength and clamping force for the 3D printed bracket to the plate and to reduce the risk of stripped treads. Stefan Hermann has conducted a strength assessment[39] of the most common methods to accomplish this, seen in figure 4.22. The torque out test showed a significantly higher torque load before failure for the threaded inserts. The directly threaded plastic gave in after 1Nm of torque. Whereas with the insert, the bolt heads themselves broke of at 3-4Nm of torque while leaving the inserts intact. The threaded insert was not incorporated into the design since the minimum order quantity for the inserts found was 500 parts. Additionally, the directly threaded hole would be sufficient with the current design.

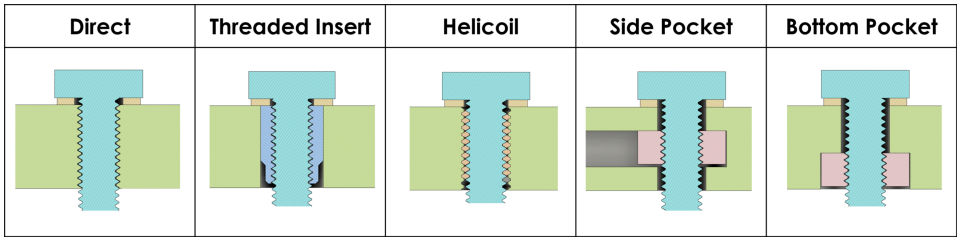

Figure 4.22: Illustration of helicoils, threaded inserts and embedded nuts[39]

Joint width

The range of motion for rotation about the Y-axis can be increased by widening the space between the joints. Based on the visualization in the GUI, the actuators will collide at a rotation angle of 67 degrees, as seen in figure 6.9. However, the platform is theoretically capable of making a full 360-degree rotation with the platform's current parameters and stroke lengths if collisions of the actuators are not taken into account. Slight modifications should be tested for the brackets to increase the platform's workspace, which can rapidly be tested by modifying the base and platform points defined in the "stewartPlatform" class in the c++ code.

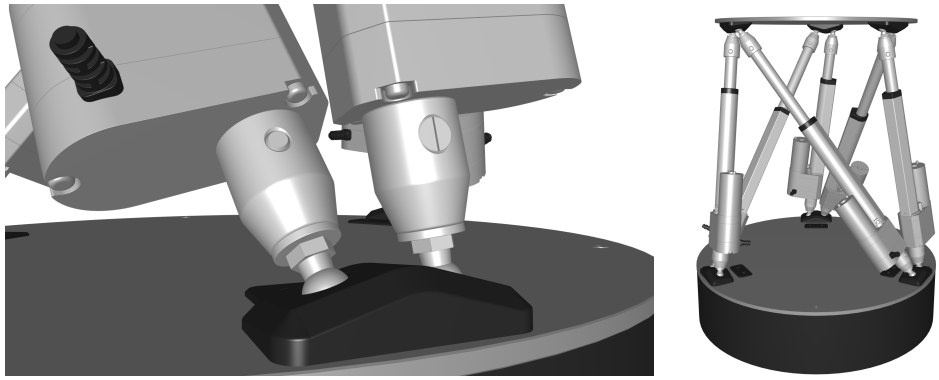

(a) (b)

Figure 4.23: Visualization from the GUI of max rotation about Y-axis before actuator collision

4.12.3 Top plate

As previously mentioned, the top plate does not have the optimal shape with regard to weight. The following section will showcase a design based on a topology study, where the new shape can be water cut, which will add minimal manufacturing cost.

Topology optimization

Solid Isotropic Material with Penalization (SIMP) is the most popular mathematical method for topology optimization. This method predicts an optimal distribution of the material within a design space, load cases, boundary conditions, manufacturing constraints, and performance requirements. According to Bendsoe (1989): "shape optimization in its most general setting should consist of a determination for every point in space whether there is material in that point or not."[40].

The objective function that is being minimized can be formulated in various ways, leading to different interpretations of what is being done. A common objective function is compliance, where minimizing compliance leads to maximizing the stiffness. To reinterpret, one can say that the goal is to minimize the component's weight without sacrificing structural integrity. The resulting shapes can be very complex to manufacture, which is not an issue for 3D printing, where "complexity is free." To get more reasonable results, programs such as SolidWorks lets one specify manufacturing controls, making the resulting shape suitable for a given manufacturing method. For the study, manufacturing controls were set such that the resulting shape could be water cut. One can also specify preserve regions around certain key features to ensure that material will not be removed there.

A quick topology study was performed only to demonstrate what kind of result and shapes that can be expected. A new study should be performed after the placement and configuration of the quick-release mechanism have been selected. The study is possible to edit, so when a good candidate for the quick-release configuration is found, only the loading conditions have to be changed, and new results can be obtained quickly. A circular pattern of 6 holes was added to the plate to represent a potential configuration of quick-release mechanism.

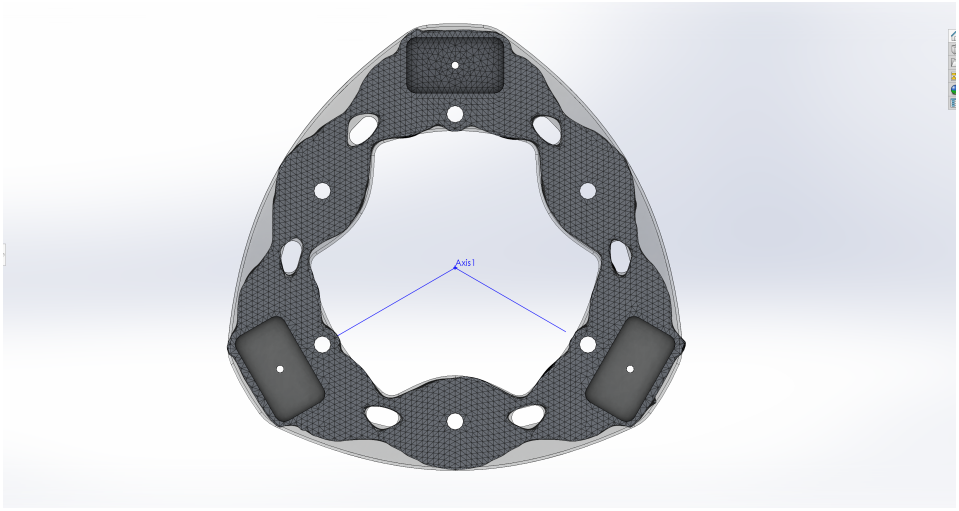

Figure 4.24: Topology optimized mesh, and design based on optimal shape

Figure 4.24, shows the smoothed mesh generated by the topology study, with a transparent cleaned-up version overlayed. More material could be removed, but the cut out regions was shaped so that it would be easy to mill, which is not necessary when water cutting. Additionally, the outer regions have more material than necessary, which was done only for aesthetics. The cleaned-up shape resulted in a weight reduction of 48%, with the same FOS for the given load case. However, how accurately this load case represents the load conditions from the quick release is questionable. Nevertheless, this demonstrates how one would approach the study and can give inspiration to future designs. The resulting shape also agrees with typical shapes found on other platforms, where a hexagonal outer shape is generally seen, and sometimes a circular cut out in the middle.

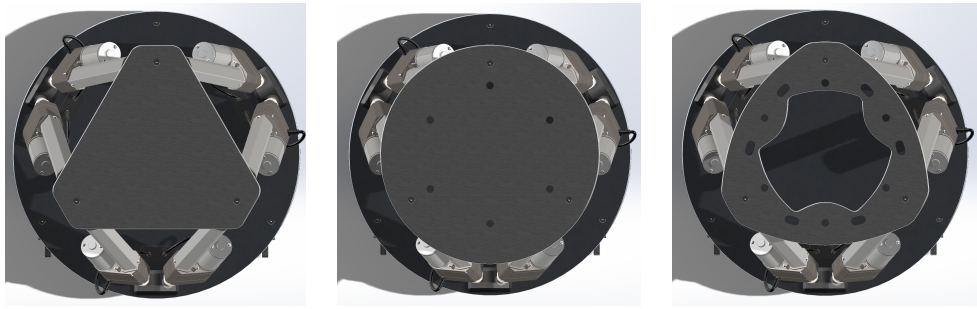

(a) (b) (c)

Figure 4.25: Hexagonal, circular and topology optimized shapes for the top plate

4.12.4 Platform feets

It was not immediately apparent how an easy to manufacture feet could be designed when placed under the brackets. Using two screws for securing the bracket would increase its size either in width or height, which is not desired as the joints should be close to the plate. Multiple options were explored, and the most cost-efficient method found is shown in figure 4.26(a), which shows a partial section view of the feet, where the feet were designed to be manufactured with a lathe.

Although, further stress reduction in the plate could be obtained by making the feet the same shape as the brackets by either 3D printing or milling the feet, which also gives more design freedom. Milling would be significantly more expensive, particularly for low volume production, and a 3D printed design would not be that scalable if higher force actuators are used in the future.

The new design would remove the three visible countersunk screws, making the platform a bit more elegant. Nevertheless, the part would be more challenging to produce, mainly because of the diameter to length ratio of the holes. This ratio could be reduced by lowering the enclosure's height and by using a longer screw. Rubber feet with large enough thread to pass through the bolt, at the given size,

can also be challenging to find, but a quick solution for that is to use helicoils.

(a) (b)

Figure 4.26: SolidWorks model of the new design for the platform feet

The first solution was accepted since a thinner plate was not desired. Additionally, the enclosure and cables would have to be rotated, the bottom cover had to be modified, and it would have a higher manufacturing cost. Nevertheless, it is a good improvement compared to the current design if higher force actuators are used.

4.12.5 Pins

The pins might seem unnecessary complex with inclusion of the threaded part. The intention was to ensure that the pin would stay in place. Additionally, the pin can be screwed tight to the shaft such that the bushings will not move if a tight tolerance is not achieved. An easier solution is to make a straight pin with a slight press fit relative to the actuator's holes. Then the pin could be hammered in making it sufficiently secured and achieving higher accuracy due to less backlash. This option was not used, since the actuator's holes were at Ø6.4, and a suitable drill and reamer were not available at that size. If left unchanged, the threaded part of the pin can be changed from 3mm to 5mm, as this will not extrude beyond the bushing, which will make the pin easier to produce.

4.12.6 Electronics enclosure

Front attachment method

The used part has a suboptimal method for attaching the front and back pieces. Initially, the front piece was intended to be a flat part, as seen in an early design in Figure 9.5 in the appendix. Using the same solution for the new design by bending the flanges inwards would reduce space for the electronics and leave less space between the Molex hub, switch, and fan. With the enclosure placed underneath the platform, as much space as possible was desired. The first and immediate idea was to make the front part as seen in Figure 4.27 (a), which is currently being

used. Since complexity is "free" in 3D printing, further design improvements were not attempted. A better solution was later found when even more room in the enclosure was desired. The new design can be seen in Figure 4.27 (b), which now seems rather obvious. Here the metal part has flanges that are folded in the opposite direction compared to the early design. The part could still be manufactured from a single sheet of metal, with minimal added time. The front part of the new design would be faster and easier to manufacture and will give 12mm more clearance for the electronics. It will also be suitable for other manufacturing methods such as water cutting or milling. There is an indentation in the middle of the part, to hide the back portion of the electronics enclosure. If the front is made by milling or water/laser cutting, this indentation can be moved to the bottom cover instead. But with both of these parts 3D printed, this will be the easiest to print.

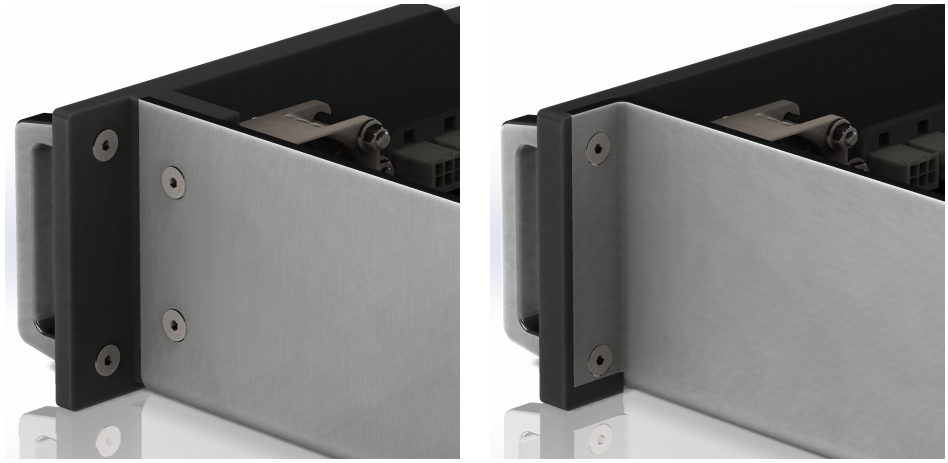

(a) (b)

Figure 4.27: SolidWorks model of old and new design for front cover

Drawer slides

The current enclosure is not attached to the rest of the platform. Instead, it is lying flat on the ground. For practical reasons, a drawer slides could be implemented into the design which could be achieved by modifying the bottom cover, enabling the slide counterpart to be mounted there. This was not added since the platform would be stationary, and it would result in less space. However, the feature can be added later if some of the space-saving suggestions are implemented.

Enclosure size

When designing the part, the enclosure was made nearly as big as possible compared to the size of the bottom plate. Using the 3D models as reference, this seemed to give sufficient space, which it did. However, more space is still desired, as the

components are tightly packed together. Furthermore, a new power inlet had to be used, which was 20-30mm deeper than the original. With the bottom plate's current size, the depth of the electronics enclosure can be increased equal amounts by modifying it, and the bottom cover. Furthermore, it is possible to gain an additional 5-10mm clearance by directly soldered the cables to the pins on the power supply.

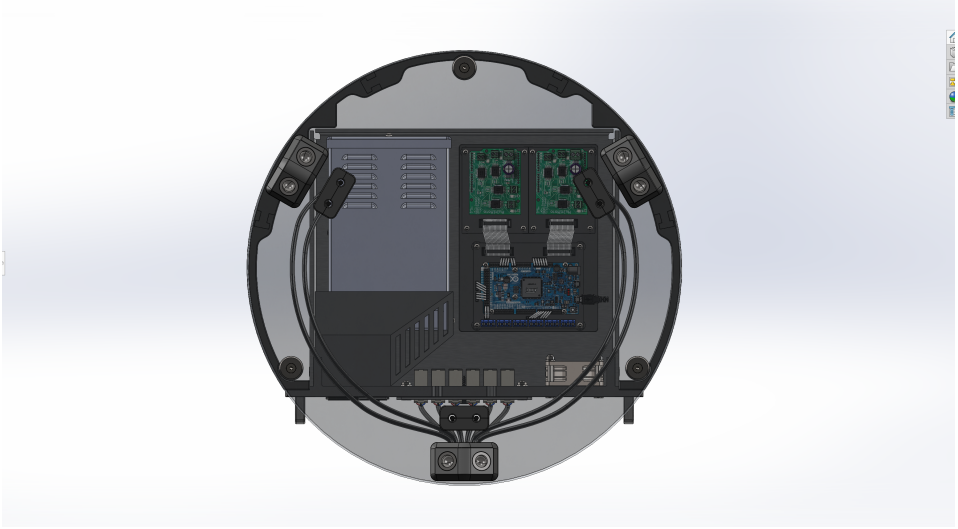

Figure 4.28: Rendering of electronics enclosure, top view

The electronics' arrangement was kept the same as from the Progressive Automations platform. However, significantly more room can be gained in the box by vertically stacking the Arduino and the motor controllers, as discussed in Section 6.12. As a last resort, the bottom cover dimensions can be increased, which will require the angled brackets to be moved further into the plate, if the same workspace is desired.

Chapter 5

Graphical user interface

This chapter will present the GUI written for the Stewart Platform. Figure 5.1 shows the main window of the GUI. The GUI is kept fairly simplistic and minimalistic, with five different groups; camera settings, display settings, manual input, demo, and status. Apart from the serial connection window based on the platform by progressive automation, the entire program was written from scratch with the scatter example[41] as a starting point, found in the Qt Creator start menu

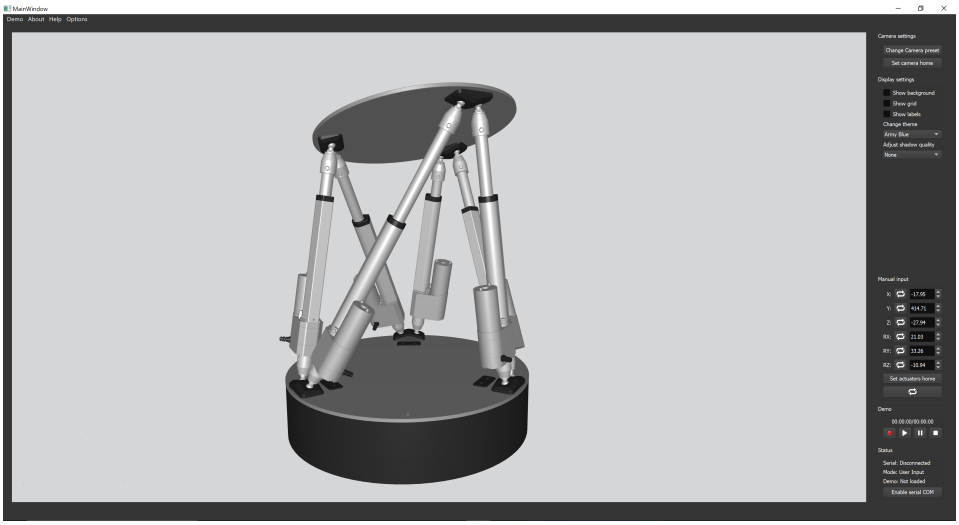

Figure 5.1: Screenshot showing the main window of the GUI

5.1 Functions

A close up picture of the different groups in the sidebar is seen in Figure 5.2. Camera settings contain two buttons, one that switches between several standard views while the other sets the camera position to a predefined home position. It is also possible to rotate and zoom in the viewport with a mouse right and middle button, respectively. The next group contains options for the graphical settings—three tickboxes, which shows/hides the background, grid, and labels. And two spinboxes, which respectively, change the background colors, and enables/adjust shadow quality. The shadow setting has a significant impact on the performance and is set to none at startup.

The manual input group, seen in Figure 5.2b, allows the user to manually change the platform's pose by writing values or using the up/down arrows. There are also buttons to set each axis home independently or set the entire platform to its home position. Additional control of the platform is possible with a 3D mouse, which will be further discussed in Section 5.5, or by running a demo. In these cases, the spinbox's values will also update according to the platform's current pose. On the top right corner, there are arrows which will switch between the pose of the platform, and a functionally yet to be implemented, which is discussed in Section 5.8.1.

Figure 5.2c, shows the two last groups. The demo group contains four buttons; record, play, pause, and stop. This function will be used for running simulation of ship motions, and the record feature was implemented for testing of the playback. Lastly, there is a label that contains the total duration of the demo and the current playback time.

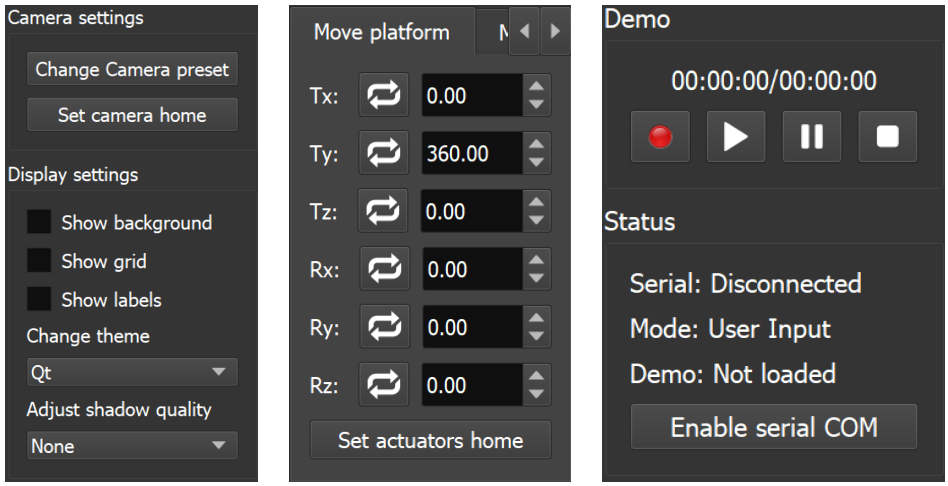

(a) (b) (c)

Figure 5.2: Close up pictures of the main GUI elements

The last group contains information about the current state of the GUI. The Serial label provides information about whether or not the platform is connected to the Arduino by displaying the port it is connected to. When a connection has been established, the enable COM button will be activated, and when toggled will send the leg lengths to the Arduino. The demo label shows which file is currently loaded for playback. When the play button is pressed for the first time, a dialog box is opened to select a file for playback. It was chosen that the file dialog would only be opened the first time, such that the demo can be repeated without extra clicks. The file dialog can later be accessed trough the menu bar under file-load demo. Mode displays the current mode the platform is in, and is currently redundant, as the greyed out or toggled buttons in the demo group would convey the same information.

5.2 Choosing framework

Qt and ROS were the frameworks initially considered for the project. With no previous experience with either, the choice was primarily based upon the available documentation and tutorials. Other deciding factors was what the department is familiar with, and deployment for a touch device such as Android or iOS, as a tablet was considered for the host. Qt was selected as it seemed to have the best resources for learning available. However, this was only intended for prototyping, where simple shapes as cylinders would be made for the visualization, and search for other frameworks would be done concurrently. However, over time, improved visualization and more features were added, and the program was never rewritten for another framework.

Moreover, as the tablet device was narrowed down to a Microsoft Surface, which would allow the code to be written for deployment for windows, more flexibility for the framework was acquired. An implementation of ROS integrated with Qt was found at the initial stage, which now seems like the best option for the final software. Nevertheless, More photorealistic options were explored for the visualization, as this would look more professional and could enable testing of the tracking software without a physical platform. Both Unreal Engine and Blender can be integrated with Qt or ROS, which can provide near photorealistic visualization in real-time. However, it would not be so straightforward to implement, and a physical platform was desired even if the testing could be performed without it. Ultimately, these ideas were scrapped to make it easier to hand over the project to other people as it would have less documentation and added complexity. Instead, the option to combine Qt with ROS is recommended. This option would provide better visualization than the current software, could communicate with other robots/projects in the lab, the people at the department are experienced with ROS, and the software can easily be deployed to work with the Microsoft Surface.

5.3 System overview and flowcharts

The software consists of three primary classes. The mouse3Dinput class is the driver and for the handling of the 3D mouse. The stewartPlatform class is responsible for calculating the kinematics and visualizing the 3D files in the scatter plot. While everything related to the frontend, and the implementation of the demo functionality, is contained in the mainwindow class. The classes are connected trough the convenient signal and slot functionality provided by the Qt framework. Simplifications could be made by merging the stewartPlatform class with the mainWindow class. However, since this was only intended for prototyping, the stewartPlatform class was first implemented with the "Eigen" library for c++, to make it easier to change to a new framework. Due to time constraints, the framework was not changed, and the Eigen library was replaced with Qt's library for vector and matrices. Considered frameworks for the project are discussed in Section 5.2. A high-level overview of the main elements in the GUI will be presented in the following flow diagrams.

5.3.1 Update mesh positions

The stewartPlatform class's primary function is to calculate the inverse kinematics and the poses for the imported 3D object. A flow diagram of the actions that occur when a pose is passed can be seen in Figure 5.3. A pose is given either trough the spinboxes, 3D mouse, or from playback of a demo. If a valid pose is given, a set of temporary vectors for the leg lengths and relevant points are calculated. The calculated leg lengths are checked against the max and minimum permissible leg lengths, and if not valid, nothing further is done, even if only one of the leg lengths is invalid. For smoother operation with the 3D mouse, it can be considered changing this behavior.

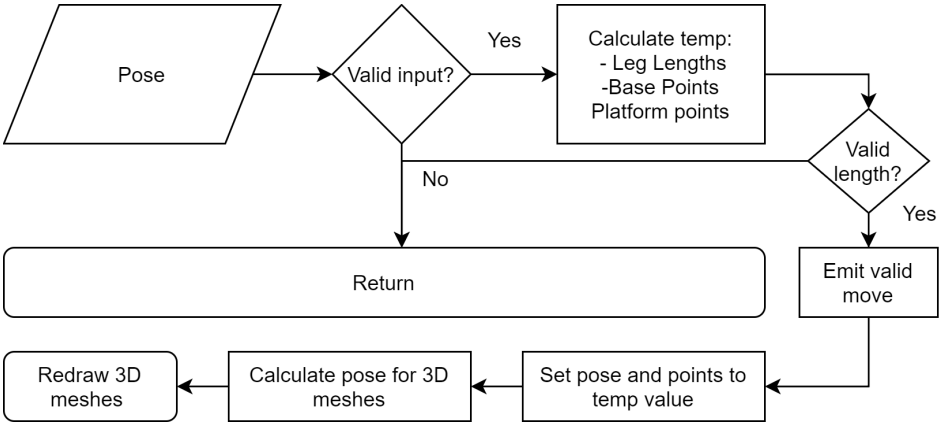

Figure 5.3: Flowchart for updating of mesh poses

With a valid leg length, the leg length and point variables are updated, and the

position and orientation for the actual imported 3D meshes are calculated. Since an MTL file could not be used for color/texture in the current framework, several meshes are imported such that independent colors could be added for individual parts/assemblies. The actuators are split in an upper and lower half with the spherical joints attached. The coordinate frames and orientation of the 3D file is conveniently placed on the spherical joints and can be examined by opening the files found in the resource folder. The top and bottom assemblies were also split in order to apply separated texture for the dark/light parts of the top and bottom assemblies. The bottom assembly remains fixed. The top plate is split, where the three angeled brackets are imported as a single file with a coordinate frame placed identically as for the light-textured top plate, such that the same transformation can be applied for all of them.

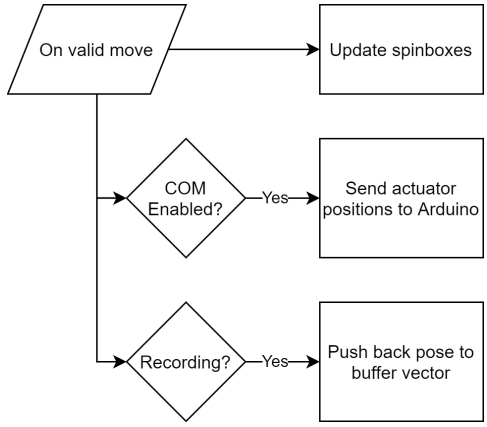

Figure 5.4: Flowchart for when a valid move is registered

As seen in Figure 5.3, a signal is emitted if a valid pose is passed—this is one of many signals that are connected to a slot in the mainWindow class. When the signal is received, the spinboxes will be updated. If the enable COM button is pressed, which can only be done if connected trough serial communication, the platform's leg lengths will be mapped to values ranging from 0-1023 and sent to the Arduino. Additionally, if the record button is pressed, the current pose is added to a buffer vector.

5.3.2 Demo

The demo functionality was implemented by writing poses to a text file. These are saved in the following format "Tx, Ty, Tz, Rx, Ry, Rz," on each line in the text document. When recording or playing back a file, 60 poses are given each second. A refresh rate of 60 was set since it both matches the update frequency of the 3D mouse and the refresh rate for most common monitors, which will ensure smooth playback. When the demo buttons are pressed, the state is changed. A timer is

implemented, which will have a timeout 60 times each second. Figure 5.7 shows a flowchart for actions that occur on timeout, depending on the current state. This implementation was chosen for its simplicity and was the first idea for how it could be implemented. Moreover, this method will not require a sophisticated path planner, as intermediate positions can be eliminated or would be relatively small.

Path planner

A simplistic path planner is implemented for the homing buttons, which is also used to move the platform to the start position of the demo, or the last position played back if the platform were moved when paused. In the path planner, the difference in leg length for the start and end pose is calculated. With information on the actuators' speed, the number of steps required to reach the end pose can be calculated based on the actuator's largest leg length difference. Step size for each axis is found from the difference in pose divided by the number of steps.

5.3.3 Play button clicked

Both the play and pause buttons are not directly connected to the stewartPlatform class to send poses. Instead, these buttons change a state variable. In early development, a single bool variable was used for storing the state. As more and more functionality and states were implemented, it would be more practical to store them in an enum. As of writing this, and several other plans for cleaning up the code have yet to be implemented. The first time the play button is pressed, a dialog box is opened. As a default, it will open the root directory to ensure that the directory is available. As will be discussed in Section 5.8.2, an option should be implemented that lets the user change the default load and save directory.

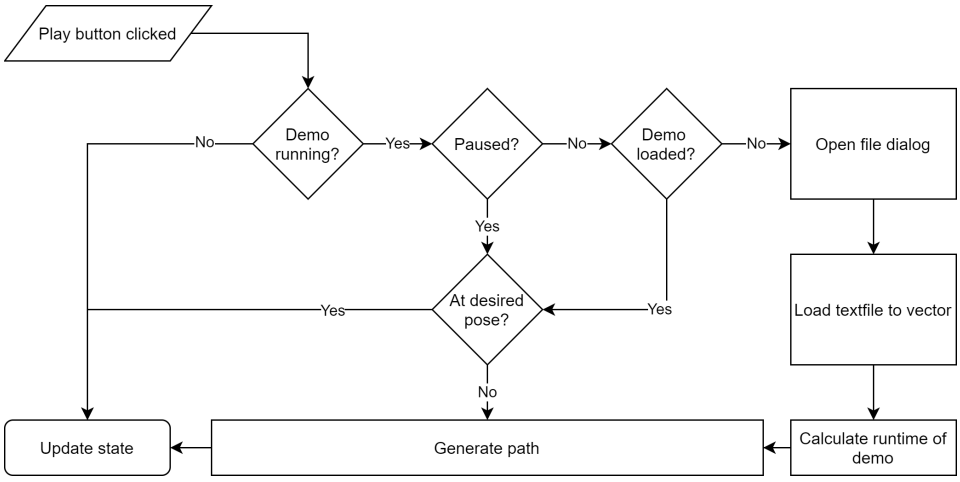

Figure 5.5: Flowchart for playback of demo

The selected file is loaded to a dynamic vector, such that the time-consuming read process does not occur during playback, which could cause memory leaks. The container used is a QVector, which has a max size of 2GB; with it, approximately 16 days worth of playback can be stored. Alternatively, an hour of recording would take approximately 5.2mb.

As previously mentioned, a path will be generated if the platform pose is not at the desired pose, which can happen if the platform is moved while the demo is paused, or the platform is not at the first pose from the demo.

5.3.4 Recording demo

When the recording button is toggled on, a dialog box is always opened, asking the user for a filename and save location. Additionally, all the other demo buttons are greyed out, and the state is changed to recording. On the "on valid move" signal, a pose will be added to a buffer vector. This means that standstill movements are not recorded, as a signal is only passed if a new valid pose is registered. This proved beneficial for recording smoother movements when using the 3D mouse. Nevertheless, this functionality was primarily added to test the playback feature. If desired, an option can be added to a preference file or a checkbox, where standstill movements can be recorded. This will require the recording action to be moved to the timeout function. The recording should also contain information on the pivot point when this feature is implemented, as discussed in Section 5.8.1.

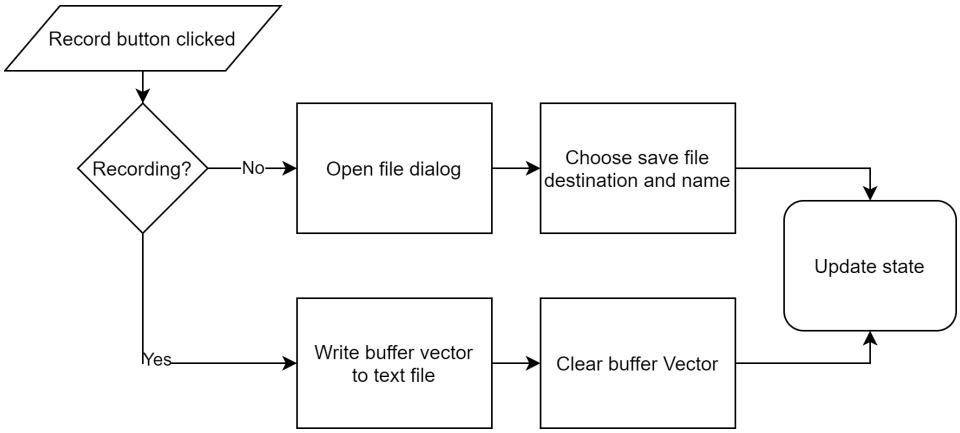

Figure 5.6: Flowchart for recording of demo

Similarly to before, a vector is used as a buffer to store the recorded data. When the record button is toggled off, this data gets written to the set recording destination and filename, and the demo buttons are reset.

5.3.5 Timeout

For playback functionality, a timer is added where a timeout occurs 60 times per second. On timeout, a function is run to check if the platform is following a generated path. Furthermore, it is checked if the path is from the demo, or from the generated paths used for homing or setting the platform to start of demo or the last position played. When homing, if the end of the generated path is not reached, the demo buttons are disabled, a signal to update the meshes is sent, and the buffer vector is incremented. If the end is reached, the buffer vector is cleared, and the play and the pause button is enabled.

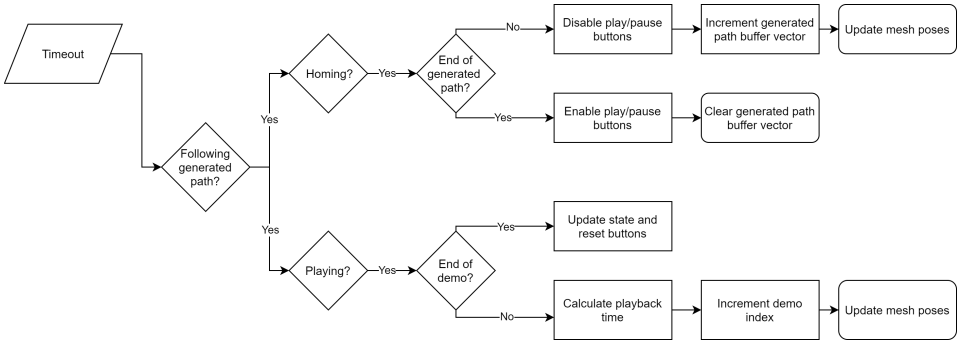

Figure 5.7: Flowchart for when timer reaches timeout

If the path the platform is following comes from the actual demo file, then it checks if it has reached the end of the demo. If it has, then the state is updated, and things are reset. If not, the current playback time is calculated, the current index is updated, and a signal to update the meshes are sent.

5.4 Simulation of ship motion

Different methods for simulation of ship motions were explored in the early stages of the project. The first method was to either collect data from ship logs or placing an IMU on a ship to record actual motions. Another possibility is to gather poses from a ship simulator. Mathematical expressions for ship motions can also be obtained where further information can be found here[42][43]. An actual demo for ship motions has not been implemented yet since the users wanted to create the simulations on their own with a previously used simulator. Depending on the simulator, some translation has to occur to make it compatible with how recordings are played back, as described in Section 5.3.2.

5.5 3Dconnexion SpaceMouse Wireless

Manual controll is added to the software trough the use of a device from 3Dconnexion, which offers the following devices:

- SpaceMouse Enterprise
- SpaceMouse Pro
- SpaceMouse Pro Wireless
- SpaceMouse Wireless
- SpaceMouse Compact

Figure 5.8: 3Dconnexion SpaceMouse Wireless[44]

All of the SpaceMouse devices can be used together with the written software, and all devices have the same patented 6-DOF sensor, which makes them suited for manual control of the Stewart platform. The SpaceMouse Wireless, shown in Figure 5.8, has been selected for this project, and will from now on be referred to as a 3D mouse. Since all the devices have the same 6-DOF sensor, the separating factors were the wireless feature and the number of buttons. The two buttons on this device were sufficient. The smaller form factor and the wireless option make it more suitable for a touch device attachment, further elaborated, and discussed in the following sections.

5.5.1 SDK and Drivers

Several drivers and existing implementations were explored for a quick implementation of the 3D mouse. Nevertheless, the first found examples were made as far back as 2011, which was not compatible with the used version of Qt. This meant

that many errors were thrown as a lot of the code was redacted. After spending a fair amount of time updating it to work with Qt5, another implementation was found in a blog post by Ascon. This implementation can be seen as a hello world implementation, where only the most basic features are implemented. This was acceptable for the current use case, as only the 6DOF joystick was needed. The code can be found on Alexandr Ershov github[45] page, and only requires a change to the main c++ file, where a single line of code must be added to install the native event filter (app.installNativeEventFilter(&mouse)). Additionally, the include path for the library files of the 3Dconnexion SDK must be added to the project file. These are not shared and must be downloaded from the 3Dconnexions website by signing up as a developer.

5.5.2 3D mouse features

The main feature of the 3D mouse is to enable manual control of the Platform. The mouse has a navigation cap, which enables six degrees of movement, as seen in Figure 5.9. The manual control is very intuitive, and the movement is done as if one were holding the top plate instead of the navigation cap. For example, lifting the cap would move the top plate up, pushing it away would move the top plate away, etc.

Figure 5.9: 3Dconnexion: Navigator cap and movements

Currently, only the right mouse buttons have features assigned to it, which opens the radial menu seen in Figure 5.10. Undo and redo have no function assigned, while the virtual NumPad does as the name suggests and opens a virtual numeric keypad where values can be entered with mouse clicks.

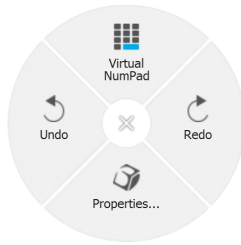

Figure 5.10: 3Dconnexion right button radial menu

The properties button opens the window displayed in Figure 5.11a. This window has a slider that controls the 3D mouse's sensitivity, which ultimately allows adjusting the speed at which the Platform is moved.

The advanced settings box opens the window seen in Figure 5.11b, allowing the user to set the speed, toggle off/on, and reverse each axis independently. The current orientation for the axes was found to be the most intuitive. Additionally, there is a checkbox to toggle off/on all translation axis trough the pan/zoom checkbox, and the same for the checkbox for the rotation axes. There is also a checkbox marked with dominant, which will restrict the movement to a single axis which the user presses the hardest. Lastly, there are two radio buttons, namely forward/backward and up/down, which is intended to be used to change which direction is responsible for zooming when using at as a 3D navigator, and will effectively swap the forward/backward and up/down direction. It is recommended to keep this at the default setting of forward/backward.

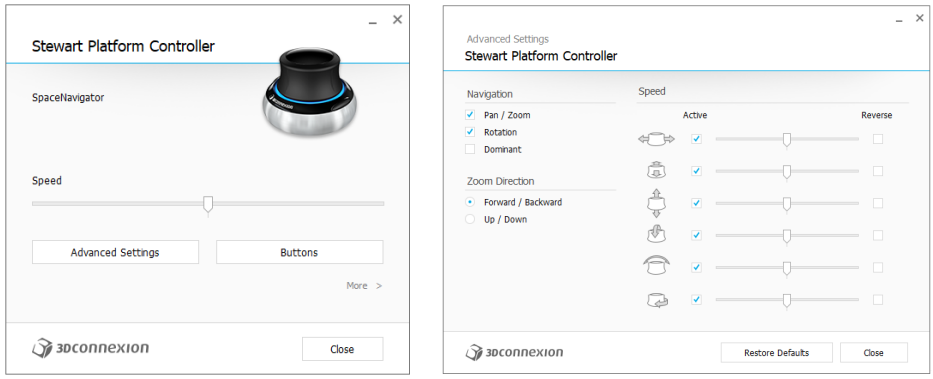

(a) (b)

Figure 5.11: 3Dconnexion (a): properties window (b): advanced 3D settings window

5.5.3 Calibration of Sensitivity

The mouse's sensitivity was set such that when moving the mouse at full force in a single axis, the simulated platform moves at the theoretical speed of the physical platform. However, these speeds only apply for movement or rotation about a single axis. Additionally, the translation speed in x and z-direction, and all rotation movements only applies when the platform is in its middle height position. Thus, combined motions at full force, or rotation and translation when the platform is in another position, can have higher or lower speeds than the platform's capability. Furthermore, these values were obtained from an older wired 3D mouse, and it seems like the new wireless mouse will have to be recalibrated, which has not been performed.

The implemented recording feature was used to find the axes' sensitivity, which records the platform's pose 60 times each second. One axis was activated at a time, and the number of recorded poses between the max and min position was counted. With a stroke length of 150 mm, speed of 50.8 mm of the actuator, and poses updated 60 times per second, 177 recorded poses is the theoretical amount needed to match the speed of the actuators. Based on this information, a number for the sensitivity was then extrapolated such that the number of recorded poses equaled 177. A similar method was used for the other axes. The platform was moved to its middle position, and similarly to before, all but a single axis was activated. A number for the other sensitivities was then found with the same method, but with a different amount for the number of expected recorded poses.

Another possible method for calibration is to look at both the number of poses and the change in leg length. With the same parameters as before, a max change in leg length is calculated as $150/50.8/60 = 0.0492$ mm. Based on this, a number for the sensitivity can be extrapolated such that the change in leg length is max 0.0492 mm.

Both methods are not particularly accurate, especially when multiple axes are moved at once, enabling the simulated platform to move faster than the physical platform. This will cause a lag between the visualized platform and waiting for the platform to adjust to the last send position. However, the current solution was deemed acceptable for several reasons. The simulated ship movements in weather conditions suitable for loading cargo from one ship to another are slow. The simulation can be slowed down without affecting the validity and testing of the vision-based tracking system since the results can be extrapolated to higher speeds. Manual control is an added feature not necessary for testing and simulating the ship's motion but was added to test the platform itself and potential future use cases. This sensitivity setting will give the best response in a single axis movement, but the platform would lag behind in combined movement. Lastly, the overall sensitivity can be rapidly changed, such that the simulation does not exceed the platform's capability.

Nevertheless, a possible solution to get a more accurate motion to the capabilities of the physical platform is to limit the new leg length to max 0.0492 mm longer than the previous length. This would require the forward kinematics for the platform to be solved with the new leg lengths, which could be both time-consuming and challenging. The Stewart platform has no known closed-form solution, and the number of solutions of the forward kinematics of the general 6–6 Stewart platform is up to 40 in the complex domain. However, a good initial guess can be found for the forward kinematics since the difference from the last known position is relatively small, and perhaps all but one solution would be eliminated. Nevertheless, this has just been briefly explored. Further information can be found in a forward kinematics solver by lee and shim[46]. This solver is written in c++, and could potentially be fast to implement.

5.5.4 User experiences

First-time users of 3D mouse found the 3D mouse's sensitivity to be challenging and typically ended up moving multiple axes simultaneously, and at to high force. New users were shown the correct technique for using a 3D mouse, which can be found in this demo by 3Dconnexion[47]. This resulted in some improvements, but ultimately time was the key, and new users quickly improved and felt comfortable with the control within a couple of hours of use. This falls in line with a survey by Technology Assessment Group[48], where the time to become comfortable and proficient is shown in Figure 5.12. Other recommendations for new users is to test the trainer and demo features that come with the 3Dconnexion software. Furthermore, the user can consider turning down the speed to make it more manageable and enabling the dominant feature, which was found to be very practical for new users to the 3D mouse, who typically unintendedly moved multiple axes simultaneously.

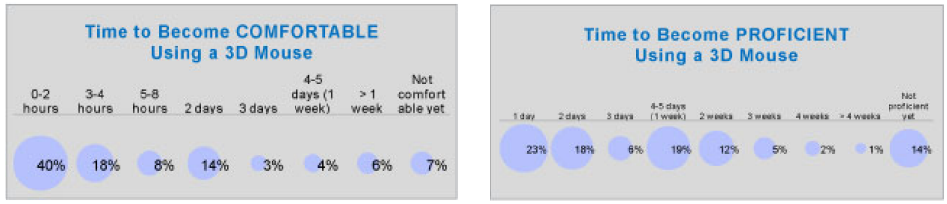

(a) (b)

Figure 5.12: 3Dconnexion survey of (a): time to become comfortable (b): time to become proficient[48]

5.6 Choosing Host PC

For the Host PC selection, future use cases, cost, and user experience were taken into consideration. The first option is to have the program run on the user's laptop, where an executable would be easily possible to download. Regardless of the chosen Host PC, this option was always intended. Nevertheless, having it run on the user's laptop might require the program to be compatible with both Windows, Linux, and MacOS. Furthermore, the laptop's performance might limit the usability of the software or limit other activities that the users can perform simultaneously because of the performance hit and occupied screen space. This would be the case with the vision-based tracking software, which needs all the performance available and screen space.

Therefore a stationary device should be allocated with the primary use for controlling the Platform. Several options for this stationary device have been explored. The simplest option would be to designate a laptop to the Platform. Alternatively, a stationary pc with a monitor can be used, which offers better performance and screen space for the same price. Another option is to have a raspberry pi or a similar microcomputer but with sufficient performance to run the program, with

a touch screen mounted to the Platform. This could be a cost-efficient solution and can be hidden by installing it under the Platform. However, the idea was quickly dismissed, as the Platform could be placed on the floor, making the user experience and ergonimics bad. Additionally, the Platform's visualization was pivoted to a more realistic representation, which would require higher performance to run. These changes might result in a larger device that would not fit or require a redesign of the Platform. Furthermore, after making a quick 3D model of this option, a sufficiently large screen would not fit well with the size of the Platform. Nevertheless, it resulted in the idea presented in Section 5.8.6.

For potential future use cases, a handheld touch device could be useful, as this would allow the user to move around freely and offer a user-friendly method for manual control of the Platform. Some of the options explored were a separate touch screen running on Ubuntu Touch, Android tablets, and iPads. All of them could offer a good end-result. However, they would be time-consuming to implement, particularly if running the program on a Windows would remain an option. This idea was dismissed, but shortly after, the idea of using a windows tablet such as the Microsoft Surface was found. Some of these windows tablets can run on Windows 10 (x64), which means no software changes are needed. The following section will present a concept for how the tablet can be used.

5.6.1 Microsoft Surface Book

A concept of how a handheld attachment for the surface book can be implemented is seen in Figure 5.13 . Here a 3D printed attachment with a keypad and 3D mouse is connected to the tablet. Straps are added to the back to represent how the tablet can be secured, as seen in Figure 5.14.

Figure 5.13: Rendering: Front of touch device concept with attachment for 3D mouse

The attachment of the surface book went trough three main iterations, where the final concept has yet to be visualized. The first option explored had a slot that encapsulated the entire tablet. This option will limit access to the ports on the tablet, and incorporation of the needed connections would be time-consuming and difficult to achieve with a 3D printed attachment. The second option was inspired by a USB-C adapter, which directly attached itself with a USB connection on the side. This option is the one shown in the figures of the concept made. However, connecting it with only the USB ports would be fragile, and the device would need additional support, which is not shown in the figures.

A better option has later been found, but a visualization of the concept is not made. Firstly, a wireless 3D mouse and keypad have been used to make attachments faster. Moreover, no cables or internal connection on the 3D printed attachment is then needed, which will make it much faster to develop. These changes leave much more flexibility for the design. Furthermore, the Microsoft Surface Pro has been changed to the Microsoft Surface Book, which has a much sturdier mechanism for attachment of keyboards. This could potentially be modified to attach to a 3D printed attachment directly. Nevertheless, with everything connected wirelessly, more straightforward options can be explored. Moreover, since there is a lag of a couple of seconds to detach with the original connection, other options might offer better user experiences and could be faster to implement.

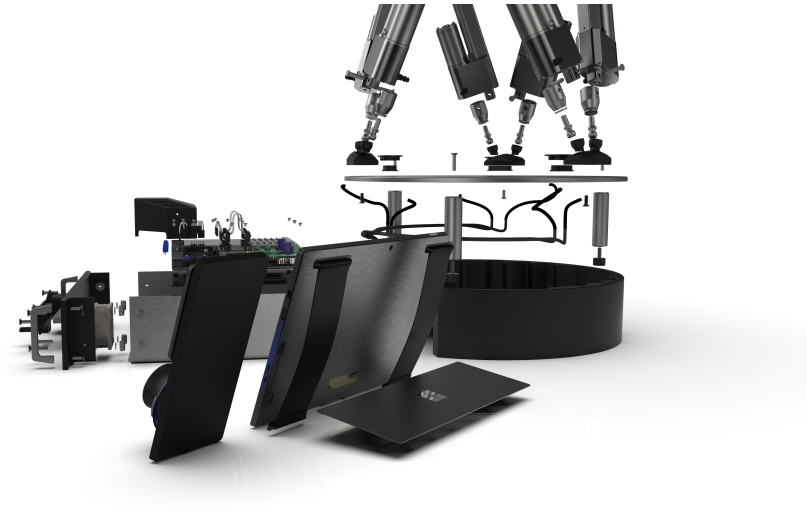

Figure 5.14: Rendering: Back of touch device concept with attachment for 3D mouse

Regardless of the option chosen, a separate 3D mouse should be bought, which always remains attached to the 3D printed attachment. This is recommended due to the heavy base of the 3D mouse needed when placed on a desk, where

the added weight will be inconvenient when holding the device. The base can be removed, but this will render the 3D mouse useless when placed on a desk, thus the recommendation of two separate 3D mouses. If the added weight of the 3D mouse is acceptable, then it would be possible to make a system for attaching the mouse quickly. Multiple 3D mouses can be connected and used to control the Platform simultaneously, so two separate 3D mouses will not cause issues.

The question to ask is if it is necessary at all to have this handheld device. Since it is recommended to buy a separate PC for operating the Platform, this was investigated to give a more informed decision, as this option can be desirable in the future. Furthermore, buying a separate PC for controlling the Platform could be more expensive than all the components bought so far; therefore, possibilities have been explored to a greater extent. It will also not require much effort to implement, as it can be run on the current software, and a simple 3D printed attachment for the devices can be 3D printed quickly. However, it is recommended to redesign the GUI for a touch-centric design, which can still be operated with a mouse and keyboard.

Furthermore, options for manual control that allow the user to move about freely are already implemented and possible with the wireless 3D mouse. This will give a similar experience as the suggested tablet, but without the visualization. However, it only has two buttons, which will limit its use as a separate controller. Nevertheless, one button can be assigned to toggle play/pause for the demo. The other button other should be kept to open a radial menu, which will give the user 4-8 options, to access the implemented features, and additional features yet to be implemented.

5.7 GUI Performance

The performance of the GUI visualization is mainly dependent upon the quality of the 3D models used. The current models were exported at very high quality. Significant performance increases are possible if the parts are exported at a lower resolution, and some details are deleted from the files. Further improvements without impacting the visuals could be achieved by smoothing, where it is possible to obtain similar visuals with a lower polygon model. This option was not found for the class used to represent the 3D models but is a standard option that should be implemented when the framework is changed to, for example, a combination of Qt and ROS. Based on information found on online forums, it seems like there is no straightforward way of finding the system requirements for the program. Some suggested running the program on a virtual machine, where it would be possible to adjust some of the settings for the hardware, but the consensus was to test it with different setups. A few setups have been tested, among them, a middle to low-end desktop with GTX 1060 and i7 8700k, which ran the program smoothly.

The option to switch between different quality 3D models can be added to the preference file. Moreover, an option of just primitive shapes, where only simple circles

and spheres are used, can also be included for maximum performance. Besides the models, the code itself can surely be improved upon. Multithreading can also be implemented by, for example, calculating rotation for each of the 3D models on separate threads.

5.8 GUI: Improvements and ideas

5.8.1 Move and display pivot point

The pivot point, which is the coordinate that gets translated and rotated trough the GUI, is at a fixed location relative to the plate. The y-coordinate is offset 8 mm below the plate, which coincides with the center of the spherical joint. While the x and z-coordinate coincides with the center of the plate. Functionality to enable rotation and translation of the pivot point similar to the one shown in this demo[49] by Physik Instrumente USA should be implemented. Currently, the GUI has a vertical tab widget that enables switching between moving the platform and moving the pivot point. However, it is not implemented, although it should be relatively quick to implement, where the calculation for the new transformation matrix is presented below. This functionality, more explicitly offsetting the origo in the y-direction, is necessary to simulate the ship motion accurately since the simulated origo must match. Nonetheless, this function is not critical in testing the vision-based tracking system but should be prioritized and implemented if enough time is available.

Another benefit is that the coordinate frame can be changed if a different coordinate frame is used for simulation. Furthermore, it can also be used for calibration by fine-tuning the rotation and translation of the pivot point to align it with the attached boat model coordinate frame. Further features would be to have a checkbox that toggles the display of the pivot point on and off.

$\boldsymbol{T}_p^b$: Transformation from base frame b to platform frame p

$\boldsymbol{T}_1^b$: Transformation from the base frame b to the pivot point frame 1

$\boldsymbol{T}_1^p$: Transformation from the platform frame p to the pivot point frame 1

The transformation $\boldsymbol{T}_p^b$ is currently used for calculation of the pose for the platform. This transformation can be kept after the pivot point functionality is added, but instead of controlling the platform, we will now control the pivot point. So in the updated program

$$\boldsymbol{T}_p^b = \boldsymbol{T}_1^b(\boldsymbol{T}_1^p)^{-1} = \boldsymbol{T}_p^b = \boldsymbol{T}_1^b\boldsymbol{T}_p^1 \tag{5.1}$$

This would also lay most of the groundwork needed to implement the other feature shown in the demo of PI's control system, namely to cast and rotate the entire coordinate system.

5.8.2 User preferences file

The created GUI has options such as changing the theme, shadows, show/disable labels, background, grid, and more. However, other options such as changing the stylesheet is currently not an option to do at run time.

A JSON file containing user preferences could be made, which is fetched at startup. This will enable the user to change the default settings, home position for the platform, calibration values for the platform, the default save/open directory, change style sheet, set a default demo to play, and more. This would be practical if the user finds himself changing the default settings at startup or multiple users with different preferences. However, this is not a problem with access to the source code and a single use case, but would be a practical functionality to implement in the future. JSON is typically suited for preference files, but other file types could also be considered.

5.8.3 Bluetooth Serial Communication

Currently, the platform is connected with a USB cable. This method was primarily chosen because it was implemented in the previous project and would reduce sources of errors during development. Nevertheless, a BlueTooth module was intended and will be a crucial future for having a handheld tablet for operating the platform. A simple app could also be made for use with a smartphone, where it would only have the demo features for loading and playing a text file, which would make the platform easy to operate, and accessible to everyone. However, there is currently no need for it.

5.8.4 Rotation axis dependant on view orientation

The 3D mouse gives an intuitive method for controlling the platform when the platform's view is in the same orientation as the mouse. However, when not using the standard view, it is challenging to comprehend how to move the mouse as it does not have the same orientation. A quick and easy fix is to rotate the physical 3D mouse equal amount to the view is rotated. Another option is to make the move commands from the 3D mouse be dependent upon the current view of the camera. This can be easily achieved as the orientation of the camera can be extracted, where the orientation about the y-axis needs to be taken into consideration. This feature should be implemented with a checkbox since it can be an unwanted behavior. For example, one might use the physical platform for reference and keep the simulator at a different view, and vice versa. Nevertheless, there is currently no desire for such a function. Besides, it is possible to look at the physical platform to make navigation more intuitive.

5.8.5 Log window

During the development, relevant information was printed to the console for debugging. In the deployed version of the GUI, no feedback other than the position

is given to the user, which was done to make the GUI more simplistic and clean. Moreover, as there currently is not much information that is not displayed needed by the user, it was decided to keep this functionality out. Even if it is unnecessary for the end-user, it can be beneficial for displaying information during debugging. It could also be hidden away as a separate window that could be opened through the menu bar, to keep the GUI minimalistic.

5.8.6 Screen attached to platform

As previously discussed, using a microcomputer with a screen attached to the platform was not desired. Nevertheless, a screen can be attached to the platform as a secondary control device or just for displaying general information. This could include the desired leg lengths and actual leg lengths, if the calibration routine was successful, poses sent from the GUI, etc. For navigation on the small screen, either a similar button and navigation system, as seen on the Prusa 3D printers, or a touch screen can be implemented.

This could be an acceptable option for testing the vision-based tracking software, as a lot of the functionality provided in the GUI is not needed when running these demos. Instead, a small selection of prerecorded demos can be recorded with the GUI and stored on the Arduino. The developed GUI would still be required to create the demo, where the leg lengths instead of the poses must be recorded. But once this is done, a standalone Host PC is not necessary to buy, and the decision can be left to future users, which can evaluate usefulness compared to price. It should be noted that this will likely require more work to complete, whereas the host PC suggested can be used as is, and could be expanded upon in the future with a 3D printed attachment.

Furthermore, the selection of one of the systems does not necessarily exclude the other. If it is never desired to run prerecorded demos from the Arduino, the screen can still function to display general information. Nevertheless, such information can always be sent to the GUI, so this does not necessarily add any value. If no value is seen in the mentioned cases, the screen can still act as a way to indicate whether or not the platform is turned on, by, for example, displaying an NTNU logo. Then again, this is a function that can be replaced with a simple LED light, or perhaps a large light strip that runs along the circumference of the bottom platform to match the aesthetics of the 3D mouse.

5.8.7 Bugs

Most of the testing of the program has been executed trough building the program in Qt Creator. However, with a final program deployed as an executable, a bug has been observed that otherwise is non-existent. This is related to manual control with the 3D mouse, where the axes remain disabled when disabling and then enabling axes in the properties menu of the 3D mouse.

5.8.8 Inserting 3D files

The ability to insert 3D files could be useful, but not necessary for this use case. A file dialog can be implemented, similar to what is used for the demo features, asking the user for the file path to the 3D file, and if desirable, a texture file. The files can then be placed relative to the top plate, and the option to control this relative position should be added. The orientation and placement for visualizing the insert file can be then be found by a composite transformation. Furthermore, the updateMeshPoses function must be updated, and a dynamic vector can be created to store the file paths.

5.8.9 GUI: Resolution and multiple screens

The program was written using a 4k display, and all features are not set to scale to match other screen resolution. Additionally, the splash screen covering up the main window while the program is loading does not detect which screen opened the software, so with multiple screens, they could be displayed at different screens. However, it is possible to detect the screen resolution and which window opened the program, so this should be easy to implement. Nevertheless, offering all this compatibility is time-consuming, but should be changed when a host PC is determined, and a different framework is used for the software.

5.8.10 Support for multiple systems

With Qt, the effort needed to make the software compatible with other operating systems such as Linux and MacOS could be minimal, as it provides several kits for deployment. With the current software, it is mainly the 3D mouse driver that needs to be reworked as it only supports 32 and 64-bit windows.

5.8.11 Sidebar

The minimum size of the GUI is now determined by the size of the buttons and functionality on the sidebar. When more functionalities are added to the software, a scrollable or hidable tab could prove beneficial since functionality can be added without increasing the GUI. The different groups could be hidable to make the sidebar more compact and readable, and with a scrolling feature. Additionally, the entire sidebar could be hidable for visualization only, or a fullscreen button can be added, which would make the visualization cover the entire screen. Furthermore, if a tablet device is used, the GUI should be designed with touch users in mind

5.8.12 Controlling platform with tablets IMU

This is a potential extra feature, which was inspired by a demo by Moog[50] where an iPad is used to control the Platform. This feature will provide less precise manual control than the 3D mouse, and would be most suited for the rotational movement. However, it could be used as a backup or as a showcase feature. It could

also be faster to implement than to create a handheld attachment, and switching from operating the Platform in a stationary manner to freehand would be faster.

5.8.13 Additional features to radial menu

The 3D mouse that will be used for controlling the platform has two buttons that features can be assigned to. Furthermore, it is possible to use radial menus with either four or eight different features, providing the possibility of a total of 16 features to be easily accessible, as of now, having this many features on quick access would likely not be beneficial. Instead, it might be best to assign one of the buttons to the most frequently used function, such as start and pause, while keeping the other button to open a radial menu.

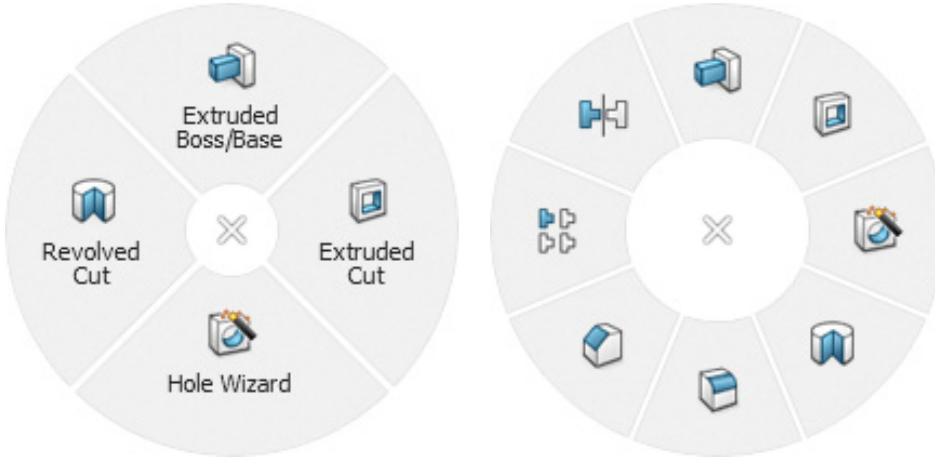

(a) (b)

Figure 5.15: 3Dconnexion radial menu

Chapter 6

Mechatronics

This chapter will present the mechatronics portion of the Stewart Platform. The PCB, Microcontroller, Actuators, Arduino Due, and the Arduino code has been reused from a previous project[51]. This was done to allow more focus to be directed towards improving the design and user interface. It should be noted that the pin assignment has been changed compared to what is described in the previous project, as it did not match the PCB. A summarization of the relevant parts from the project is presented in this section. Further information about the system can be found on Progressive Automations GitHub page[52], which contains the project rapport, code, PCB files, and more.

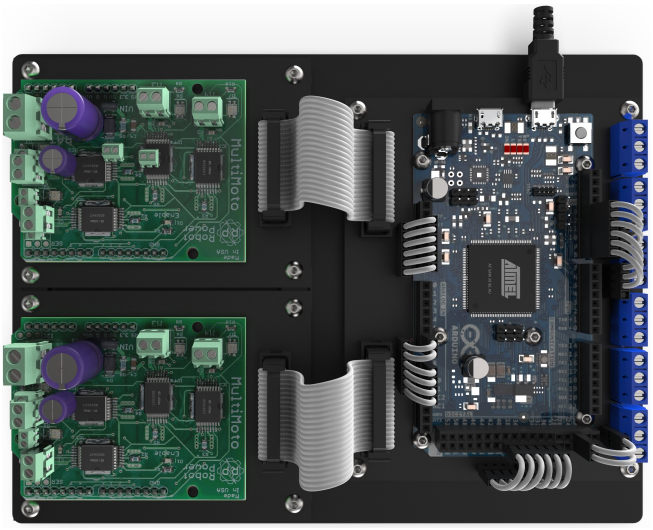

Figure 6.1: Rendering of motor controllers and Arduino Due assembly

The cables and parts that get soldered to the PCB were modeled in SolidWorks, as seen in Figure 6.1. This was done to make it as fast as possible for someone else to complete the project, as it was uncertain if it was possible to gain access to the workshop. Nevertheless, these details were not entirely completed as the school reopening was announced. Faster methods also exist for creating a good overview of the wiring diagram, such as the app found on circuit.io.

6.1 Arduino Due

The Arduino Due is a microcontroller based on the Atmel SAM3X8E ARM Cortex-M3 CPU, making it the first Arduino board based on a 32-bit ARM core microcontroller. The Arduino Due is programmed and used similarly to the other ATMega based Arduino boards. The Due also has the same footprint and pin layout as the Mega 2560 board. However, there are a few important differences and extensions that are relevant to this project. Further information can be found on Arduinos website[53].

- **Voltage:** The due runs at 3.3V. Connecting to higher voltages like the 5V commonly used will cause damage to the Due.
- **Serial ports:** The due have two USB ports available. The native port supports serial communication using the SerialUSB object and a Programming port, which is the default for uploading sketches and communicating with the Due.
- **ADC and PWM resolutions:** The Due resolution for analog read and write for ADC and PWM can be set to 12 bit, compared to the 10 and 8-bit, respectively, that the other boards use.

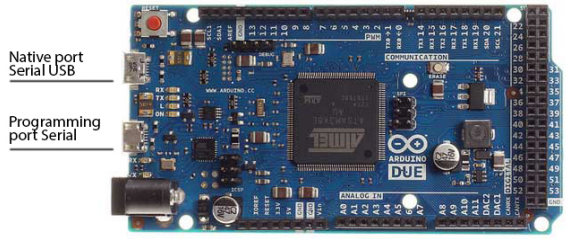

Figure 6.2: Arduino Due[54]

In the platform by progressive automation, the Arduino Mega was first used. After extensive effort to improve the Arduino code's performance, they swapped it out with the Due. The Arduino Due is the best offering from Arduino when it comes to large projects and performance, where it performed 7.6 times better than the Mega according to this benchmark[55].

6.2 Linear Actuators

The PA-14P linear actuator by Progressive Automations, seen in Figure 6.3, was chosen for the project. Elaboration for the choice is explained in Section 4.1.2, and details and datasheet for the actuator can be found in the Appendix. A 3D model was available for the actuators but with a low amount of detail. The model was modified in SolidWorks, where cables, screws, and other missing details were added. A feedback system was necessary to control the actuators' position and speed. Three main options are available: Potentiometer, Hall sensor, and Optical sensor feedback. The following description of the feedback sensors is based on a blog post by Frigelli Automations[56] and further supplemented with information from various sources.

Figure 6.3: Progressive automation feedback actuator PA-14P-4-35[25]

6.2.1 Potentiometer feedback

A potentiometer is a resistor with three terminals where one of the contacts can be adjusted. When adjusting the contact, the length is changed, which effectively increases or decreases the resistance. The resulting configuration is essentially an adjustable voltage divider, where the measured voltage is dependent on the position of the adjustable connector, which allows the distance to be measured.

Advantages

Potentiometers are relatively stable and do not require a homing cycle. Furthermore, the feedback is directly related to the position, so losing power or memory will not affect the control cycle. Additionally, a potentiometer can be added separately, since it does not have to be built into the system.

Disadvantages

The feedback signal can become erratic since the resistive material can wear out over time. The feedback signal is also greatly affected by electrical noise, causing

inaccurate position readings. Furthermore, the potentiometer's repeatability is low, which results in different readings for the same potentiometer type.

Another major disadvantage is that linear actuators have a limited stroke length. Typically they are equipped with a rotary potentiometer, with a max number of turns before maxing out. However, linear potentiometers can be used, which does not impose limitations for the stroke length. Nevertheless, the signal gets worse the longer the stroke length, due to instability of the resistive element. Thus, potentiometers are limited to shorter stroke lengths.

6.2.2 Hall sensor feedback

In a hall effect sensor, a magnetic trigger wheel is installed inside the gearbox of the actuator. Figure 6.4 shows a trigger wheel and a sensor. The trigger wheel is placed close to a sensor, such that every time a tooth passes it, the surrounding magnetic field will cause the sensor's output to be either high or low. This will produce a square wave signal, which can be used to calculate the RPM, which again can be used to calculate the length of the actuators. The Hall sensor comes in two options; directional and non-directional.

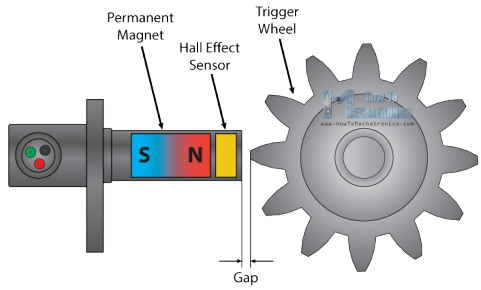

Figure 6.4: Hall effect sensor[57]

Advantages

The stable square wave signal makes the Hall effect sensor reliable, with good repeatability and accurate position control.

Disadvantages

Since the Hall sensor only produces a signal as the magnetic trigger wheel is rotated, the sensor needs to perform a homing cycle such that a relative position can be calculated. This is typically performed by fully retracting the actuators and then fully extending it while counting the number of the pulses. The number of pulses can be mapped to the stroke length, and then a relative position can be calculated as new pulses are registered.

6.2.3 Optical sensor feedback

The optical sensor feedback works similarly to a hall effect sensor, but instead of a magnetic trigger wheel, a small flat disc with holes or slits is used instead. A led shines toward a Photosensor, and will either pass through the holes or be blocked by the disc, as seen in Figure 6.5. This produced a square wave signal which can be used to calculate the actuator's length.

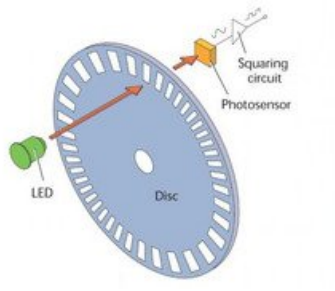

Figure 6.5: Optical Sensor Feedback

Advantages

The optical disc can be manufactured with many more holes than a hall effect sensor can have teeth, which means that more pulses are registered per rotation, which results in a higher resolution. Thus the optical sensor is more reliable, offers better repeatability and position control.

Disadvantages

Like the hall effect sensor, the optical sensor also has to complete a homing cycle to calculate a relative position. Additionally, the control device will have to be faster to account for the increased number of pulses. Lastly, optical sensors that are typically used do not know the direction, and one would have to program polarity direction as part of the system. The direction can be determined based on the polarity of the positive and negative actuator wires.

6.3 H-bridge Motor controller

A motor controller is needed since the rated current and voltage for the actuators exceeds the Arduino capabilities. The selection is based upon the previous project decision, where two microcontrollers with four channels each are used, enabling full speed control with PWM and direction control. Three actuators are connected to each motor controller, leaving two leftover channels that can be used in case any of them fail. The controller can take an input voltage ranging from 3-36v, and where each channel is rated 6.5A continuous and 8A peak, which is sufficient for the 12v 5A actuators selected.

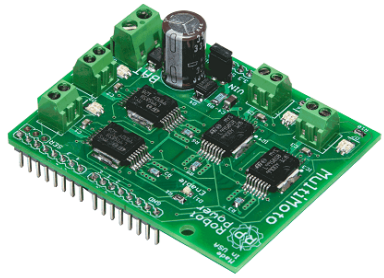

Figure 6.6: Motor controller: MultiMoto Arduino Shield LC-82[58]

6.4 Power supply

Each actuator is rated to draw 5A of current at max load. With six actuators, at least 30A is needed. The power supply seen in Figure 6.7 was chosen. As all the actuators are not intended to be running at max capacity, this option was ok. Although, it would not leave any room for upgrading or adding components to the platform, and could cause problems at near max capacity depending on the quality of the power supply. 3D model for the power supply was not available, so a model was made in Solidworks mainly for visualization and for making dependent parts.

Figure 6.7: Mean Well 360W, 12V, 30A Power Supply[59]

6.5 IMU

A 6-axis IMU is a sensor composed of a 3-axis accelerometer and a 3-axis gyroscope, enabling translation and rotational movement to be measured across the x, y, and z-axes. There is also a possibility of a 9-axis IMU with a 3-axis magnetometer added, which as the name suggests, measures magnetic fields. Further information on the IMU can be found on CEVA's Experts blog[60],

Figure 6.8: Cross domain development kit[61]

To measure the actual pose of the Platform, an IMU can be placed underneath the top plate. To keep things clean, the IMU should be wireless. Some options were explored, but the Platform's end users have bought several of the IMU units seen in Figure 6.8, which will not only be used for the Platform. This unit is a fully integrated hardware and software development kit, with a 9-axis IMU and sensors for pressure, temperature, humidity, acoustic, and light. This was selected since software can be developed independently for the unit, enabling it to be used on several projects and robots. The kit comes with an API for quick and easy development. It can also be connected to wirelessly trough BlueTooth or WiFi. This is a good temporary solution, but cheaper options could be used as the kit offers more functionality than needed. Furthermore, higher accuracy IMU exists. Selection and integration of the IMU have not been performed, where this task will be left to the user to determine based on precision, cost, and development time. To achieve accurate placement of the IMU relative to the top plate, a precisely manufactured slot can be machined, similar to what is used for the angled brackets. However, it is uncertain if this is needed. Research has been conducted on the importance of IMU placement, but this has not been investigated thoroughly. Furthermore, for this specific use case, it might be beneficial to place the IMU on the model boat instead.

6.5.1 Importance of an IMU

If the developed Stewart Platform were able to position itself precisely relative to the simulator, an IMU would not have been necessary. As will be presented in

Chapter 7, the designed Platform with the current actuators leaves much room for improvement. Having accurate information on the ground truth position is desired to achieve more certainty of the vision-based tracking software's performance. With an IMU, it can be possible to achieve accurate ground truth data, even with low accuracy and precision of the produced Stewart Platform. Thus, with an IMU implemented, substantial cost savings can be achieved, and a platform with lower precision can be produced. Moreover, it should be noted that there will be deviations of the simulated ship motion compared to what is planned, but this will not impact the testing and validation of the tracking software since only ground truth data is needed.

6.6 Printed Circut Boards

The PCB files were found on the Progressive Automation's GitHub[52], and an order was placed on PCBWay. There are three PCBs, where each is designed to mate with their respective Arduino/Multimoto boards and is connected with a 20-pin ribbon cable, which was done to maximize modularity. Each Multimoto board had a maximum of four channels, so two were needed. This left two extra channels, where support was added such that all four channels could be used if one would become faulty. The potentiometer headers on the PCB are preceded by a low-pass filter with a $10nF$ SMD capacitors in parallel with the $10k\omega$ potentiometers resistance, as seen in the schematics in Figure 9.9 in the Appendix. This was done to reduce noise in the readings, which showed improvements in signal clarity when measuring with the oscilloscope. However, it was not determined if this would be the optimal value across all actuators, and the capacitance should also be retested and fitted for the new platform. Similar parts that could be used with the PCB were found in Norwegian resellers, and were hand soldered to the PCB. A complete list of parts and article numbers and further details of the electronics layouts and schematics can be found in the Appendix.

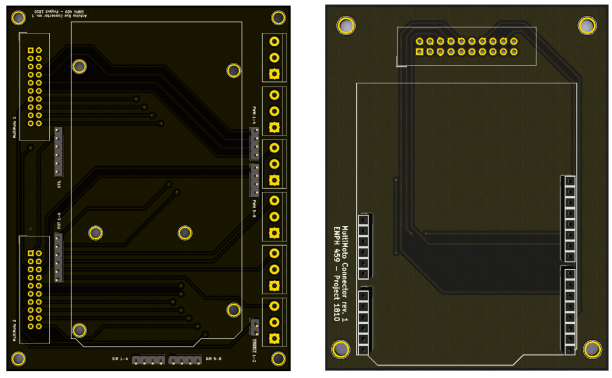

(a) (b)

Figure 6.9: PCB for the motor controller and the Arduino Due

6.7 System Overview

The actuators are controlled via the Arduino Due microcontroller. In the GUI, lengths for each of the actuators are calculated and mapped to a value ranging from 0-1023. A string containing these mapped lengths is sent to the Arduino over a USB serial connection, where a PID feedback system is used to move the actuators to the desired position, using the potentiometers reading as input.

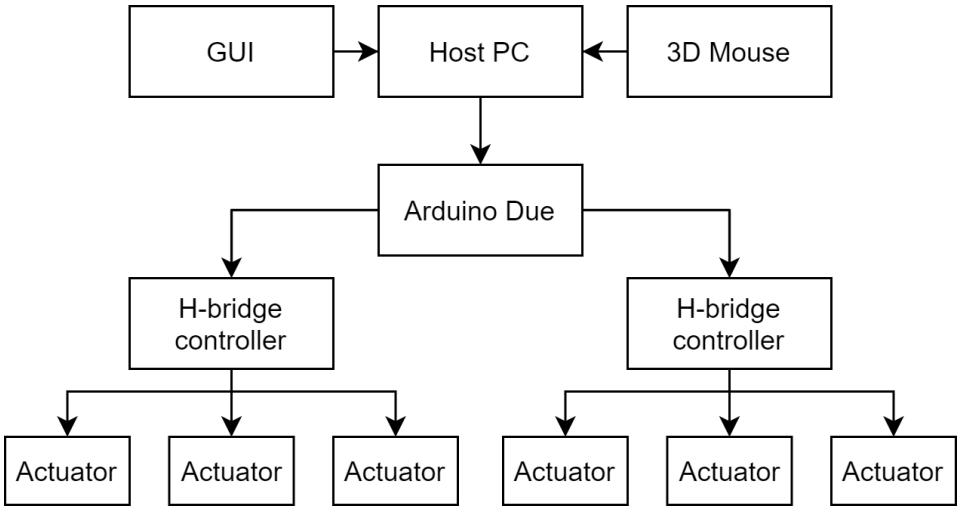

Figure 6.10: System-level diagram for the platform

Theoretically, the measured value from the potentiometer should be in the range of 0-1023, although the actual readings ranged from 50-650. The platform performs a calibration routine at startup to account for this. Here averaged readings are taken at maximum extension and retraction. With known max and min position for the potentiometer readings, the received values get mapped to the calibrated values. If the calibration fails or the readings are significantly different from what is expected - such as when the motor controllers are not powered after reset, a set of default values are used based on previous readings. The calibration routine is performed every time the platform is powered on to account for a potential shift in readings that can happen over time, which is acceptable since the calibration is relatively brief at less than ten seconds.

Figure 6.11 shows the flow diagram for the Arduino Due. When the program starts, it first waits to see if a serial connection to the host is made. Then it initializes the pin outputs and performs the calibration routine before it enters an infinite loop to move the actuators to the last set position.

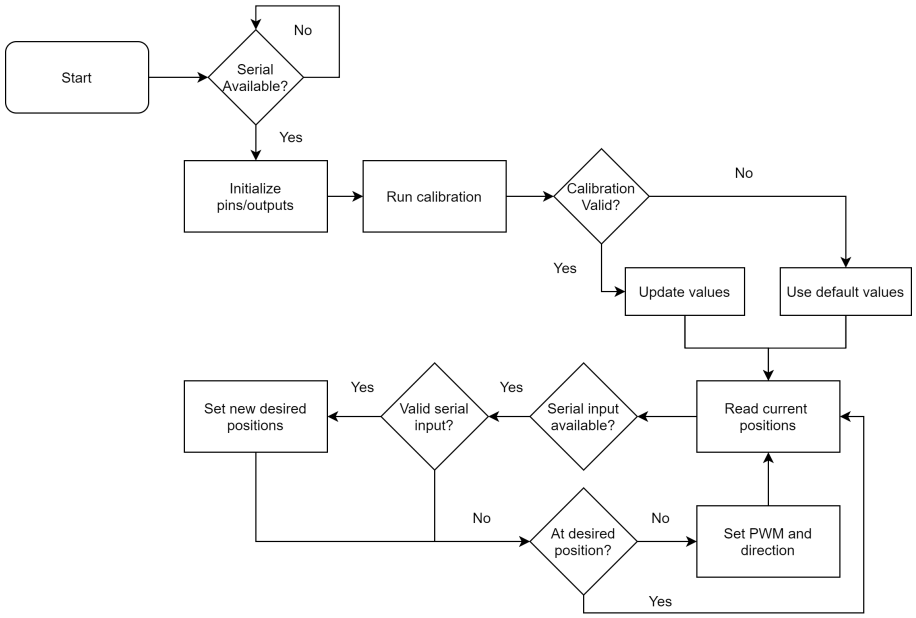

Figure 6.11: Flow diagram for the Arduino Due

6.8 Suggested improvements

Although the current PID values worked great, it can not be reasoned that these values would be optimal for the new Platform, so the values should be re-tuned.

The Arduino code has not been extensively examined and likely has many areas that could be improved. Instead, the time was focused on other aspects of the Platform. Nevertheless, immediate observations show that the actuators have varying speeds, which are currently not fully accounted for in the Arduino code. This is most easily observed during the calibration routine, where all the actuators do not extend fully at the same time. With the frequent position updates, this is not a big problem. Additionally, the stroke lengths are not exact, as discussed in Chapter 7, so the mapping results in slightly wrong positions, which should be accounted for.

6.8.1 Signal clarity

The potentiometer readings were measured to range from approximately 50 to 650, with some variations between them. The readings were also quite noisy when placed in a steady position, which falls in line with what mentioned about the disadvantages of the potentiometer feedback. An average of 255 readings is measured for a single position, where the observed range was ten units. The code has a threshold for when the PID regulator accepts the position, where this was set to four units in the previous project. This indicates that improvements are possible.

Ten units equate to roughly 2.5mm when a range of 600 units is mapped to a stroke length of 150mm. Although the actuators could theoretically keep moving 2.5mm in and out, the observed platform is quite stable, and any movement has not been observed with the naked eye. This might be due to the fast change in readings and the relatively slow response from the PID regulator; nevertheless, a high pitched sound is formed since the actuators are continuously adjusting. The threshold at which the PID regulator keeps adjusting can be increased to eliminate the sound. However, this could result in a loss in precision for the actuators. Instead, it would be better to minimize signal noise. Options that can be tested are shielded cables/tape, increasing distance from the power supply and motor controller, and using a different rated capacitor for the low pass filter—Alternatively switching to an optical or hall effect feedback.

ADC resolution

The Arduino code currently uses 10-bit for the potentiometer readings. However, as mentioned, the Arduino Due is capable of both 12bit ADC and PWM resolution. This will increase the range to 0-4095, which the lengths can be mapped to, which can give four times as high resolution. However, there will be questionable benefits from increasing the resolution with the current signal noise, thus, not currently implemented. However, it is quick to change, as the only the analogRead() function must be replaced with analogReadResolution().

6.8.2 Vertial stacking

A new motor controller with six or more channels, preferably a shield that can be stacked vertically on top of the Arduino due, is desired to maximize available space within the enclosure. This is illustrated in Figure 6.12. With more space, there will be more room for airflow for the power supply and might reduce interference with increased distance between the power supply and the Arduino. This also enables shorter wires to be used, which could further improve signal quality and result in a cleaner setup. If a motor controller is found, but does not fit the Arduino due as a shield, then a PCB can be designed as a shield for the Due, with the new motor controller attached to it.

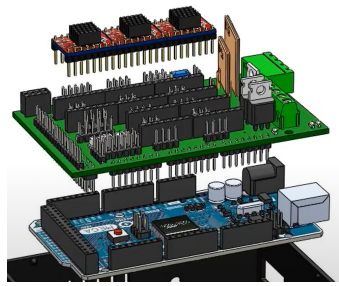

Figure 6.12: Vertical stacking of motor controller[62]

Pre-manufactured board

An alternative to vertical stacking is to order a pre-manufactured board from the actuators vendor, which could be faster and better to implement than reducing the size by vertical stacking, adjusting the low pass filter, improving cable management, and achieving a clean setup. With the mechatronics' current complexity, where the only job is to move the actuators to a given position, it could be acceptable. Nevertheless, one would have less control of the system and would leave fewer possibilities to expand it. However, it could still be combined with an external microcontroller, which will probably be needed, as a suitable control board is yet not found. Furthermore, new actuators would most likely be needed if one is found, as the control boards are made to a set range of actuators.

6.8.3 Power supply

There were not many power supplies to choose from, available at Norwegian resellers. However, as will be discussed, a more compact and flat power supply is desired in order to make the height of the enclosure smaller. Although this is dependent on some of the other space-saving methods are implemented. Furthermore, a higher wattage power supply could be considered, which will allow additions to be made to the Platform.

Heat dissipation

There might be some concerns about heat accumulation within the enclosure. For heat dissipation, 10cm on the four sides around the power supply, and 5cm on the ventilation side should be kept, according to the datasheet found in the Appendix. This was not achieved with the current size of the enclosure. Additionally, the power supply is not mounted in an upright position, as instructed in the datasheet, although this is mainly to avoid rain. Based on results from the Progressive Automation report, their platform worked well with a load of 6%. Nevertheless, with a newly designed platform, another power supply with less space between components and operations at a higher load of approximately 15% of total capacity, this might be a problem.

The derating curve for the power supply shows that the power supply can deliver 100% of its rated power up to an ambient temperature of 35 degrees Celcius. At the max ambient temperature of 60 degrees Celcius the delivered power is reduced to 50%. A fan is added to the design to improve airflow, and initial testing without it shows no signs of problems, however, this has yet to be adequately tested. Moreover, more space can be gained for the power supply by, for example, vertical stacking. The sides of the enclosure facing the power supply could also be trimmed to give more breathing room. Lastly, additional fans can be added to the sides of the bottom cover to create a push and pull configuration, which will greatly improve the airflow. If it turns out to be a problem, a temporary solution is to slide out the enclosure from under the plate, flip it around, and reconnected to give more breathing room.

Chapter 7

Results

This chapter will present the developed Platform. It will also include the calibration procedure planned for the Platform, all of which have not been performed due to available time. Additional pictures, videos, and project files are attached to the delivery, which is also accessible on my GitHub repository[63].

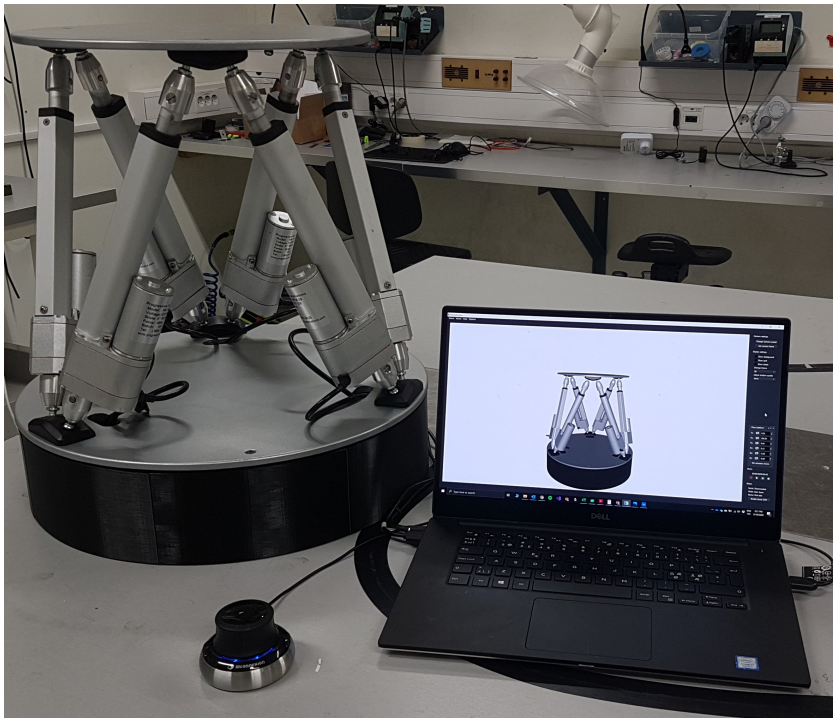

Figure 7.1: Produced platform

7.1 Model ship

Figure 7.4 shows the developed platform with a boat model attached. This is a handmade downscaled version of the Bourbon Orca by SavyBoat[64]. An accurate 3D model[65] of this ship was also found. The 3D model could be imported to the GUI visualization with a function described in Section 5.8.8, or it could be implemented directly in the program. However, this functionality was not important for the end-user. Nevertheless, other tracking methods rely on a 3D object, and this model can be considered if needed.

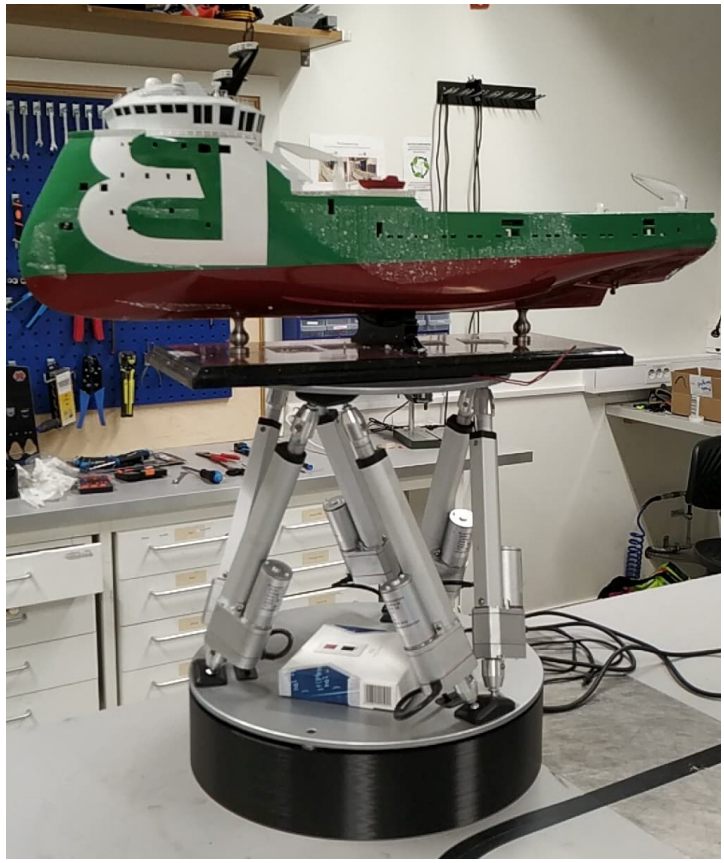

Figure 7.2: Produced platform with ship model attached

The model is quite large compared to the platform and weighs approximately 10 kg. Although looking slightly odd, the size is not an issue, and the weight is well within the platform's capabilities. The model is temporarily secured. However, an intermediate plate should be manufactured once the quick release mechanism arrives. The model has two supports that can be used for attachment to the intermediate plate.

7.2 Electronics enclosure

Figure 7.3 shows the electronics enclosure from the early testing of the actuators, which uses the prototype version, laser cut from wood. The MDF material is 2mm thicker than what was used for the design. This, combined with the fact that the cables could not be folded as close to the plate as desired, caused a slight interference, making it difficult to insert. This can easily be fixed by making the height 3-5mm shorter. Furthermore, as previously mentioned, the power inlet had to be replaced, which was 20-30mm deeper, leaving barely enough space for the power supply. There is not much room left over for the inside width since it is restricted by the dimension between the feet, which was the motivation for implementing vertical stacking, as described in Section 6.12, and other methods for increasing available space in the enclosure was discussed in Section 4.12.6. The front part of the electronics enclosure was redesigned as presented in Section 4.12.6, which gives a little more room inside the enclosure and a much better overall design also suited for other manufacturing methods.

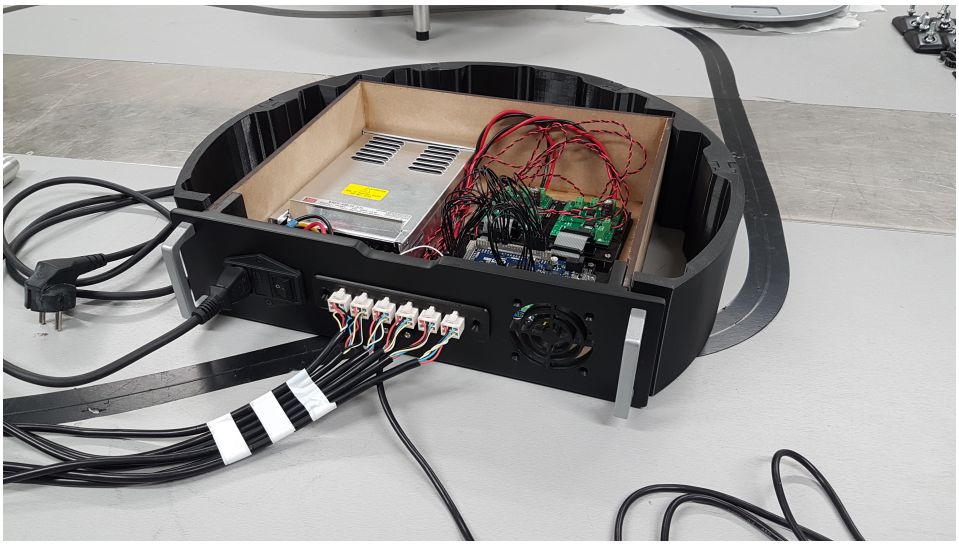

Figure 7.3: Picture of electronics enclosure from early testing

The figure shows the bottom cover, which has been split into five parts that are pressed together. This was later printed as a single piece with a larger 3D printer, and the thicker portions where the parts are pressed together could be removed.

7.3 Plates

Due to availability, 8mm carbon Steel was used for the plates instead of the intended 7mm aluminum, which increased the top and bottom plate weight from 1.8/2.8kg to 5.8/9.5 kg, respectively. This was acceptable for the bottom plate, and might even provide additional stability. For the top plate, 4,2% of load capacity is lost. Nevertheless, the platform is currently loaded at approximately 15% of max capacity. Additionally, both a topology optimized shape and quick release mechanism were under development, where the weight of the top plate is expected to be halved. So these changes were accepted, as it is intended to be replaced.

Figure 7.4: Produced top and bottom plates with brackets attached

As for the surface finish, the plates were painted instead of brushed due to the change in material. This gave an acceptable result, but upon closer inspection, one can observe particles attached to the plate due to having to paint outside. One could consider using vinyl wrap where any appearance would be possible to obtain, and it will also be easier to obtain an excellent finish with the equipment available. A good brushed finish is also easier to obtain, where several DIY procedures can be found on YouTube. A layer of clear coat can be applied afterward, and with a brushed finish, any scratches and marks would be less noticeable.

7.4 Joint friction

Since the ordered spherical joints are produced with such a wide tolerance, some of the ordered joints had much friction, which is to be expected of such low-cost joints. When mounted in the housing, some of them would freely rotate, influenced only by its gravity. The worst required approximately 1 kg of force to rotate, which was tested by hanging items of known weight from the joint. Due to this friction, some load capacity is lost as the actuators have to apply extra force. Since some of the joints worked smoothly, one could try ordering a larger batch and select the ones with the least friction, which will not require any redesign.

7.5 Surface finish

Figure 7.5 shows a closeup of the produced bracket and grommet. Of the 3D printed parts, only the front part of the electronics enclosure and the brackets have been sanded and painted. These were done mostly as an experiment to test what surface finish is to be expected. With planned changes to nearly all the parts, other aspects were prioritized. However, this procedure is explained in Section 4.11.3, and can easily be done by anyone without any experience.

Figure 7.5: Closeup of produced bracket and grommet

7.6 Actuator Backlash

The actuators consist of a lead screw used to extend and retract the shaft, which can be subjected to backlash. The appendix contains the actuators' datasheet, which gives insight into the actuator's internal components. With the used actuators, the backlash ranged from 0.05mm to 0.2mm. Since the actuators are in compression, this effect will not be as noticeable. However, it indicates the actuators' precision, as the backlash must be surpassed before the direction can be reversed.

7.7 Cable management

It was planned to cut the original cables from the actuators down to size. Thirty new crimp terminals must then be attached, which were performed for the female end for the Molex connectors, and can be a tedious process. When trimming, there should be some leftover length such that a slightly larger base can be used. Additionally, some extra length will be needed if the new design for the platform feet is implemented since the enclosure will be rotated 120 degrees. However,

trimming the cables could make each of the individual cables shorter, which would enable a cleaner look. Combining this with a 3D printed clip, as shown in the concepts, a cleaner look for a final product can be achieved. A temporary solution is shown in the figures below.

(a) (b)

Figure 7.6: Actuators Cable management

7.8 Calibration

The following section will present some of the calibration and measurements performed. a functionality similar to what is described in Section 5.8.1 should be implemented to compensate for the innacuracies from manufacturing by rotating and translating the Platform to zero it out. The calibration values can be implemented in the preference file, described in Section 5.8.2, such that the GUI will display zero across all values for when using the pivot point feature.

7.8.1 Calibration of actuator lengths

All the actuators assemblies should be of equal length, to get a motion that corresponds to the simulated one. Lengths based on the 3D model can be seen in Figure 7.7, where the 371.96mm value in the retracted position and 521.96mm value corresponds to the length between the two spherical joints rotation point, which is the values used for the leg lengths in the simulation.

The following measurement was performed with a large digital vernier caliper, and a depth micrometer as this was readily available in the workshop. The accuracy of the micrometer and caliper was not verified with a gauge block, and in-depth calculation for the uncertainties in the following measurement will not be performed. These were the initial measurements done, which gave a basic understanding of the leg lengths and accuracy expected from the Platform. More precise measurements should be performed when the suggested improvements are implemented, and more precise equipment is available, to avoid rework.

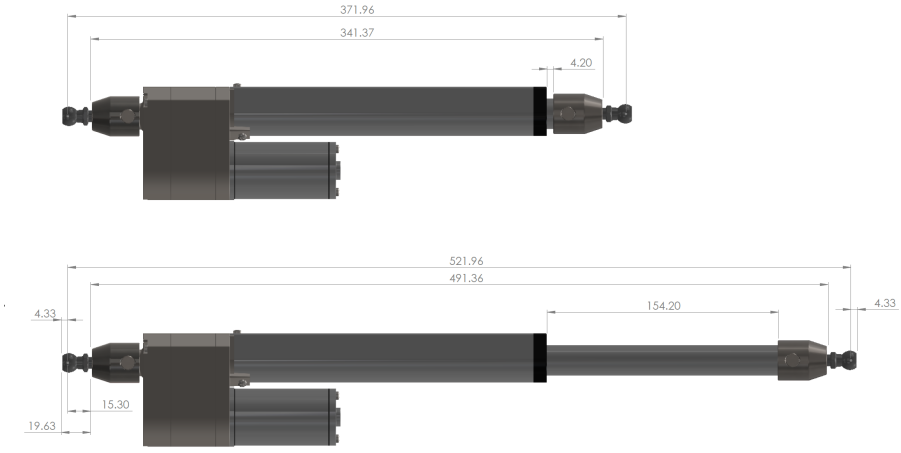

Figure 7.7: Actuator assembly: lengths used for calibration

7.8.2 Retracted and extended lengths

The measurement was done in two steps since the length of interest falls within the spherical ball. First, the lengths between the upper and lower bushing were measured fully extended and retracted. Then the distance from the bushings face to the flat portion of the spherical joint was measured. With these measurements, a distance to the point of rotation can be calculated, and combining it with the first measurement, gave the results presented in the tables below. A more accurate measurement could be achieved by measuring the distance with the spherical joints attached.

MAX						
Actuator	1	2	3	4	5	6
Theoretical length mm	491.36	491.36	491.36	491.36	491.36	491.36
Measured length mm	489.04	489.47	489.15	488.98	489.49	489.17
Avg length			**489.21**			
Range			**0.52**			

Table 7.1: Measurements of the actuators fully extended

Furthermore, the calculated measurement relies on the tolerance of the spherical joint. More advanced equipment is necessary to measure that distance. Even then, it still would be almost as challenging and time-consuming as re-manufacturing the spherical joints oneself, where it could be possible to rely on the precision on the lathe. The datasheet for the spherical joint, which can be found in the appendix, does not contain the tolerance for the length measured. However, a related tolerance is at $\pm 0.2mm$, which indicates the uncertainty expected from the measurements. That being said, some of the uncertainty is accounted for in the measurement.

MIN						
Actuator	1	2	3	4	5	6
Theoretical length mm	341.36	341.36	341.36	341.36	341.36	341.36
Measured length mm	337.53	337.74	337.88	337.44	338.04	337.69
Avg length			**337.72**			
Range			**0.615**			

Table 7.2: Measurements of the actuators fully retracted

The results show a systematic difference between the lengths extracted from the 3D model and the measurements. This can easily be compensated for in the 3D model, by changing the limit mate, such that the 4.2mm and 154.20mm measurement seen in Figure 7.7 match the measured values. The range in the values is of more interest, where it was planned to manufacture washers to compensate for the differences, by placing them between the bushings and the spherical joints.

7.8.3 Measured Stroke Length

An average stroke length was found to 151.49mm, which is 1.49mm more than specified. The higher stroke length and variation must be accounted for in the software to achieve a more accurate simulation. So the longer stroke lengths must be limited and mapped differently to the (0-1023) range used in the Arduino code. Any changes to the 3D models are not necessary with how they are modeled, and how origins are placed.

Calculated Stroke Length						
Actuator	1	2	3	4	5	6
Stroke Length mm	151.52	151.73	151.27	151.54	151.44	151.475
Average Stroke Length			**151.49**			
Range			**0.46**			

Table 7.3: Calculated stroke lengths for the actuators

7.8.4 Feedback Measurements

When measuring the maximum and minimum lengths, the actuators are at its limit and will not be influenced by PID regulation's precision. Thus, accurate measurement for the stroke length is achieved by looking at the difference in the values. The middle position measurement is done to evaluate the precision of the feedback system. Here the position is set to half of the potentiometer range, where the theoretical values correspond to the middle of the measured maximum and minimum lengths. Since the potentiometer readings are mapped to values between approximately 50-650 units, one unit would correspond to a length of 0.25mm, which would theoretically be the highest possible precision that can be achieved. If the potentiometer had spanned the full range from 0-1023, this would have been reduced to 0.15mm. This could be reduced further by using 12-bit resolution for the ADC, but the signal clarity has to be improved before these changes would be beneficial. The observed range is 0.55mm, which is far better than what was expected based on the noisy readings mentioned in Section 6.8.1, where the readings spanned ten units. Nevertheless, these were the average of two measurements, and several more should be performed to get more accurate information by calculating the uncertainty of these measurements.

Middle						
Actuator	1	2	3	4	5	6
PWM (0-1023)	512	512	512	512	512	512
Theoretical length mm	413.28	413.60	413.51	413.21	413.77	413.43
Measured length mm	413.47	413.71	413.23	413.17	413.42	413.29
Deviation	**0.19**	**0.11**	**-0.29**	**0.04**	**-0.36**	**-0.15**
Range			**0.55**			

Table 7.4: Measurement of actuators at middle position

Summarized Measurements	
Avg. Length: Max	489.21
Avg. Length: Min	337.72
Avg. Length: Stroke	151.49
Avg. Range: Max	0.52
Avg. Range: Min	0.62
Avg. Range: Stroke	0.46
Avg. Range: Middle	0.55

Table 7.5: Summarized measurements for the actuators

7.8.5 Calibration with CMM

Will not go into great detail of how a detailed calibration routine can be performed; instead, the readers are referred to standard calibration routines ISO-230 for machine testing. The standard is split into several parts, and have standardized methods that could be applicable to test the repeatability, speed, and accuracy of the Platform. Furthermore, the professor in charge of the CMM should be consulted. With much more experience, he could offer valuable insight into the specifics for the calibration.

Before the CMM is used, the quick fasteners method mentioned in Section 4.12.1 should be implemented. With it, an intermediate plate should be manufactured with three flat planes such that the orientation of the top plate can be found compared to the bottom plate. The calibrated values will then be for the attached intermediate plate, which would be relative to the fastener holes, and would then be the same for all attached loads. The suggested quick-release fasteners had a repeatability of 0.01mm, which would be very precise, compared to the other sources of errors. Additionally, the whole Platform would not have to be recalibrated if a new load is used; instead, the load could be calibrated relative to the intermediate plate.

With three planes on the intermediate plate, it would be possible to find the orientation relative to the bottom plate. This can be measured with an interferometer or similar device, which will give a highly accurate reading. Furthermore, precise locations for the position of the base points and platform points can be measured independently.

Given the measured pose, forward kinematics can be calculated to find a corresponding set of leg lengths that will take into account the inaccuracies of the angeled brackets. New washers with these measurements can be manufactured to get a better starting point for the calibration. The measurements can be performed again, which now should be more precise. Lastly, the errors which can not be resolved by manufacturing spacers or improving manufacturing precision can be accounted for with the move pivot point feature.

7.8.6 Measured range of motion

The joints have a maximum pivot angle of 25 Degrees; however, with the current configuration, higher angles are possible to achieve. Setting an accurate limit for the joints would require the angle between the bracket's face and the actuator's length axis to be calculated. Experiments were performed to check if the joints would naturally limit themselves by stopping further movements when the maximum angle is achieved. Where only the rotation about the y-axis was restricted to avoid collisions between the actuators. After several tests, it seemed that the platform would naturally stop when reaching max angles. However, it was later observed that the joints left marks on the bushing house, and two weeks after the first test, one of the joints popped out when showcasing the platform.

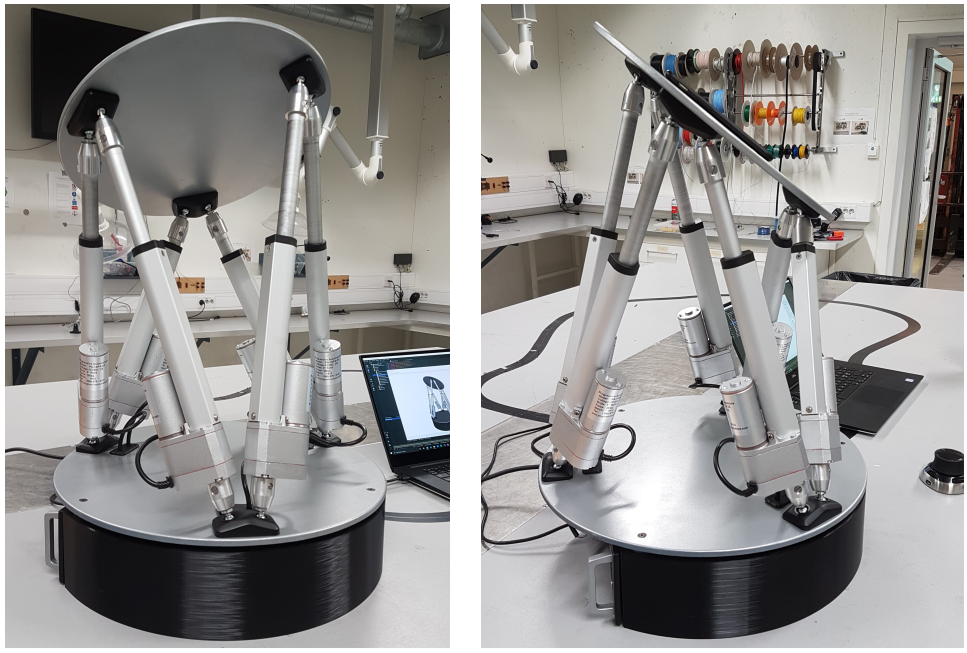

(a) (b)

Figure 7.8: Platform in combined rotation

Thus further limitations have to be set, which was accomplished by setting the platforms max angle about the x and z-axis to 25 degrees. This will not give an accurate limit for the joints since depending upon the platform's position, the angle of the joints themself will be different. However, since 25 degrees or less is sufficient for the current use case, accurate calculations of the joint angle have not been performed. Additionally, by rotating the boat relative to the platforms coordinate frame, angles as high as 36 degrees are possible because of combined rotation. Moreover, one should consider ordering universal joints to increase the

range of motion instead.

A quick method for measuring the range of motion was done with an app on a smartphone to get a general idea of the platform's capabilities. The phone was placed on top of the platform and zeroed out. At maximum, minimum, and intermediate position, no change in the angle was observed, although some deviation was expected due to the different leg and stroke lengths. However, the accuracy of this measuring method is questionable, where the resolutions were 0.2 degrees. Figure 7.8 shows the platform at a combined rotation close to what is max achievable, measured to 36.6 degrees. Measurement of a single axis rotation of 25 degrees was performed to test the accuracy, measured to an angle of 24.6. The measurement is within the uncertainty range but indicates a slight difference between theoretical and actual pose, which is expected.

7.9 Price

The Appendix contains a list of all the components ordered for the project. In total, close to 16.000 NOK have been used on this project, including the cost for 3D printing filament, paint, glue, and several spare parts left over due to order quantity. The manufacturing cost is not included in this price as it was performed internally. However, a price estimate from an external manufacturing company, Stryvo A/S, is attached in the Appendix, quoted at 12.040 NOK, which gives a good estimation of the expected cost. Compared to the cheapest and most comparable commercially available platforms by Acrome, a significant cost saving has been achieved. They had two versions quoted at 5200€ and 8000€, excluding shipping and taxes, where the later would be the more comparable Platform.

Furthermore, the back portion of the electronics can be laser cut from MDF without sacrificing the Platform's performance, which will save an estimated 1520 NOK. Further price reduction is possible by replacing the parts with 3D printed and laser cut wood, although this will sacrifice capacity and accuracy. Nevertheless, extensive work has been put into the development of the Platform. If this time were accounted for, the development cost would exceed the price of Acrome's Platform many times over.

7.10 Manufacturing tolerances

Generous tolerances were set for the production for ease of manufacturing and to ensure parts would fit. Furthermore, new design/ideas will be found, and high accuracy was not that important if an IMU is used. The parts could be manufactured with higher precision to achieve a motion that is true to the simulation, which can be considered for future use cases. However, with the current actuators, it is questionable if it is worth it.

Certain tolerances do not have to be set that high either since, for some dimensions, it is more important that all parts are produced equally, which is more obtainable

when producing it with CNC machines. Furthermore, as discussed, some manufacturing errors can be calibrated away. However, the tolerances that should be considered changed is the bore for the actuator bushings, to center them better on the actuators. The pin can also be changed, which will make it easier to manufacture and eliminate backlash in the bushings if made with a press fit tolerance. This would require a custom Ø6.4 drill and reamer to be ordered. Lastly, the slot for the angled brackets can be made more precise. However, with a 3D printed bracket, there is a limit in how precise this can be placed, and one should consider milling this part instead.

Chapter 8

Discussion

The objective was to develop a mechanism to simulate ship motions, which would be used to test and validate a vision-based system. A Stewart platform was selected for the mechanism, and it was decided that the Platform would be made instead of bought, mainly to reduce cost. Thus the design, GUI, inverse kinematics, and mechatronic system had to be implemented. Furthermore, several platforms have been explored during the development process, and if necessary, a more informed decision can be made before one is bought.

Accurate simulations of ship motion are not necessary to test and validate the tracking software. Thus it was concluded that as long as accurate ground truth data is available for the Platform pose, the produced Platform would be sufficient. The ground truth data could be gathered in one of two ways. Either by using the poses used for controlling the Platform, or through an IMU. If the poses sent from the Platform were to be used, then there will be inaccuracies due to the actuators' precision and the manufacturing errors. The manufacturing errors can be reduced and calibrated away. However, the resolution, backlash, and inaccuracies from the used actuators would remain. Thus more precise actuators would be required, such as hall effect or optical sensor feedback, which will increase the cost. The bushings were designed, such that the actuators could easily be replaced, only requiring dimension change and not change to the overall design. Nevertheless, as stated several times, for this specific application, an IMU is an easier and cheaper method for gathering ground truth data.

There remains some work before the Platform can be used to test the tracking software, namely the implementation of the IMU and generation of ship motions. Both of these have been explored; however, the end-user would take responsibility for implementing them. Demo features have been implemented in the GUI, which will enable playback of motions, although the generated motions must be in the format described. Another key feature for more accurate ship motions, is the move pivot point feature, as discussed in Section 5.8.1, which is yet to be developed.

However, once a minimum viable working platform was achieved for the given use case, the focus would be directed toward a pre-study, allowing many more ideas and features to be explored. Thus many things are left unfinished, as sacrificed had to be made with the given timeframe.

Each chapter contains and discusses some of the ideas and suggestions found, which other people can consider implementing. With the current user and use-case, little restrictions were set; however, during product development processes, one should focus closely on what the end-users need, want, and do not know that they want. There is a famous quote attributed to Henry Ford: "If I had asked people what they wanted, they would have said faster horses." Since a Stewart platform is not a novel idea, many new and useful features would be hard to find. Instead, existing and similar machines were explored to get a picture of what more demanding users would want. Although not novel ideas, little or no Platforms exist with all of the features discussed implemented.

The scientific relevance and significance of the performed work have not been discussed yet. It has been stated that cost was one of the primary reasons for developing the Platform. It did end up at a significantly lower price than commercially available platforms, such as the offerings by Acrome. However, if development time is considered, then it can be argued that the time would have been better spent improving or developing a control system for an existing platform. One of the encouragements for taking on the development was that several open-source platforms were found with servo motors. Surely, there would be a good open-source platform in a higher price class suitable for the current use-case; however, it proved more challenging than expected to find. The one from progressive automation was used as a base point, where the mechatronics system have been reused. This version does not seem to have gained much traction, and the developed Platform might fill this gap.

Releasing an open-source version of this Platform was kept in mind throughout the development process. Different solutions were explored to make it configurable to make it more relevant for a wide variety of tasks and price classes. Firstly, both a low-cost prototype version has been made and explored. For more accurate operations, the joints angled brackets, and parts can be manufactured with high tolerances, and the actuators can be swapped out. The SolidWorks equations feature was intended and discussed in Section 3.4.1, which allows an entirely new configuration of the Platform to be rebuilt within minutes. Controlled and changed trough a text file containing the bare minimum of dimensions needed for the Platform. This can make the Platform viable for a wide range of dimensions and stroke lengths before the overall design should be changed. All of this can be contained within a single assembly, with configurations enabling the parts to be switched between, for example, prototype/manufactured parts, and different shapes for the top plate. There is still much work to be done, but with high quality renders and a Stewart Platform set apart from most of the DIY projects, it could gain traction as an open-source version.

8.1 Personal remark

Another major reason for developing the Platform was that I got the chance to learn and apply all the various major fields I studied in the last several years, which would be a valuable experience for the job I will be starting in.

Chapter 9

Conclusion

A Stewart Platform was developed within the given timeframe. All the necessary features needed for testing the vision-based tracking system have been developed, except for generating the ship motion and the IMU implementation, which the end-user would take responsibility for. At a certain stage, all new ideas and improvements were gathered to be applied all at once, which is presented and discussed throughout the thesis. Thus lower precision for the manufacturing and different materials has been accepted for the platform. This, combined with the fact that the used actuators are not as precise, makes the poses sent to control the platform less reliable as ground truth data. Remanufacturing the parts, implementing the move pivot point feature, and calibration of the platform are all things that can be performed to increase the precision of the platform. Nevertheless, with potentiometer feedback, accurate positions are not possible, which would require more expensive actuators with optical or hall effect sensors. Attachment of the actuators was made with this in mind, where the bushings and pins are designed to fit standard actuator shapes only requiring a change to the dimension and not the overall design. However, it was concluded that it was unnecessary for the given use-case, as long as accurate ground truth poses can be obtained from an IMU.

Another goal for the project was to reduce the cost. The components bought for the platform was just below 16.000 NOK, and the price for manufacturing is quoted at 12.040. This gave a final price roughly 4-5 times cheaper than the cheapest and most similar option made by Acrome. Additionally, the cost could have been reduced further for this specific use case, by replacing the metal parts with wood and 3D printed parts. Either way, this is a significant cost saving, as the work was performed for free; however, if development time were factored in, it would have exceeded the price of buying many times over.

The time might have been better served to develop a control system for an existing platform; nevertheless, the project has given me valuable experience and allowed me to test almost all of the fields I have been studying, in addition to the new

skills developed. Furthermore, there are no good low-medium cost open source platforms available, and this platform might fill this gap and could be beneficial for other researchers. An equation driven 3D model can also be implemented when all the suggestions are added to the platform. This will enable other researchers to choose parameters suitable for their needs and generate 3D models and production drawings for an entirely new platform for their specific use case. With easily interchangeable actuators, this design will cover a wide range of use cases and price ranges. All of which could be contained within a single assembly with multiple configurations for switching between different parts. However, this remains a future plan.

9.1 Future work

Future work on this platform will depend entirely on use cases and how much money one is willing to invest. However, the different design choices can be implemented in the same model, which will allow people to select the configuration suitable to their needs and price range. Several new features have been presented throughout the various chapters, as well as suggestions for improving the platform's precision. The following list contains a summary of most of the suggestions and features mentioned throughout the thesis.

- Reduce potentiometer noise and increase ADC resolution. Or use optical/hall effect sensors instead to increase actuator precision.
- Manufacture with tighter tolerances
- Perform calibration of the platform
- Implement the move pivot point feature
- Replace/implement IMU
- replace the spherical joints
- Vertical stacking of motor controllers
- Optimize/clean up Arduino/c++ code, and integrate Qt with ROS.
- Implement quick release mechanism
- topology optimized shape for the top plate
- Redesign of bushing pins
- Redesign of platform feet
- Develop and produce new angled brackets with a wider distance between joints and with threaded inserts
- Produce new electronics enclosure with the new design, with 2-5mm more clearance for the cables.

- Improving Cable Management in electronics enclosure and for actuator cables
- Serial communication over BlueTooth
- Implement User preference file
- Buy a separate Host PC, and develop handheld attachment for it
- Make a touch-centric UI.
- Support for different operating systems
- Support for multiple screens and resolutions
- Make the design equation driven
- Add equations and configurations to the model

For the design parts, both the low cost and higher precision modification can be added to the same model trough configurations, already performed with the top plate, which can be switched between the different shapes with a single click. A text file and implementation of equations can also be considered. With little experience in programming and mechatronics, there is certainly much room for improvements in the things that I am not even aware of. One can also explore other Stewart Platform control systems, to get an idea of other and useful features that have not been discussed.

9.2 Ongoing commitments

The developed software for the GUI was left somewhat unfinished, and will eventually be cleaned up and better documented. If questions about dependencies, setup, or anything related to the project, I will be available for questions. I will also be developing some of the ideas mentioned, such as the handheld device, quick release mechanism, move pivot point feature, Topology optimized shape, and more. This will be performed as a side project and eventually released as an open-source platform. However, when this is performed is uncertain.

Bibliography

[1] D. F. Elset, "Crane payload stabilization using lagrangian kinematics and euler angles," Master's thesis, NTNU, 2019.

[2] K. M. Lynch and F. C. Park, *Modern Robotics*. Cambridge University Press, 2017.

[3] G. Sanderson. (2018). Visualizing quaternions an explorable video series, [Online]. Available: `https://eater.net/quaternions`.

[4] CalQlata^{TM}. (2011). Rao calculator (vessel response amplitudes). Figure: Ship DOF, [Online]. Available: `https://www.calqlata.com/productpages/00081-help.html`.

[5] *Oxford Dictionary of English. 3rd ed.* Oxford University Press, 2013, Prototype.

[6] K. Ulrich and S. Eppinger, *Product design Process, 4th ed. McGraw-Hill, New York 448 pp.* 2012.

[7] C. W. Elverum and T. Welo, "On the use of directional and incremental prototyping in the development of high novelty products: Two case studies in the automotive industry," *Journal of engineering and technology management*, vol. 38, pp. 71–88, 2015.

[8] M. Beaudouin-Lafon and W. E. Mackay, "Prototyping tools and techniques," in *Human-Computer Interaction*, CRC Press, 2009, pp. 137–160.

[9] M. McCurdy, C. Connors, G. Pyrzak, B. Kanefsky, and A. Vera, "Breaking the fidelity barrier: An examination of our current characterization of prototypes and an example of a mixed-fidelity success," in *Proceedings of the SIGCHI conference on Human Factors in computing systems*, ACM, 2006, pp. 1233–1242.

[10] D. K. Sobek II, A. C. Ward, and J. K. Liker, "Toyota's principles of set-based concurrent engineering," *MIT Sloan Management Review*, vol. 40, no. 2, p. 67, 1999.

[11] T. R. Browning, "On customer value and improvement in product development processes," *Systems Engineering*, vol. 6, no. 1, pp. 49–61, 2003.

[12] C. Floyd, "A systematic look at prototyping," in *Approaches to prototyping*, Springer, 1984, pp. 1–18.

[13] T. Welo, "On the application of lean principles in product development: A commentary on models and practices," *International Journal of Product Development*, vol. 13, no. 4, pp. 316–343, 2011.

[14] J. A. Landay and B. A. Myers, "Sketching interfaces: Toward more human interface design," *Computer*, vol. 34, no. 3, pp. 56–64, 2001.

[15] D. G. Ullman, *The mechanical design process: Part 1*, 2010.

[16] I. Systems. (2012). Creating intelligent models using solidworks equations [webcast]. [Online; accessed 8-June-2020], Youtube, [Online]. Available: https://www.youtube.com/watch?v=Xx-VWpV6oCc.

[17] B. Dasgupta and T. Mruthyunjaya, "The stewart platform manipulator: A review," *Mechanism and machine theory*, vol. 35, no. 1, pp. 15–40, 2000.

[18] O. Stepanenko. (2019). Kinematics — 6-dof motion platform. [Online; accessed 13-June-2020], Youtube, [Online]. Available: https://www.youtube.com/watch?v=m78S4eHpSHU.

[19] ——, (2019). Kinematics — serial robot vs. parallel robot. [Online; accessed 13-June-2020], Youtube, [Online]. Available: https://www.youtube.com/watch?v=3fbmguBgVPA.

[20] Circular-Base-Stewart-Platform. (2017). Circular-base-stewart-platform, part 10, the motion-demo. [Online; accessed 13-June-2020], Youtube, [Online]. Available: https://www.youtube.com/watch?v=RR4pmNEWuo4&t=194s.

[21] MaxPlanckSociety. (2015). Cablerobot-simulator. [Online; accessed 13-June-2020], Youtube, [Online]. Available: https://www.youtube.com/watch?v=cJCsomGwdk0.

[22] M. -. (2014). Ministew - servo actuated stewart platform. [Online; accessed 13-June-2020], Youtube, [Online]. Available: https://www.youtube.com/watch?v=jVgYo1qos7w.

[23] P. Automations. (2018). 6-axis stewart platform project using linear actuators. [Online; accessed 14-June-2020], Youtube, [Online]. Available: https://www.youtube.com/watch?v=6xm1bDBc1p0.

[24] (). P16-p linear actuator with feedback. [Online; accessed 6-March-2020], Actuonix Motion Devices, [Online]. Available: https://www.actuonix.com/P16-P-Linear-Actuator-p/p16-p.htm.

[25] (). Feedback linear actuator model: Pa-14p-4-35. [Online; accessed 6-March-2020], Progressive automation, [Online]. Available: https://www.progressiveautomations.com/products/linear-actuator-with-potentiometer?variant=18277322391619.

[26] ACROME. (2018). Acrome stewart platform with custom sizes. [Online; accessed 13-June-2020], Youtube, [Online]. Available: https://www.youtube.com/watch?v=vlCH4zhIqmM.

[27] V. Mishra and R. Mathur, "Determination of height of a modified stewart platform for various sizes of flexible base," *Procedia Engineering*, vol. 41, pp. 360–366, Dec. 2012. DOI: 10.1016/j.proeng.2012.07.185.

[28] A. M. Devices. (2018). Probots 6 degrees of freedom stewart platform. [Online; accessed 13-June-2020], Youtube, [Online]. Available: https://www.youtube.com/watch?v=r9ayBAY1p6E&feature=youtu.be&t=60.

[29] (). Flange bearing with ball stud, male thread, gfsm-ag, igubal®. [Online; accessed 6-March-2020], Igus, [Online]. Available: https://www.igus.no/product/384.

[30] (). In-line ball and socket joint, agrm lc, with steel pin, igubal®. [Online; accessed 6-March-2020], Igus, [Online]. Available: https://www.igus.co.uk/product/324.

[31] (). Igus news pages 27-32. [Online; accessed 6-March-2020], Igus, [Online]. Available: https://www.hennlich.cz/fileadmin/user_upload/HSK/Aktuality/IGUS_news_27-32.pdf.

[32] Myostat. (2016). Fastest way to program a 6dof hexapod 6-axis motion platform: Software, mechanics, controller. [Online; accessed 6-March-2020], Hephaist, [Online]. Available: http://www.myostat.ca/SRJoint#.

[33] (). Clip bearing zclm, igubal®. [Online; accessed 6-March-2020], Igus, [Online]. Available: https://www.igus.co.uk/product/17503.

[34] (). Huco universal joint 105.32.4848, single, plain, bore 20 x 20mm, 86mm length. [Online; accessed 6-March-2020], Huco, [Online]. Available: https://no.rs-online.com/web/p/universal-joints/5113820/.

[35] J. Korber. (2017). Make your 3d printed part (surface) look awesome! tutorial. [Online; accessed 8-June-2020], Youtube, [Online]. Available: https://www.youtube.com/watch?v=0vgynnYzo08.

[36] (). Magnet-lock clamping receptacles. [Online; accessed 11-June-2020], Imao Corporation, [Online]. Available: https://www.imao.biz/catalog/en/categoryviews/?categorycode=&category=%5C$501978&page=1.

[37] (). Button-locking pins. [Online; accessed 11-June-2020], Imao Corporation, [Online]. Available: https://www.imao.biz/catalog/en/categoryviews/?categorycode=&category=%5C$490171&page=1.

[38] (). One-touch flex locator clampers. [Online; accessed 11-June-2020], Imao Corporation, [Online]. Available: https://www.imao.biz/catalog/en/categoryviews/?categorycode=&category=%5C$902317&page=1.

[39] S. Hermann. (2020). Helicoils, threaded insets and embedded nuts in 3d prints - strength & strength assessment. [Online; accessed 11-June-2020], CNC Kitchen, [Online]. Available: https://www.cnckitchen.com/blog/helicoils-threaded-insets-and-embedded-nuts-in-3d-prints-strength-amp-strength-assessment.

[40] M. P. Bendsøe, "Optimal shape design as a material distribution problem," *Structural optimization*, vol. 1, no. 4, pp. 193–202, 1989.

[41] T. Q. Company. (2020). Scatter example, [Online]. Available: https://doc.qt.io/qt-5/qtdatavisualization-scatter-example.html.

[42] S.-K. Ueng, D. Lin, and C.-H. Liu, "A ship motion simulation system," *Virtual Reality*, vol. 12, pp. 65–76, Mar. 2008. DOI: 10.1007/s10055-008-0088-8.

[43] M. B. Kjelland, I. Tyapin, G. Hovland, and M. R. Hansen, "Tool-point control for a redundant heave compensated hydraulic manipulator," *IFAC Proceedings Volumes*, vol. 45, no. 8, pp. 299–304, 2012.

[44] *Spacemousewireless*, https://www.3dconnexion.eu/spacemouse_wireless/eu/, [Online; accessed 13-June-2020].

[45] A. Ershov, *Qt5and3dmouse*, https://github.com/ershovdz/Qt5And3DMouse/blob/master/main.cpp, 2017.

[46] T.-Y. Lee and J.-K. Shim, "Forward kinematics of the general 6–6 stewart platform using algebraic elimination," *Mechanism and Machine Theory*, vol. 36, no. 9, pp. 1073–1085, 2001.

[47] 3Dconnexion. (2012). Using a 3d mouse - correct technique. [Online; accessed 13-June-2020], Youtube, [Online]. Available: https://www.youtube.com/watch?v=CCabW4BtJEE.

[48] T. A. Group, *The economic payback of 3d mice for cad design engineers*, https://www.3dconnexion.com/fileadmin/user_upload/manuals_docs/english_intl/3dx_whitepaper_cadpayback_en_intl.pdf, [Online; accessed 13-June-2020].

[49] P. I. U. .-. P. M. Control. (2016). Fastest way to program a 6dof hexapod 6-axis motion platform: Software, mechanics, controller. [Online; accessed 13-June-2020], Youtube, [Online]. Available: https://www.youtube.com/watch?v=hkoTRNfivbU&t=174s.

[50] Moog. (2011). Ipad controlling a moog electric motion base. [Online; accessed 13-June-2020], Youtube, [Online]. Available: https://www.youtube.com/watch?v=aB-QLuSpm4g.

[51] D. N. Tim Branch Henry Liu, "Stewart platform with electronics control and leap motion interaction," Project, The University Of British Columbia, 2018.

[52] P. Automations, *Stewart-platform*, https://github.com/progressiveautomations/Stewart-Platform, 2018.

[53] *Getting started with the arduino due*, https://www.arduino.cc/en/Guide/ArduinoDue, 2015.

[54] (). Arduino due - 32 bit processor model: Lc-062. [Online; accessed 6-March-2020], Progressive automation, [Online]. Available: https://www.progressiveautomations.com/products/lc-062?_pos=1&_sid=630d1af47&_ss=r.

[55] N. Koumaris, *Arduino due vs arduino mega*, https://educ8s.tv/arduino-due-vs-arduino-mega/, 2015.

[56] F. A. Team, *Don't buy a feedback linear actuator until you read this*, https://www.firgelliauto.com/blogs/news/don-t-buy-a-feedback-linear-actuator-until-you-read-these-important-tips, 2018.

[57] D. Nedelkovski, *What is hall effect and how hall effect sensors work*, https://howtomechatronics.com/how-it-works/electrical-engineering/hall-effect-hall-effect-sensors-work/, 2015.

[58] (). Multimoto arduino shield model: Lc-82. [Online; accessed 6-March-2020], Progressive automation, [Online]. Available: https://www.progressiveautomations.com/products/lc-82?_pos=13&_sid=7c07c431d&_ss=r.

[59] (). Erpf-400-12 - vekslende strømforsyning, 360w, 12v, 30a. [Online; accessed 6-March-2020], Mean Well Enterprises, [Online]. Available: https://www.elfadistrelec.no/no/vekslende-stromforsyning-360w-12v-30a-mean-well-erpf-400-12/p/30134146?q=str%5C%c3%5C%b8mforsyning+30a+12v&pos=2&origPos=2&origPageSize=10&track=true.

[60] C. Pao, *What is an imu sensor?* https://www.ceva-dsp.com/ourblog/what-is-an-imu-sensor/, 2018.

[61] (). Cross domain developement kit. [Online; accessed 20-June-2020], Bosch, [Online]. Available: https://www.bosch-connectivity.com/products/cross-domain/cross-domain-developement-kit/.

[62] D. X. (2019). Delta x - the first open source delta robot kit in the world - full. [Online; accessed 17-June-2020], Youtube, [Online]. Available: https://www.youtube.com/watch?v=dx5dYdQ7NDo&t=72s.

[63] F. Berglid, *Stewartplatform*, https://github.com/Berglid/StewartPlatform, 2020.

[64] SavyBoat. (). Bourbon orca. [Online; accessed 24-April-2020], [Online]. Available: https://savyboat.com/shop/bourbon-orca/?fbclid=IwAR2Izo4M3I8vk7VqZe5yttmo8VE1EFtk44_d0aM6vo_frXEVCuHH6n3VMwU.

[65] ArqArt3D. (). Anchor handling tug supply vessel bourbon orca 3d model. [Online; accessed 24-April-2020], [Online]. Available: https://savyboat.com/shop/bourbon-orca/?fbclid=IwAR2Izo4M3I8vk7VqZe5yttmo8VE1EFtk44_d0aM6vo_frXEVCuHH6n3VMwU.

Appendix

9.3 Previous designs

9.3.1 Actuator size comparison

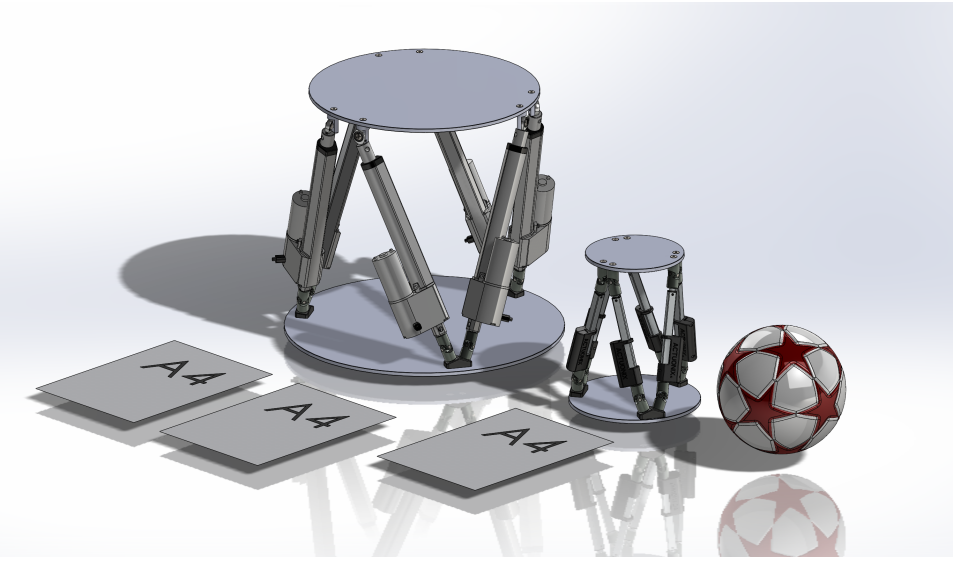

Figure 9.1: Size comparison 1: Actuonix P16-P vs Progressive Automation PA-14P actuators

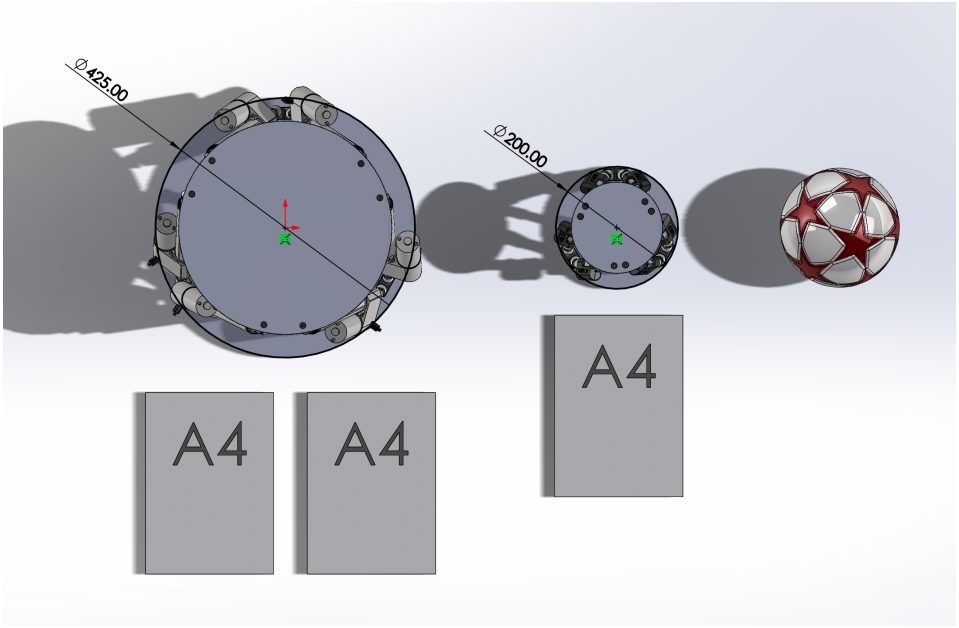

Figure 9.2: Size comparison 2: Actuonix P16-P vs Progressive Automation PA-14P actuators

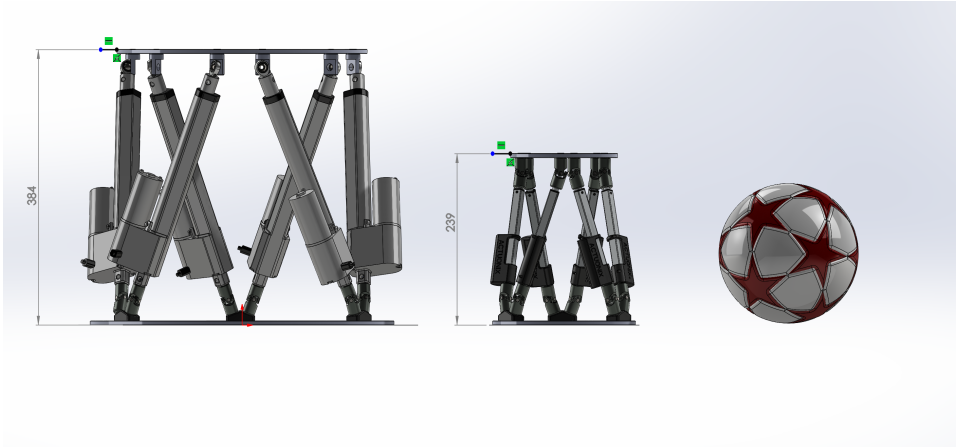

Figure 9.3: Size comparison 3: Actuonix P16-P vs Progressive Automation PA-14P actuators

9.3.2 Side mounted enclosure

Early design with side mounted electronics, and the joint housing in its original form.

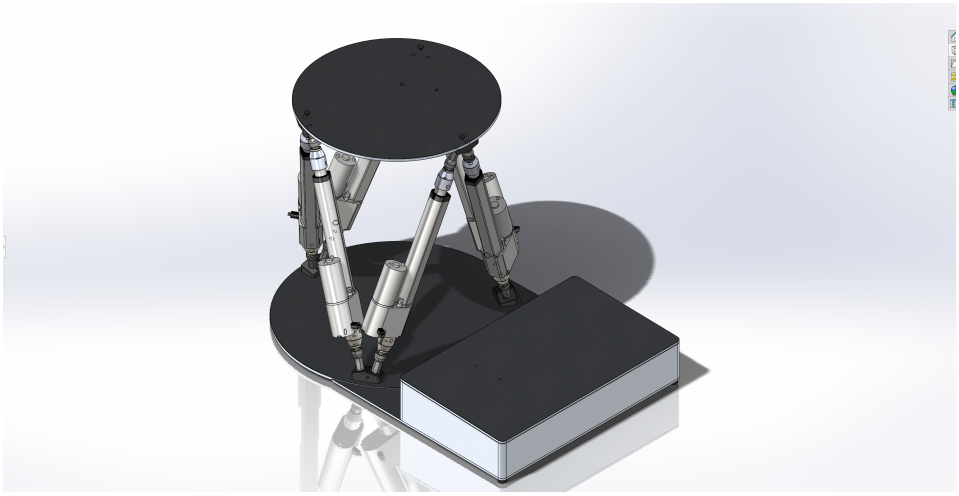

Figure 9.4: Side mounted enclosure 1

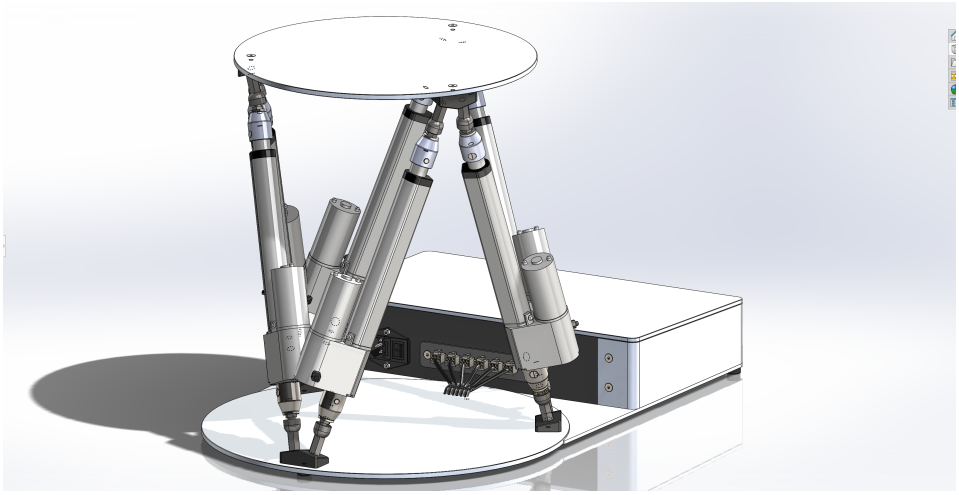

Figure 9.5: Side mounted enclosure 2

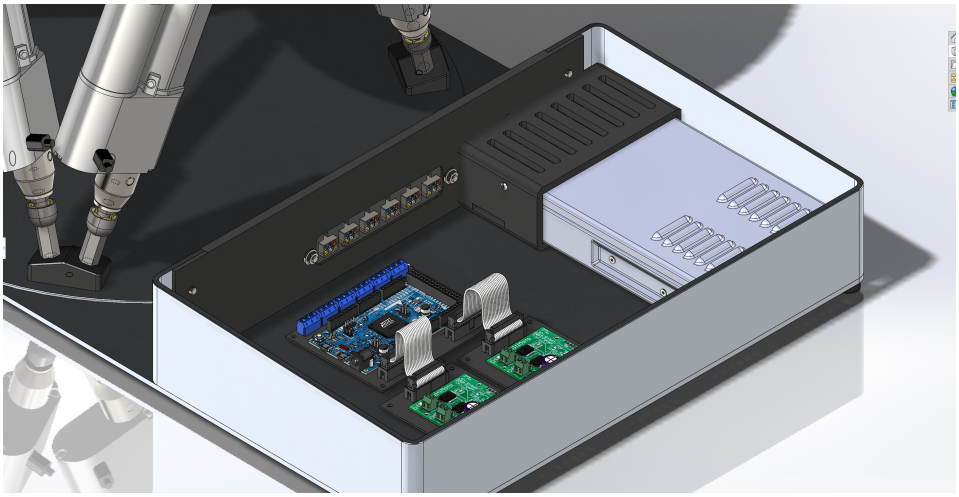

Figure 9.6: Side mounted enclosure 3

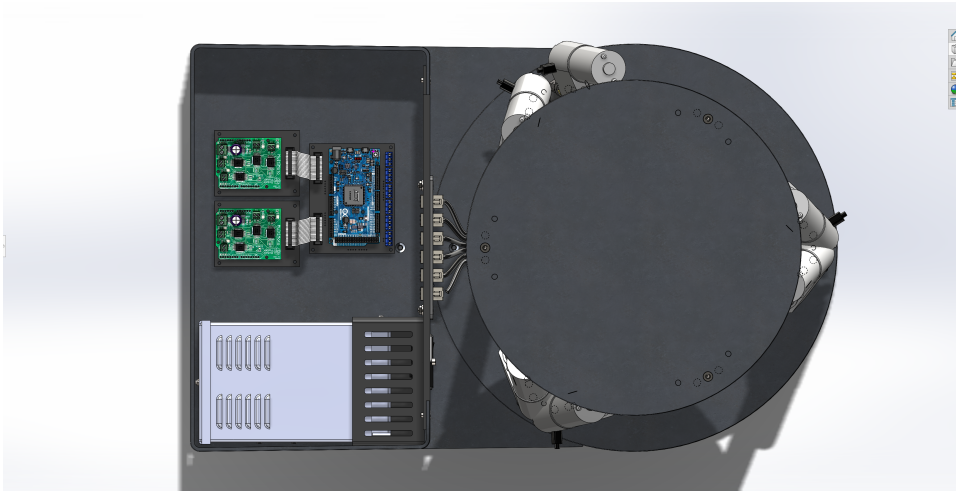

Figure 9.7: Side mounted enclosure 4

9.4 Wiring diagram

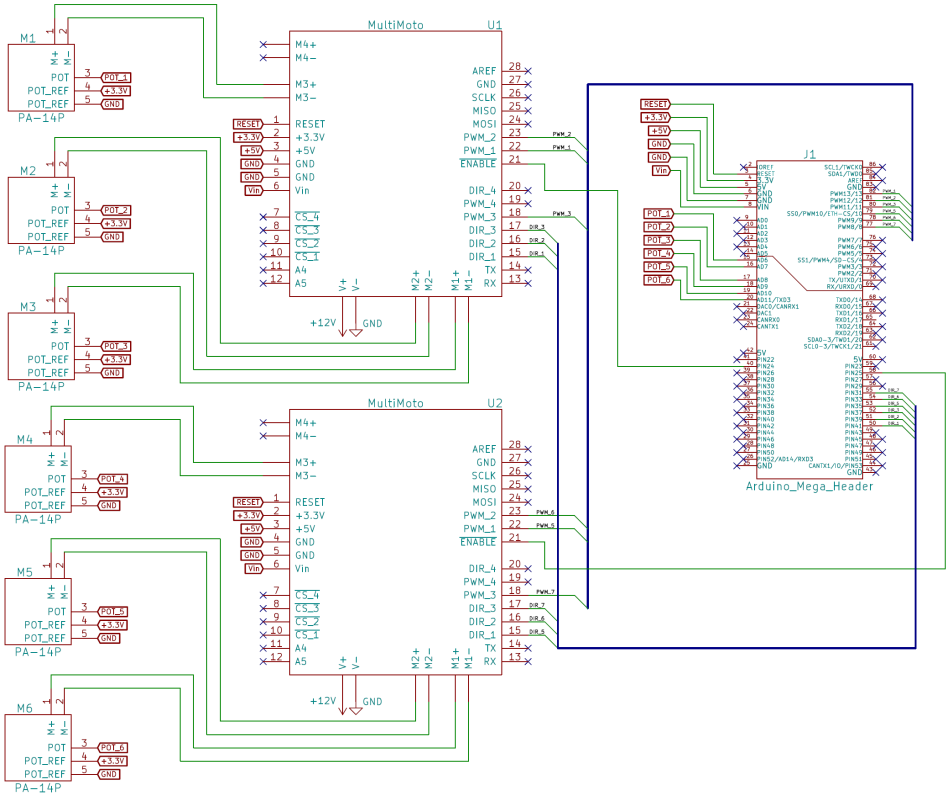

Figure 9.8: Overall wiring diagram

Note: An Arduino Mega header is used instead of an Arduino Due. However, the pin layout is identical.

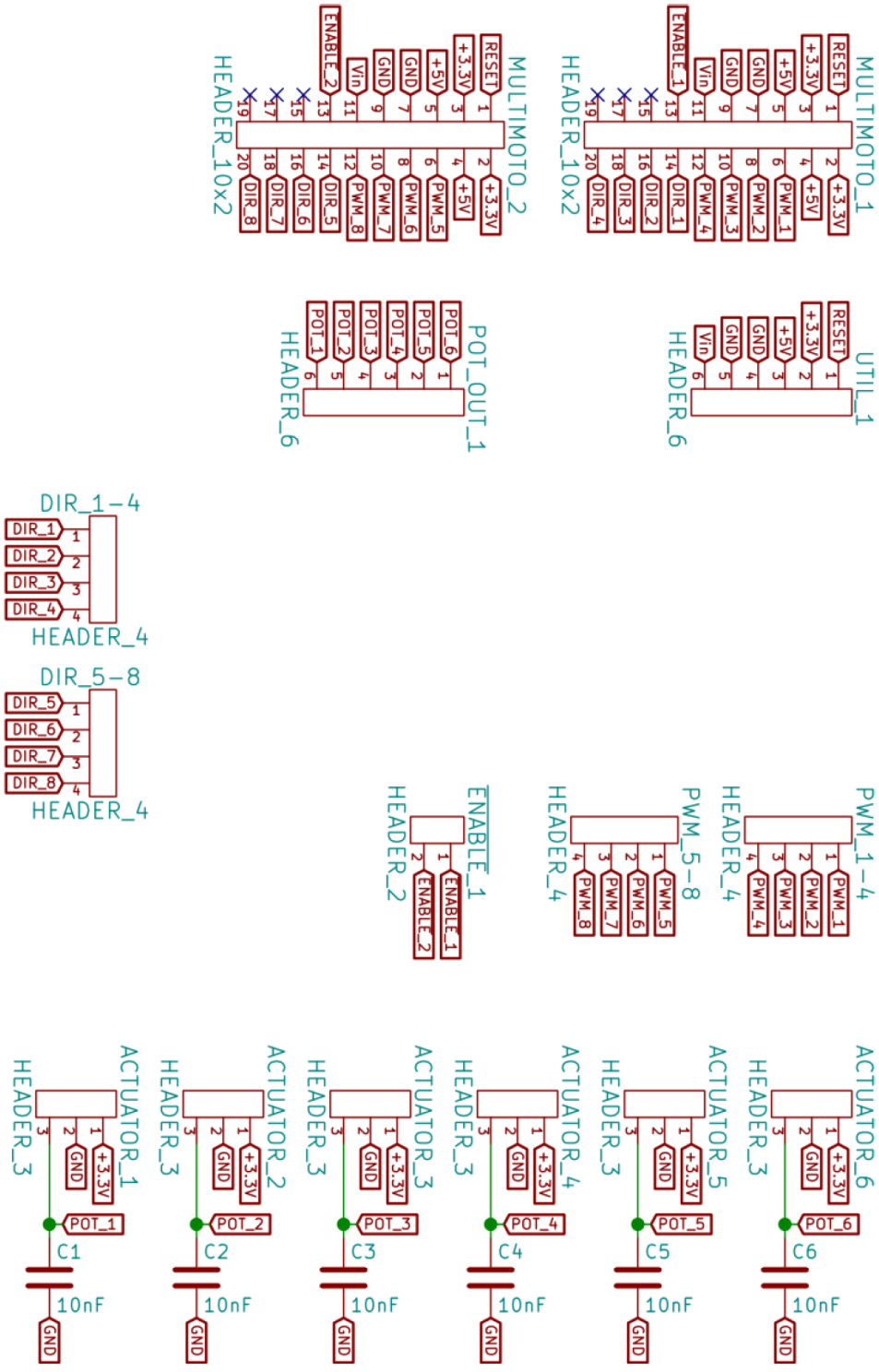

Figure 9.9: Pin/header layout for the Arduino connector PCB

9.5 Platform Parameters

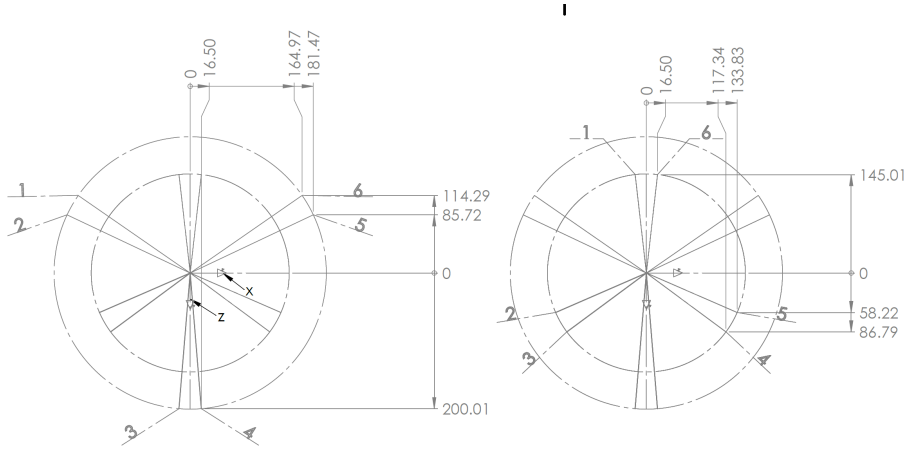

	Base coordinates (x, y z)		
1	- 164.97	0	- 114.29
2	- 181.47	0	- 85.72
3	- 16.50	0	200.01
4	16.50	0	200.01
5	181.47	0	- 85.72
6	164.97	0	- 114.29

	Platform coordinates (x, y z)		
1	- 16.50	0	- 145.01
2	- 133.83	0	58.22
3	- 117.34	0	86.79
4	117.34	0	86.79
5	133.83	0	58.22
6	16.50	0	- 145.01

Figure 9.10: Platform parameters

** Spesifikasjon av vare/tjeneste
  Artikkelnr..................: PA-14P
  Antall......................: 6
  Mengdeenhet.................: 1
  Beskrivelse.................: 12v Feedback linear actuator Stroke = 6 Inch, Force = 35lbs, Speed = 2.00"/sec
  Pris pr. enhet..............: 138.99 Ekskl. mva
  Valuta......................: USD

  Artikkelnr..................: LC-062
  Antall......................: 1
  Mengdeenhet.................: 1
  Beskrivelse.................: ARDUINO DUE - 32 BIT PROCESSOR
  Pris pr. enhet..............: 47.50 Ekskl. mva
  Valuta......................: USD

  Artikkelnr..................: LC-82
  Antall......................: 2
  Mengdeenhet.................: 1
  Beskrivelse.................: MULTIMOTO ARDUINO SHIELD
  Pris pr. enhet..............: 48.99 Ekskl. mva
  Valuta......................: USD

  Artikkelnr..................: 301-34-146
  Antall......................: 1
  Mengdeenhet.................: 1
  Beskrivelse.................: ERPF-400-12 - Vekslende strømforsyning, 360W, 12V, 30A, MEAN WELL
  Pris pr. enhet..............: 514.00 Ekskl. mva
  Valuta......................: NOK

  Artikkelnr..................: 301-76-072
  Antall......................: 1
  Mengdeenhet.................: 1
  Beskrivelse.................: AF-C06-SD - IEC Inlet Single Phase EMI Filter 250VAC 6A, Ohmite
  Pris pr. enhet..............: 188.00 Ekskl. mva
  Valuta......................: NOK

  Artikkelnr..................:
  Antall......................: 1
  Mengdeenhet.................: 1
  Beskrivelse.................: Frakt actuatorzone
  Pris pr. enhet..............: 81.58 Ekskl. mva
  Valuta......................: USD

** Spesifikasjon av vare/tjeneste
  Artikkelnr..................: AGRM-08-LC-MS
  Antall......................: 13
  Mengdeenhet.................: 1
  Beskrivelse.................: IGUBAL IN-LINE BALL AND SOCKET AGRM-08-LC-MS
  Pris pr. enhet..............: 32.3 Ekskl. mva
  Valuta......................: NOK

** Spesifikasjon av vare/tjeneste
  Artikkelnr.....: 300-93-707
  Antall.....: 6
  Mengdeenhet.....: 1
  Beskrivelse.....: IDC-flatkabelsokkel 2.54mm Antall kontakter=20
  Pris pr. enhet.....: 14,88 Inkl. mva
  Valuta.....: NOK

  Artikkelnr.....: 301-12-335
  Antall.....: 10
  Mengdeenhet.....: 1
  Beskrivelse.....: Stiftlist DIN 41651, 20 Poles
  Pris pr. enhet.....: 2,44 Inkl. mva
  Valuta.....: NOK

  Artikkelnr.....: 301-25-774
  Antall.....: 1
  Mengdeenhet.....: 1
  Beskrivelse.....: USB A Plug to USB Micro-B Plug Cable 1.8m Svart
  Pris pr. enhet.....: 33,38 Inkl. mva
  Valuta.....: NOk

  Artikkelnr.....: 165-72-413
  Antall.....: 20
  Mengdeenhet.....: 1
  Beskrivelse.....: C0805C103K5RACTU - Keramisk kondensator 10 nF 50 VDC 0805
  Pris pr. enhet.....: 1,47 Inkl. mva
  Valuta.....: NOK

  Artikkelnr.....: 300-93-647
  Antall.....: 25
  Mengdeenhet.....: 1
  Beskrivelse.....: Rett Hann Kretskorthode, Hullmontert, 1 Rekker, 6 Kontakter, 2.54mm Pitch
  Pris pr. enhet.....: 0,98175 Inkl. mva
  Valuta.....: NOK

  Artikkelnr.....: 300-93-645
  Antall.....: 50
  Mengdeenhet.....: 1
  Beskrivelse.....: Rett Hann Kretskorthode, Hullmontert, 1 Rekker, 4 Kontakter, 2.54mm Pitch
  Pris pr. enhet.....: 0,63625 Inkl. mva
  Valuta.....: NOK

  Artikkelnr.....: 300-93-643
  Antall.....: 100
  Mengdeenhet.....: 1
  Beskrivelse.....: Rett Hann Kretskorthode, Hullmontert, 1 Rekker, 2 Kontakter, 2.54mm Pitch
  Pris pr. enhet.....: 0,34675 Inkl. mva
  Valuta.....: NOK

  Artikkelnr.....: 301-15-110

Antall.....: 10
Mengdeenhet.....: 10
Beskrivelse.....: Jumpertråd, hann - hunn, Pakke med 10 stykk, 150 mm, Svart
Pris pr. enhet.....: 9,81 Inkl. mva
Valuta.....: NOK

Artikkelnr.....: 300-65-157
Antall.....: 10
Mengdeenhet.....: 1
Beskrivelse.....: SL, Hylse Krympehus, 4 Poler, 1 Antall rader, 2.54mm Pitch
Pris pr. enhet.....: 3,75 Inkl. mva
Valuta.....: NOK

Artikkelnr.....: 143-56-614
Antall.....: 10
Mengdeenhet.....: 1
Beskrivelse.....: C-Grid III, Hylse Hus, 6 Poler, 1 Antall rader, 2.54mm Pitch
Pris pr. enhet.....: 4,46 Inkl. mva
Valuta.....: NOK

Artikkelnr.....: 301-58-043
Antall.....: 10
Mengdeenhet.....: 1
Beskrivelse.....: SL, Hylse Hus, 2 Poler, 1 Antall rader, 2.54mm Pitch
Pris pr. enhet.....: 3,19 Inkl. mva
Valuta.....: NOK

Artikkelnr.....: 301-58-045
Antall.....: 10
Mengdeenhet.....: 1
Beskrivelse.....: SL, Hylse Hus, 3 Poler, 1 Antall rader, 2.54mm Pitch
Pris pr. enhet.....: 3,31 Inkl. mva
Valuta.....: NOK

Artikkelnr.....: 180-87-389
Antall.....: 1
Mengdeenhet.....: 1
Beskrivelse.....: LOCTITE 460, NORDIC - Superlim 20 g
Pris pr. enhet.....: 523,75 Inkl. mva
Valuta.....: NOK

Artikkelnr.....: 301-45-374
Antall.....: 1
Mengdeenhet.....: 1
Beskrivelse.....: Strømledning Type F (CEE 7/4) - IEC 60320 C13 2m Svart
Pris pr. enhet.....: 33,50 Inkl. mva
Valuta.....: NOK

Artikkelnr.....: 144-02-012
Antall.....: 7
Mengdeenhet.....: 1

Beskrivelse.....: Mini-Fit Jr., Plugg Krympehus, 6 Poler, 2 Antall rader, 4.2mm Pitch
Pris pr. enhet.....: 5,86 Inkl. mva
Valuta.....: NOK

Artikkelnr.....: 144-02-265
Antall.....: 50
Mengdeenhet.....: 1
Beskrivelse.....: Krympestift, Hann, Tinn, 18 ... 24AWG
Pris pr. enhet.....: 0,926875 Inkl. mva
Valuta.....: NOK

Artikkelnr.....: 300-43-059
Antall.....: 12
Mengdeenhet.....: 1
Beskrivelse.....: Rekkeklemme for kretskort 0.13 ... 1.31mm² / 26 ... 16AWG 5.08mm Pitch, 3 Poler
Pris pr. enhet.....: 4,29 Inkl. mva
Valuta.....: NOK

Artikkelnr.....: 141168
Antall.....: 1
Mengdeenhet.....: 1
Beskrivelse.....: Panel Mount Extension USB Cable Micro B Male to Micro B Female
Pris pr. enhet.....: 79 Inkl. mva
Valuta.....: NOK

Artikkelnr.....:
Antall.....: 1
Mengdeenhet.....: 1
Beskrivelse.....: Frakt digital impulse
Pris pr. enhet.....: 99 Inkl. mva
Valuta.....: NOK

** Spesifikasjon av vare/tjeneste
Artikkelnr.....: 257-8640
Antall.....: 1
Mengdeenhet.....: 4
Beskrivelse.....: FIBET Cylindrical M6 Zinc Plated Steel Anti Vibration Feet 2012VE18-60 45.4kg Compression Load ,20mm dia. Natural Rubber
Pris pr. enhet.....: 20,12 Ekskl. mva
Valuta.....: NOK

Artikkelnr.....: 724-3336
Antall.....: 1
Mengdeenhet.....: 1
Beskrivelse.....: 3M 20 Way Flat Ribbon Cable, 25.04 mm Width, Series HF365
Pris pr. enhet.....: 184,27 Ekskl. mva
Valuta.....: NOK

Artikkelnr.....: 123-0958
Antall.....: 1
Mengdeenhet.....: 1

Beskrivelse.....: RS PRO 2m Power Cable, Low Smoke Zero Halogen (LSZH) C13, IEC to CEE 7/7, Schuko (Male, Right Angle)
Pris pr. enhet.....: 163,21 Ekskl. mva
Valuta.....: NOK

Artikkelnr.....: 468-443
Antall.....: 1
Mengdeenhet.....: 1
Beskrivelse.....: Hi-Bond HB397F Transparent Double Sided Polyester Tape, 9mm x 50m, 0.23mm
Pris pr. enhet.....: 58,72 Ekskl. mva
Valuta.....: NOK

Artikkelnr.....:
Antall.....: 1
Mengdeenhet.....: 1
Beskrivelse.....: Eventuelle tillegg (frakt, miljøgebyr etc.)
Pris pr. enhet.....: 0 Ekskl. mva
Valuta.....: NOK

PROGRESSIVE AUTOMATIONS

FORWARD THINKING

PA-14P

Data Sheet

Contents

Specifications

Load (LBS)		No Load Current (A)				Full Load Current (A)				Speed (inch/sec)	
Dynamic	Static	12VDC	24VDC	36VDC	48VDC	12VDC	24VDC	36VDC	48VDC	No Load	Full Load
35	75	1.0	0.5	0.3	0.3	5.0	2.5	1.7	1.3	2.00	1.38
50	100	1.0	0.5	0.3	0.3	5.0	2.5	1.7	1.3	1.14	0.83
75	150	1.0	0.5	0.3	0.3	5.0	2.5	1.7	1.3	0.95	0.70
110	220	1.0	0.5	0.3	0.3	5.0	2.5	1.7	1.3	0.79	0.59
150	300	1.0	0.5	0.3	0.3	5.0	2.5	1.7	1.3	0.37	0.28

Stroke	1" to 40"
Limit Switch	Internal - Non-Adjustable
Limit Switch Feedback	Customizable
Screw Type	ACME Screw
Motor Type	Brushed or Brushless DC Motor
Connector Type	See Page 5
Wire Length	40" (customizable)
Housing Material	6062 Aluminum Alloy
Rod Material	Aluminum Alloy/Stainless Steel (customizable)
Gear Material	Polyformaldehyde (35 lbs only)/Powder Metallurgy Steel Alloy
Color (Shaft)	Silver
Color (Motor End)	Silver
Noise	<45dB
Duty Cycle	25% (5 minutes on, 15 minutes off)
Operational Temperature	-25ºC to 65ºC (-13ºF to 149ºF)
Protection Class	IP54 (IP65 customizable)
Feedback Options	Potentiometer (see page 5)
Certifications	CE/RoHS
Mounting Brackets	See Page 6
Mounting Ends	Customizable

Dimensions

(Dimensions in inches)

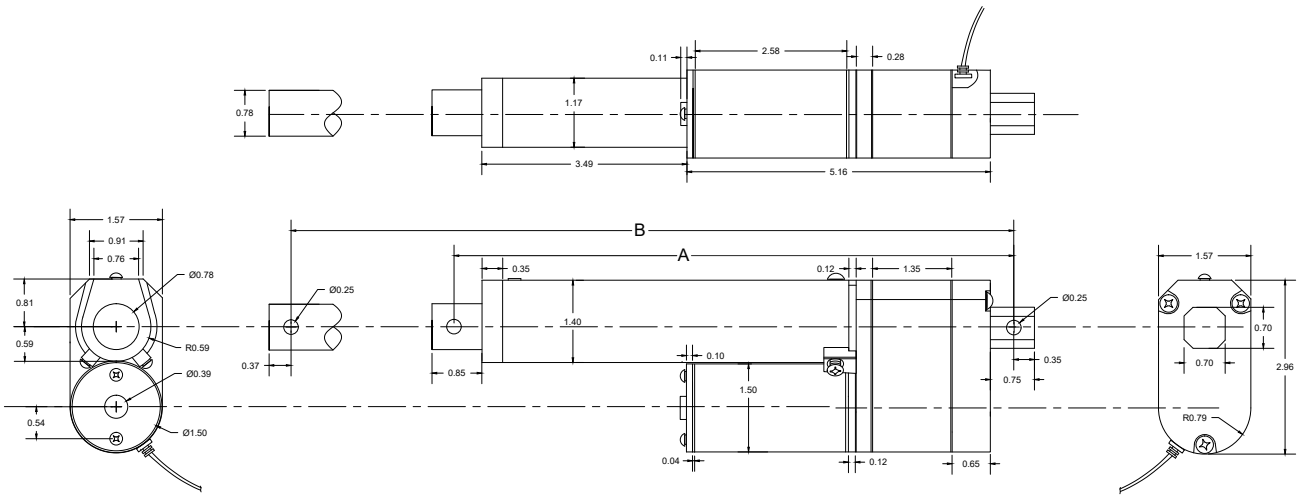

Hole to Hole

	Stroke	1	2	3	4	6	8	9	10	12	14	16	18	20	22	24	30	40
PA-14P	A	6.51	7.51	8.51	9.51	11.51	13.51	14.51	15.51	17.51	19.51	21.51	23.51	25.51	27.51	29.51	35.51	45.51
	B	7.51	9.51	11.51	13.51	17.51	21.51	23.51	25.51	29.51	33.51	37.51	41.51	45.51	49.51	53.51	66.61	85.51

For Stroke Length

A = Stroke Length + 5.51"

B = Stroke Length x 2 + 5.51"

Speed vs Load

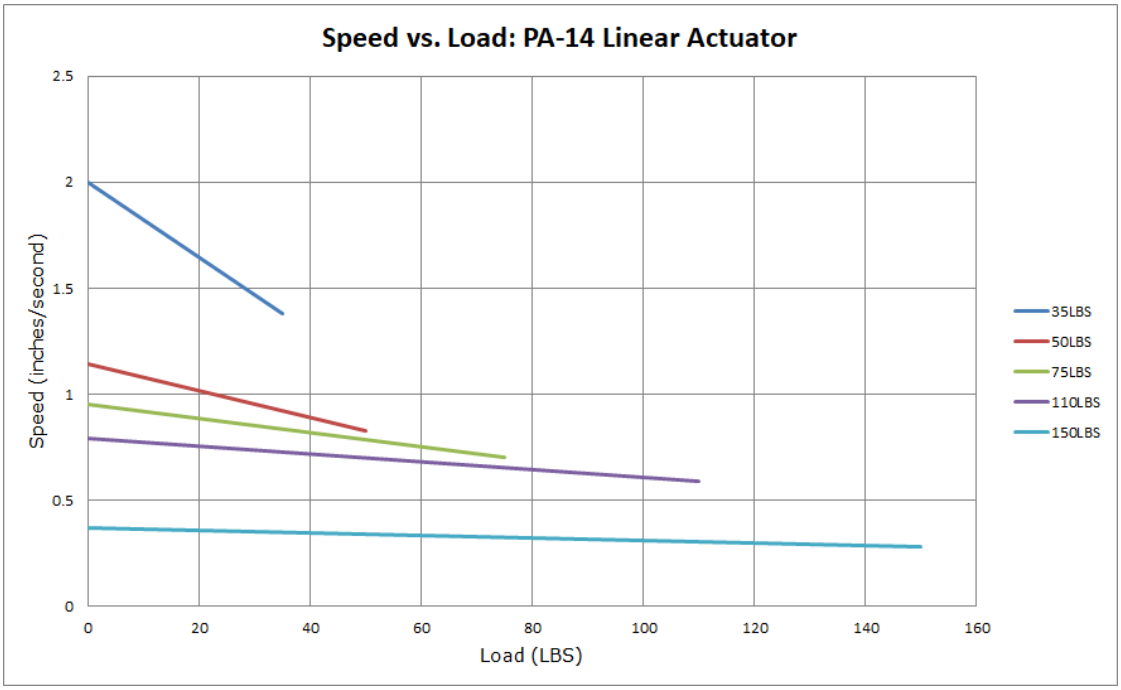

Current vs Load

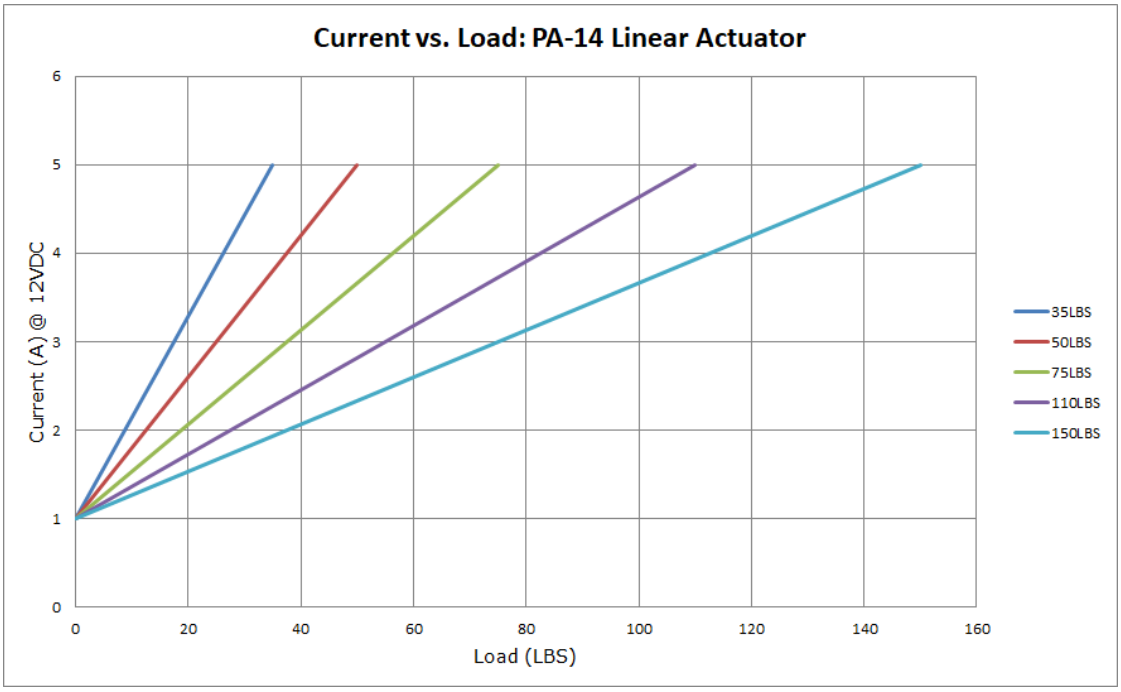

Connectors & Feedback

2-Pin Connector (Standard)

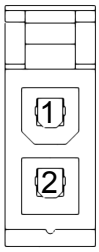

Motor	
1	2
M-	M+

Component	Part Name	Part Number	Mating Part Number
Housing	Molex Mini Fit Jr 2-Pin Receptacle	39-01-2025	39-01-3029/ 39-01-2026

Potentiometer Specifications

*For Stroke Length up to 40"

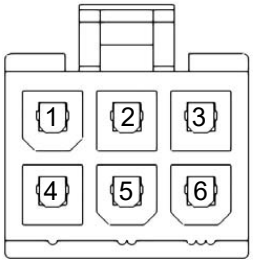

Motor		Potentiometer			
4	5	2	3	1	6
-	GND (White wire)	Actuator Negative (Red Wire)	Potentiometer (Blue Wire)	Actuator Positive (Black Wire)	5V (Yellow Wire)

Resistance*	Number of Turns	Tolerance
0-10kΩ	10	+/- 5%

*Actual resistance value may vary within the 0-10kΩ range based on stroke length

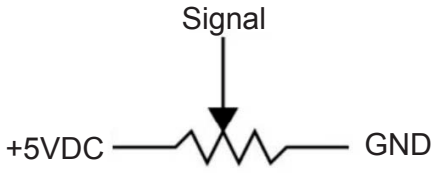

Mounting Brackets

(Dimensions in inches)

BRK-14

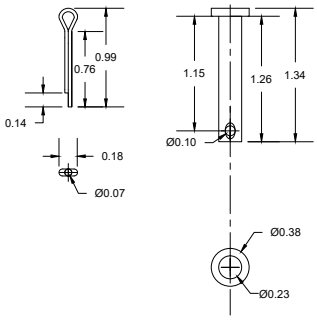

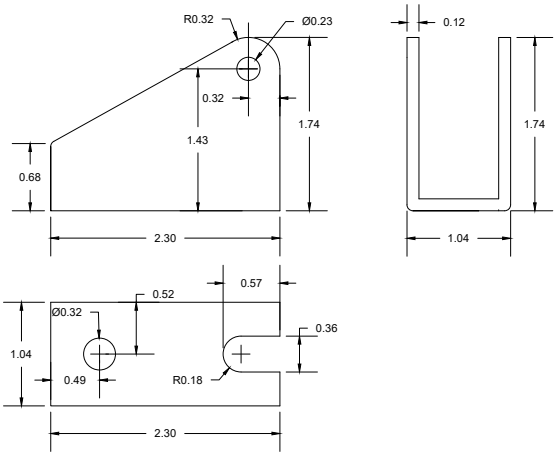

BRK-03

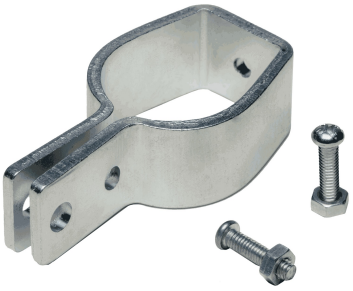

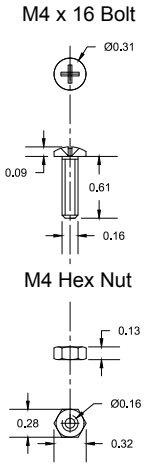

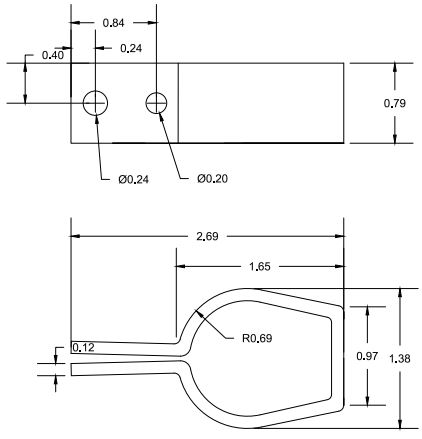

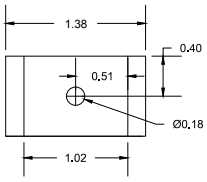

Internal Components

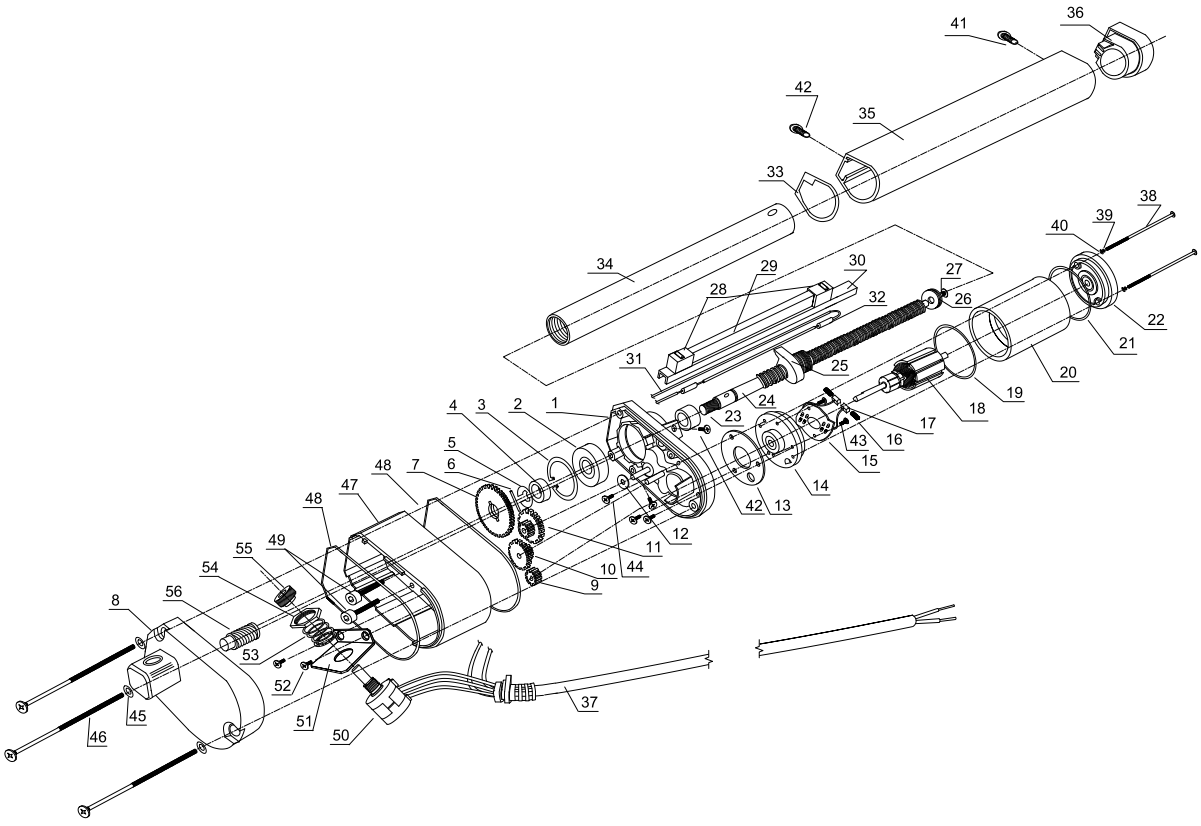

Internal Descriptions

Item	Description	Qty
1	Actuator base	1
2	Shaft Bearing	1
3	Shaft Bearing Lock	1
4	Shaft Base Spacer	1
5	Shaft Base Spacer Lock	1
6	Shaft Gear Wheel Holder	1
7	Shaft Gear Wheel	1
8	Base Cover with Mounting Support	1
9	Electric Motor Gear Wheel	1
10	Small Intermediate Gear Wheel	1
11	Medium Intermediate Gear Wheel	1
12	Teflon Washer	1
13	Electric Motor Base Washer	1
14	Electric Motor Base	1
15	Brush Holder PCB	1
16	Electric Motor Brush	2
17	Electric Motor Brush Spring	2
18	Electric Motor Rotor	1
19	Motor Enclosure Bottom Washer	1
20	Electric Motor Encloser with Stator	1
21	Motor Enclosure Top Washer	1
22	Electric Motor Cap with Rotor Bearing	1
23	Shaft Spacer	1
24	Treaded Shaft Drive / Lead Screw	1
25	Shaft Base with Limit Switches Arm	1
26	Shaft Drive End Support	1
27	Shaft Drive End Support Screw	1
28	Limit Switch	2

Item	Description	Qty
29	Limit Switches Spacer	1
30	Limit Switches Base	1
31	Limit Switches Wiring	1
32	Diode	2
33	Shaft Encloser Bottom Washer	1
34	Shaft with Mounting Hole	1
35	Shaft Encloser	1
36	Shaft Enclosure Top Cap	1
37	Power Cable	1
38	Motor Enclosure Screw	2
39	Motor Screw Spring Washer	2
40	Motor Screw Washer	2
41	Shaft Eclosure Top Cap Screw	1
42	Shaft Enclosure Base Screw	3
43	Brush Holder PCB Screw	2
44	Motor Base Screw	3
45	Base Cover Washer	3
46	Base Cover Screw	3
47	Base Extension	1
48	Base Extension gasket	2
49	Base Extension Screw	2
50	Potentiometer	1
51	Potentiometer Bracket	1
52	Potentiometer Bracket Screw	2
53	Potentiometer Washer	3
54	Potentiometer Nut	1
55	Potentiometer Gear	1
56	Shaft Gear	1

400W Single Output Switching Power Supply

ERPF-400 series

Features

- Universal AC input / Full range
  (Withstand 300VAC surge input for 5 seconds)
- Built-in active PFC function
- High efficiency up to 91%
- Design against rain splash
- Protections: Short circuit / Overload / Over voltage/ Over temperature
- Cooling by free air convection
- LED indicator for power on
- Low cost,high reliability
- 100% full load burn-in test
- 3 years warranty

Applications

- LED strip lighting
- LED channel letters
- LED moving sign

Description

ERPF-400 series is a 400W single output enclosed type AC/DC power supply with the active PFC design. It adopts an aluminum case and the interior is semi-potted, protecting the internal electronic components from rain splash and dust. With the complete protection functions, ERPF-400 is suitable for the applications such as outdoor LED channel letters, billboard, commercial signs, etc.

Model Encoding

ERPF - 400 - 24

- 24 — Output voltage(12V/24V/48V)
- 400 — Output wattage
- ERPF — Series name

400W Single Output Switching Power Supply **ERPF-400 series**

SPECIFICATION

MODEL		ERPF-400-12	ERPF-400-24	ERPF-400-48
OUTPUT	DC VOLTAGE	12V	24V	48V
	RATED CURRENT	30A	16.7A	8.3A
	CURRENT RANGE Note.5	0 ~ 30A	0 ~ 16.7A	0 ~ 8.3A
	RATED POWER	360W	400.8W	398.4W
	RIPPLE & NOISE (max.) Note.2	150mVp-p	150mVp-p	240mVp-p
	VOLTAGE ADJ. RANGE	10.8 ~ 13.2V	21.6 ~ 26.4V	43.2 ~ 52.8V
	VOLTAGE TOLERANCE Note.3	±1.0%	±1.0%	±1.0%
	LINE REGULATION	±0.5%	±0.5%	±0.5%
	LOAD REGULATION	±0.5%	±0.5%	±0.5%
	SETUP, RISE TIME	2000ms, 100ms/230VAC; 3000ms, 100ms/115VAC at full load		
	HOLD UP TIME (Typ.)	10ms/230VAC; 10ms/115VAC at full load		
INPUT	VOLTAGE RANGE Note.4	90 ~ 264VAC 127 ~ 370VDC		
	FREQUENCY RANGE	47 ~ 63Hz		
	POWER FACTOR (Typ.)	PF≧0.95/230VAC, PF≧0.98/115VAC		
	EFFICIENCY (Typ.)	89%	90%	91%
	AC CURRENT (Typ.)	2.5A/230VAC 3A/115VAC		
	INRUSH CURRENT (Typ.)	cold start 45A/115VAC, 90A/230VAC		
	LEAKAGE CURRENT	<1mA / 240VAC		
PROTECTION	OVER LOAD	105 ~ 135% rated output power		
		Protection type : Constant current limiting, recovers automatically after fault condition is removed		
	SHORT CIRCUIT	Protection type : Constant current limiting, recovers automatically after fault condition is removed		
	OVER VOLTAGE	13.8 ~ 16.2V	27.6 ~ 32.4V	55.2 ~ 64.8V
		Protection type :Shut down O/P voltage, re-power on to recover		
	OVER TEMPERATURE	Shut down O/P voltage, recovers automatically after temperature goes down		
ENVIRONMENT	WORKING TEMP.	-30 ~ +60℃ (Refer to output load derating curve)		
	WORKING HUMIDITY	20 ~ 90% RH non-condensing		
	STORAGE TEMP., HUMIDITY	-30 ~ +85℃, 10 ~ 95% RH		
	TEMP. COEFFICIENT	±0.1%/℃ (0 ~ 35℃)		
	VIBRATION	10 ~ 500Hz, 3G 10min./1cycle, 60min. each along X, Y, Z axes		
SAFETY & EMC (Note.6)	SAFETY STANDARDS	IEC/EN/UL 60950-1,CCC GB4943.1-2011, EAC TP TC 004 approved		
	WITHSTAND VOLTAGE	I/P-O/P:3KVAC I/P-FG:2KVAC O/P-FG:0.5KVAC		
	ISOLATION RESISTANCE	I/P-O/P, I/P-FG, O/P-FG:100M Ohms/500VDC / 25℃/ 70% RH		
	EMC EMISSION	Compliance to EN55032 (CISPR32) class A, GB9254 classA, GB17625.1; EN61000-3-2;EN61000-3-3, EAC TP TC 020		
	EMC IMMUNITY	Compliance to EN61000-4-2,3,4,5,6,8,11;light industry level,criteria A, EAC TP TC 020		
OTHERS	MTBF	233.422Khrs min. MIL-HDBK-217F (25℃)		
	DIMENSION	220.4*130*48mm (L*W*H)		
	PACKING	1.1Kg; 9pcs / 11Kg / 0.63CUFT		
NOTE	1. All parameters NOT specially mentioned are measured at 230VAC input, rated load and 25℃ of ambient temperature. 2. Ripple & noise are measured at 20MHz of bandwidth by using a 12" twisted pair-wire terminated with a 0.1uf & 47uf parallel capacitor. 3. Tolerance : includes set up tolerance, line regulation and load regulation. 4. Derating may be needed under low input voltages. Please check the static characteristics for more details. 5. Please refer to "Static Characteristics". 6. The power supply is considered a component which will be installed into a final equipment. All the EMC tests are been executed by mounting the unit on a 450mm*450mm metal plate with 1mm of thickness. The final equipment must be re-confirmed that it still meets EMC directives. For guidance on how to perform these EMC tests, please refer to "EMI testing of component power supplies." (as available on http://www.meanwell.com).			

■ Mechanical Specification

Case No.230 Unit:mm

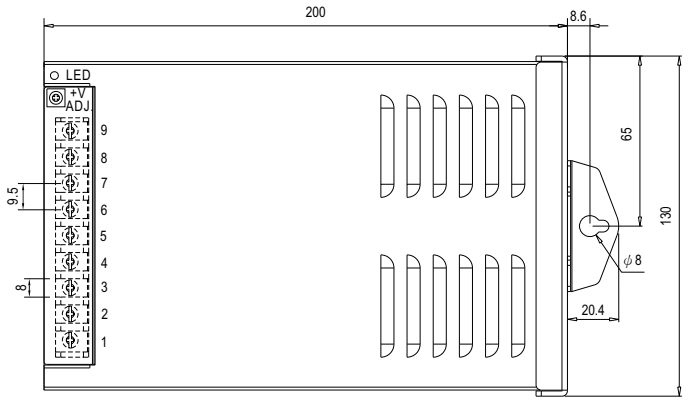

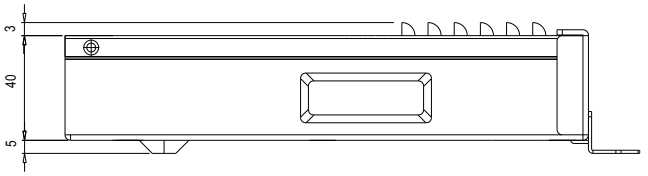

Terminal Pin No. assignment :

Pin No.	Assignment	Pin No.	Assignment	Max mounting torque
1	AC/L	4~6	DC OUTPUT +V	8Kgf-cm
2	AC/N	7~9	DC OUTPUT -V	
3	FG ⏚			

■ Block Diagram

fosc : 80KHz

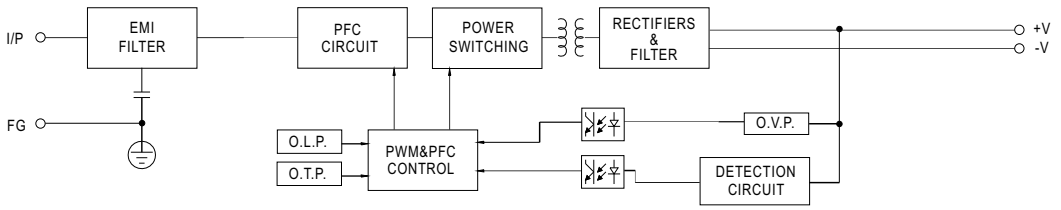

■ Derating Curve

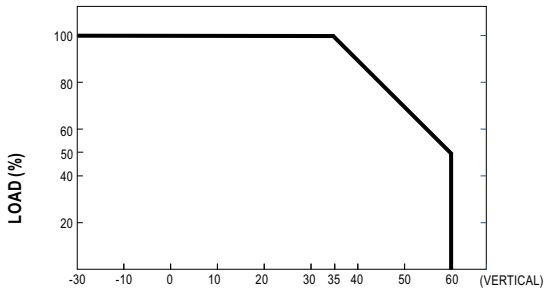

AMBIENT TEMPERATURE (℃)

■ Static Characteristics

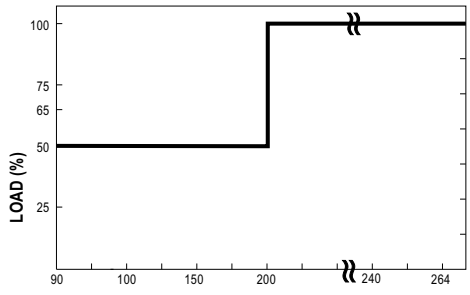

INPUT VOLTAGE (VAC) 60Hz

■ Installation

1.ERPF-400 should be installed in an upright position,leaning forward,backward or lay flat are not allowed

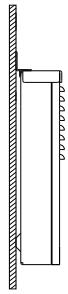

Correct installation method

2.For heat dissipation, distance of 10cm from 4 sides(up/down/right/left) and 5cm from the ventilation hole side should be kept, shown as below:

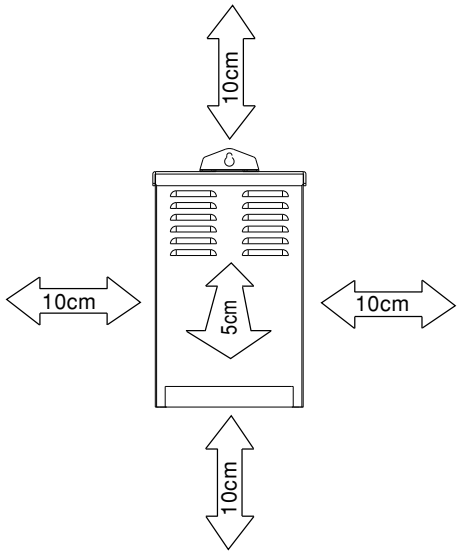

igubal® Rod Ends - Product range

In-line ball and socket - AGRM and AGLM

- For all mechanical combinations
- Very easy hand assembly
- Maintenance free operation
- Corrosion-and chemical-resistant
- Good vibration-dampening qualities
- Ball stud made of plastic or metal[19)]

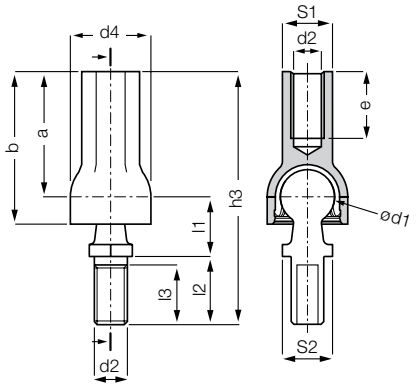

Order key

Type			Size
AG	...	M	- 08
Dimensional E series	Thread L = Left hand thread R = Right hand thread	Metric	Inner-Ø [mm]

Material:
Housing - **igumid G ➤ Page 1373**
Spherical cap - **iglide® L280 (W300)***

Dimensions [mm]

Part No.	Part No.	d1	d2	d4	l1	l2	l3	h3	S1	S2	a	b	e	Pivot angle	
Right thread	Left thread	+0.1		+0.5	+0.2	+0.3		+0.5			+0.3	+0.5			
		–0.1		–0.5	–0.2	–0.3	Min.	–0.5			–0.3	–0.5	Min.	Recommended	Maximum
AGRM-08	AGLM-08	13.0	M8	19.3	13.0	16.5	13.5	59.0	SW12	SW11	29.5	36.5	16.0	18°	25°

[19)] Metal stud option: MS = metal stud, only available with right-hand thread. Example: WGRM-05 LC MS

Technical data

Part No.		Max. axial tensile force		max. axial compressive force		Maximum assembling force	Weight
Right thread	Left thread	Short term	Long term	Short term	Long term		
		[lbs]	[lbs]	[lbs]	[lbs]	[lbs]	[g]
AGRM-08	AGLM-08	56	28	225	112	25	7.8

*W300 is the European material equivalent for iglide® L280.

STRYVO

NTNU Trondheim

7491 TRONDHEIM
Norge

Kontaktperson: Frode Berglid
Telefon:
Epost: frobe@stud.ntnu.no

Tilbud: 21001

Side: 1 av 2
Dato: 20.04.2020

Forespørselsdato: 16.04.2020
Forespørsel: Stewart platform pristilbud
Vår kontaktperson: Terje Blaalid
Deres kundenummer: 13608
Gyldig til: 27.04.2020

Betalingsbetingelse: Netto pr 14 dager
Leveringsbetingelse: EXW STRYVO AS

På grunn av den svært urolige valutasituasjonen må vi ta valutaforbehold for dette tilbudet.
Om NOK (Norsk krone) endrer seg vesentlig forbeholder vi oss retten til å justere prisene i henhold til svingninger i valuta.

#	Antall	Varebeskrivelse	Levering	Stk. pris	Sum
1	1,00	Bottom plate ALUMINIUMSPLATE 6mm 6082 T6 kvalitet.	ca 6 uker fra PO/Avtales	1.780,00	1.780,00
2	1,00	Top plate ALUMINIUMSPLATE 6mm 6082 T6 kvalitet.	ca 6 uker fra PO/Avtales	1.690,00	1.690,00
3	6,00	Bushing lower Rund 304 Ø30	ca 6 uker fra PO/Avtales	320,00	1.920,00
4	6,00	Bushing upper Rund 304 Ø30	ca 6 uker fra PO/Avtales	320,00	1.920,00
5	1,00	Circuit box back ALUMINIUMSPLATE 4mm 5052/5754 kvalitet.	ca 6 uker fra PO/Avtales	1.520,00	1.520,00
6	12,00	Pin M10, Ø6,3 Rund 304 Ø12	ca 6 uker fra PO/Avtales	210,00	2.520,00
7	3,00	Platform feet Rund 304 Ø25	ca 6 uker fra PO/Avtales	230,00	690,00
		Sum eks. mva.			12.040,00

Stryvo AS, Vipevegen 8, 6783 Stryn
Tlf: +47 57 87 28 00, Web: www.stryvo.no
E-mail: post@stryvo.no

Bankgiro: 3705.14.24108
Foretaksregisteret nr:
NO992808314MVA

IBAN: NO9737051424108
SWIFT: SOFJNO22

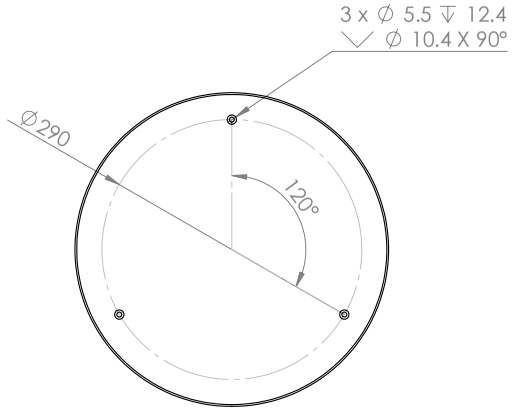

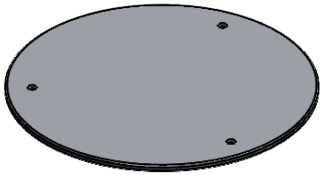

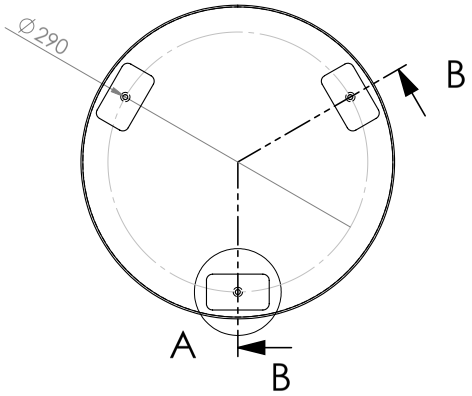

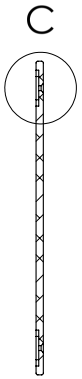

SECTION B-B

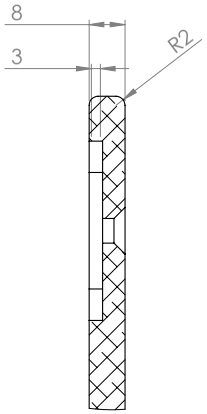

DETAIL C
SCALE 1 : 1

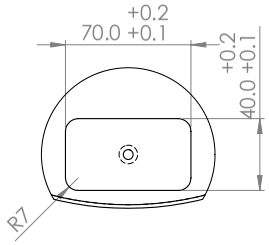

DETAIL A
SCALE 2 : 5

Material: **Aluminum**		This drawing and any information or descriptive material set out on it are the confidential and copyright property of ***Company Name***. © and MUST NOT BE DISCLOSED, COPIED, LOANED in whole or part or used for any purpose without the written permission of ***Company Name***.	Description: **Top plate**
Finish:			Drawn by: **FB** / Drawn Date:
Unless Otherwise Stated: Linear Tol.: **±0.2**, Angular Tol.: **0°15'** Surface Finish: **0.8µm** All Dimensions: **mm**		Document Type:	Checked/Approved by: / Checked/Approved Date:
Drawing Scale: **1:5**		**Project nr:** 90034201	
Approx Weight: **2.00** Kg	Drawing Produced In Accordance With: **BS8888**	Legal Owner: Frode berglid +47 90622810 frobe@stud.ntnu.no	Part Number:
Projection Method: **First Angle**	Sheet Size: **A3**		Drawing Number: / Sheet: **1 of 1** / Revision:

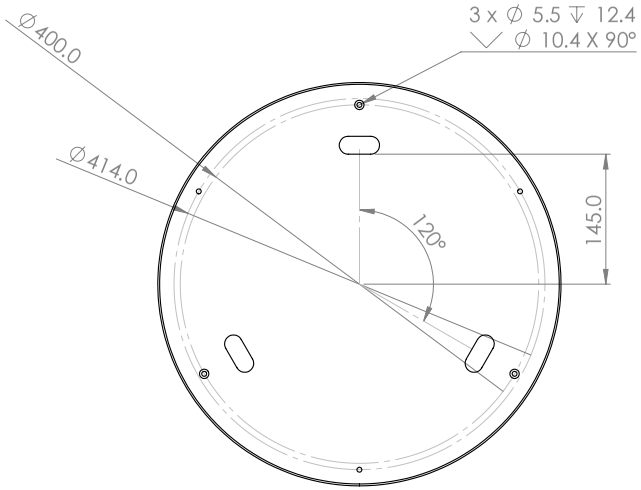

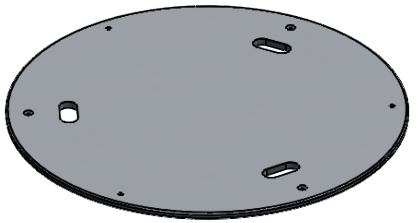

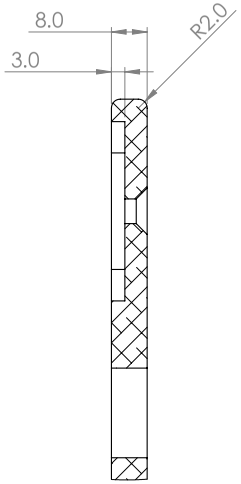

DETAIL D

SCALE 1 : 1

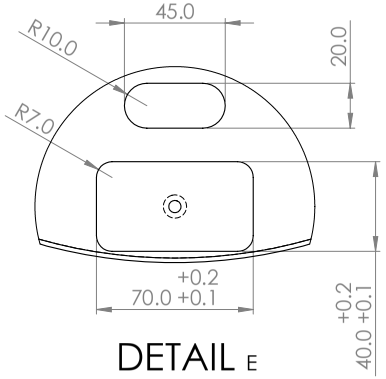

DETAIL E

SCALE 1 : 2

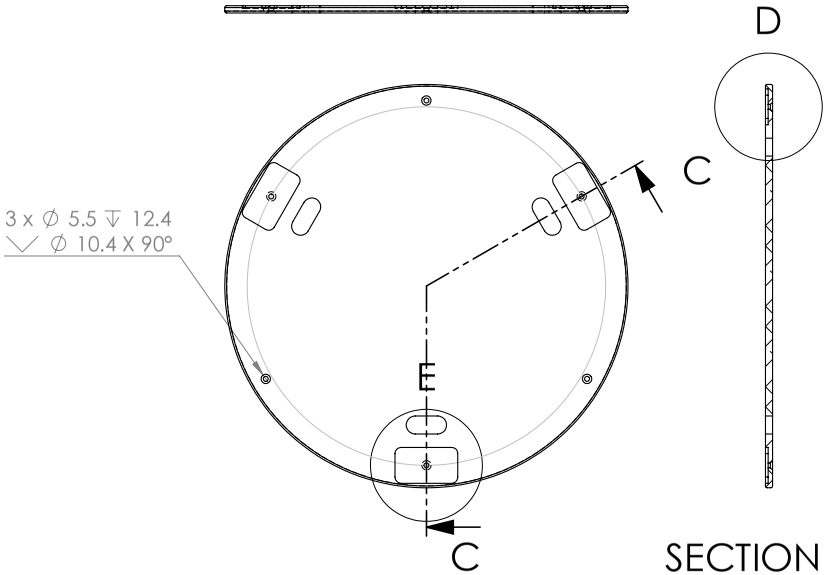

SECTION C-C

OBS: Holes countersunk on opposite side

Material: **Aluminium**		This drawing and any information or descriptive material set out on it are the confidential and copyright property of ***Company Name***. © and MUST NOT BE DISCLOSED, COPIED, LOANED in whole or part or used for any purpose without the written permission of ***Company Name***.	Description: **Bottom plate rev1** **1 Part**
Finish:			Drawn by: **FB** / Drawn Date:
Unless Otherwise Stated: Linear Tol.: **±0.2**, Angular Tol.: **0°15'** Surface Finish: **0.8µm** All Dimensions: **mm**		Document Type:	Checked/Approved by: / Checked/Approved Date:
Drawing Scale: **1:5**		**Project nr:** 90034201	
Approx Weight: **3.31** Kg	Drawing Produced In Accordance With: **BS8888**	Legal Owner: Frode berglid +47 90622810 frobe@stud.ntnu.no	Part Number:
Projection Method: **First Angle**	Sheet Size: **A3**		Drawing Number: / Sheet: **1 of 1** / Revision:

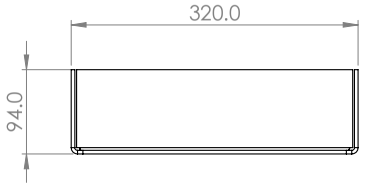

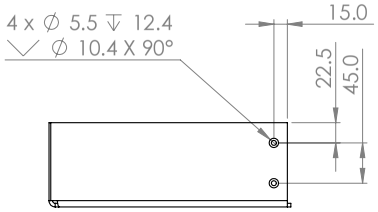

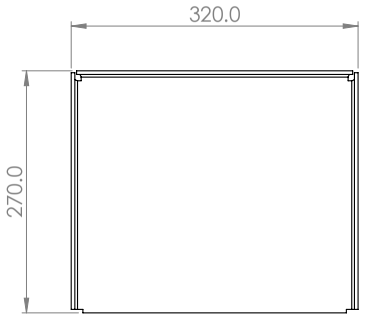

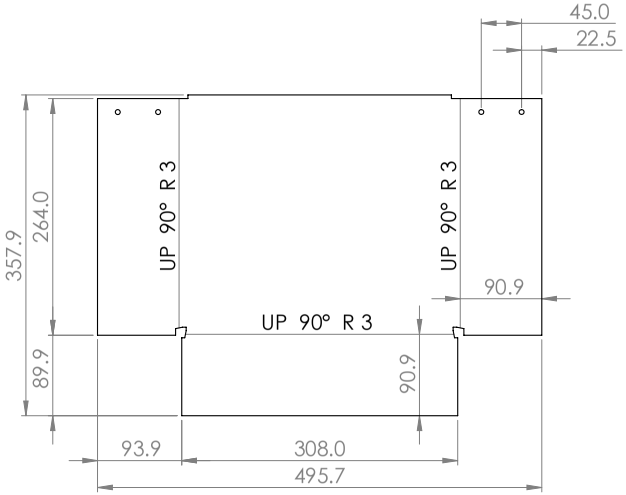

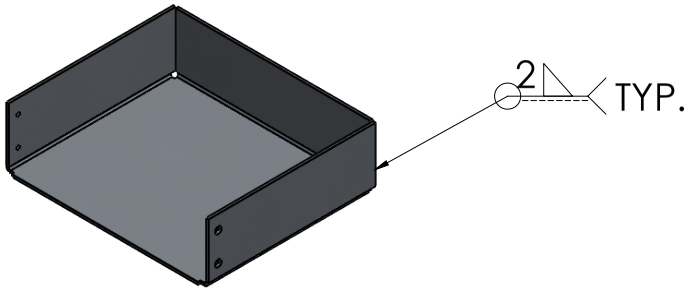

Material: **Aluminium**	This drawing and any information or descriptive material set out on it are the confidential and copyright property of ***Company Name***. © and MUST NOT BE DISCLOSED, COPIED, LOANED in whole or part or used for any purpose without the written permission of ***Company Name***.	Description: **Circut box back**	
Finish:			
Unless Otherwise Stated: Linear Tol.: **±0.2**, Angular Tol.: **0°15'** Surface Finish: **0.8µm** All Dimensions: **mm**	Document Type:	Drawn by: **FB**	Drawn Date:
Drawing Scale: **1:5**	**Project nr:** 90034201	Checked/Approved by:	Checked/Approved Date:
Approx Weight: **1.72** Kg / Drawing Produced In Accordance With: **BS8888**	Legal Owner: Frode berglid +47 90622810 frobe@stud.ntnu.no	Part Number:	
Projection Method: **First Angle** / Sheet Size: **A3**		Drawing Number:	Sheet: **1 of 1** / Revision:

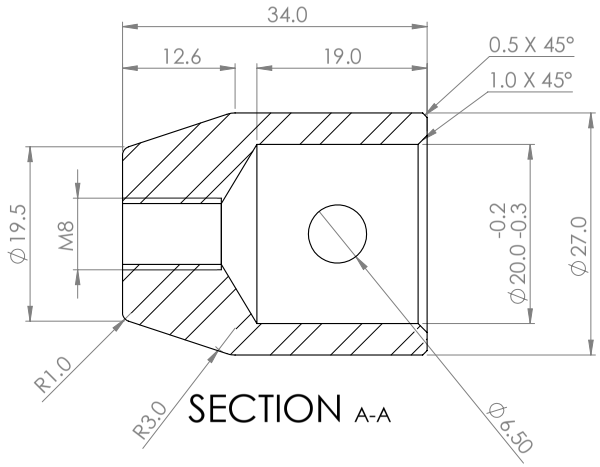

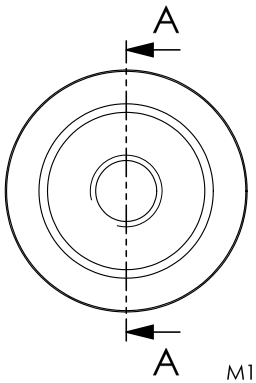

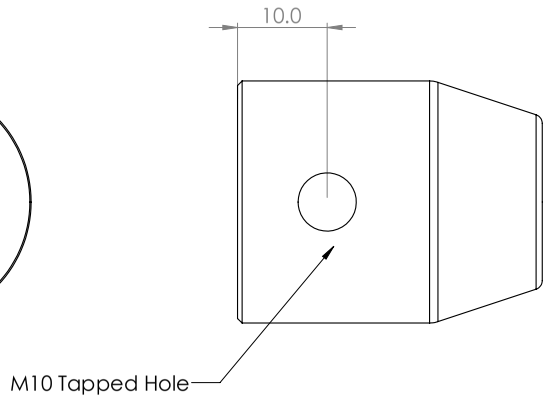

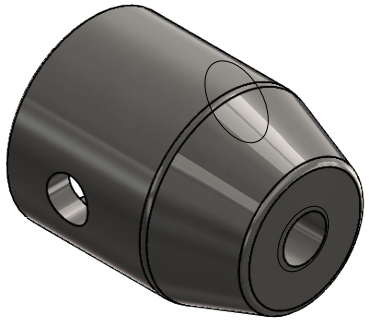

OBS: Ø6.5 hole on one side, and tapped M10 on the other side

Material: **AISI 304**		This drawing and any information or descriptive material set out on it are the confidential and copyright property of ***Company Name***. © and MUST NOT BE DISCLOSED, COPIED, LOANED in whole or part or used for any purpose without the written permission of ***Company Name***.	Description: **Bushing lower 6 Pieces**
Finish:			Drawn by: **FB** / Drawn Date:
Unless Otherwise Stated: Linear Tol.: **±0.2**, Angular Tol.: **0°15'** Surface Finish: **0.8µm** All Dimensions: **mm**		Document Type:	Checked/Approved by: / Checked/Approved Date:
Drawing Scale: **2:1**		**Project nr:** 90034201	
Approx Weight: **82.20** g	Drawing Produced In Accordance With: **BS8888**	Legal Owner: Frode berglid +47 90622810 frobe@stud.ntnu.no	Part Number:
Projection Method: **First Angle**	Sheet Size: **A3**		Drawing Number: / Sheet: **1 of 1** / Revision:

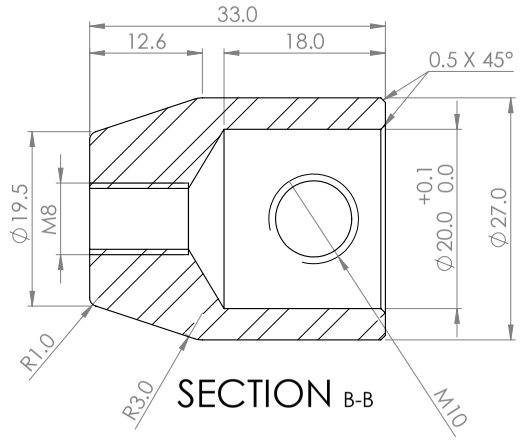

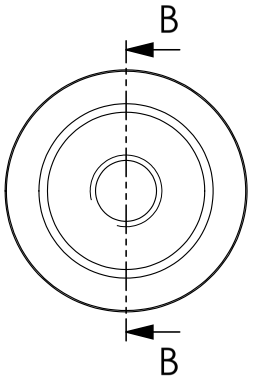

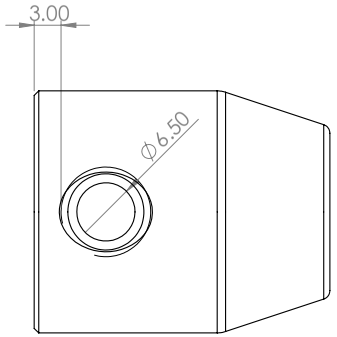

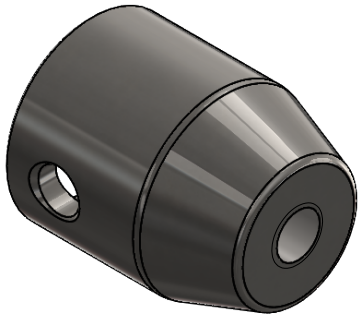

OBS: Ø6.5 hole on one side, and tapped M10 on the other side

Material: **AISI 304**	This drawing and any information or descriptive material set out on it are the confidential and copyright property of ***Company Name***. © and MUST NOT BE DISCLOSED, COPIED, LOANED in whole or part or used for any purpose without the written permission of ***Company Name***.	Description: **Bushing upper 6 Pieces**	
Finish:		Drawn by: **FB**	Drawn Date:
Unless Otherwise Stated: Linear Tol.: **±0.2**, Angular Tol.: **0°15'** Surface Finish: **0.8µm** All Dimensions: **mm**	Document Type:	Checked/Approved by:	Checked/Approved Date:
Drawing Scale: **2:1**	**Project nr:** 90034201		
Approx Weight: **80.25** g / Drawing Produced In Accordance With: **BS8888**	Legal Owner: Frode berglid +47 90622810 frobe@stud.ntnu.no	Part Number:	
Projection Method: **First Angle** / Sheet Size: **A3**		Drawing Number:	Sheet: **1 of 1** / Revision:

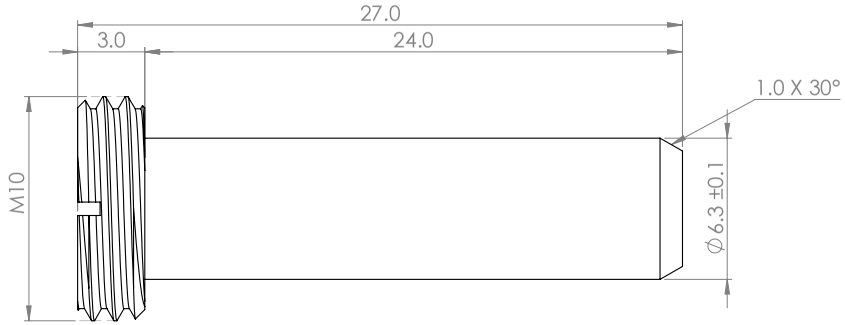

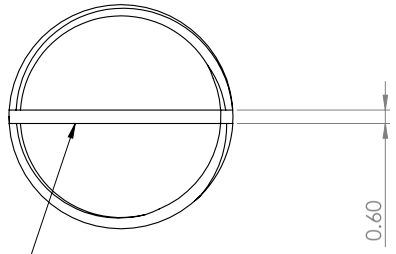

Slot for screwdriver.
Accuracy not important, check funcionality with a screwdriver

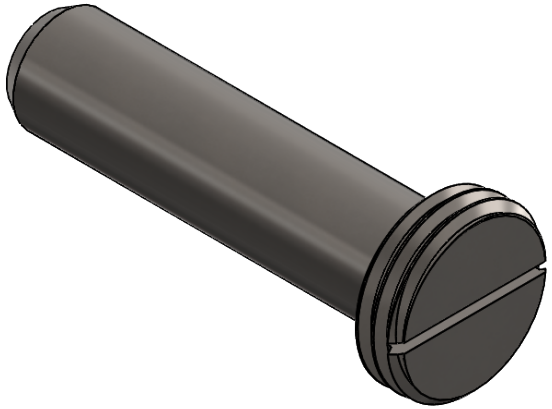

Make from M10 threaded rod. Or 304/316 bar

Material: **Stainless Steel (ferritic)**		Description: **Pin M10, Ø6.3 12 Pieces**	
Finish:		Drawn by: **FB**	Drawn Date:
Unless Otherwise Stated: Linear Tol.: **±0.2**, Angular Tol.: **0°15'** Surface Finish: **0.8µm** All Dimensions: **mm**	Document Type:	Checked/Approved by:	Checked/Approved Date:
Drawing Scale: **5:1**	**Project nr:** 90034201		
Approx Weight: **7.36** g / Drawing Produced In Accordance With: **BS8888**	Legal Owner: Frode berglid +47 90622810 frobe@stud.ntnu.no	Part Number:	
Projection Method: **First Angle** / Sheet Size: **A3**		Drawing Number:	Sheet: **1 of 1** / Revision:

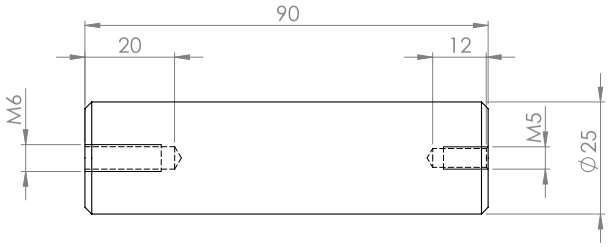

Material: **AISI 304**	This drawing and any information or descriptive material set out on it are the confidential and copyright property of ***Company Name***. © and MUST NOT BE DISCLOSED, COPIED, LOANED in whole or part or used for any purpose without the written permission of ***Company Name***.	Description: **Platform feet 3 PCS**	
Finish:		Drawn by: **FB**	Drawn Date:
Unless Otherwise Stated: Linear Tol.: **±0.2**, Angular Tol.: **0°15'** Surface Finish: **0.8µm** All Dimensions: **mm**	Document Type:	Checked/Approved by:	Checked/Approved Date:
Drawing Scale: **1:1**	**Project nr:** 90034201		
Approx Weight: **0.34** Kg / Drawing Produced In Accordance With: **BS8888**	Legal Owner: Frode berglid +47 90622810 frobe@stud.ntnu.no	Part Number:	
Projection Method: **First Angle** / Sheet Size: **A3**		Drawing Number:	Sheet: **1 of 1** / Revision:

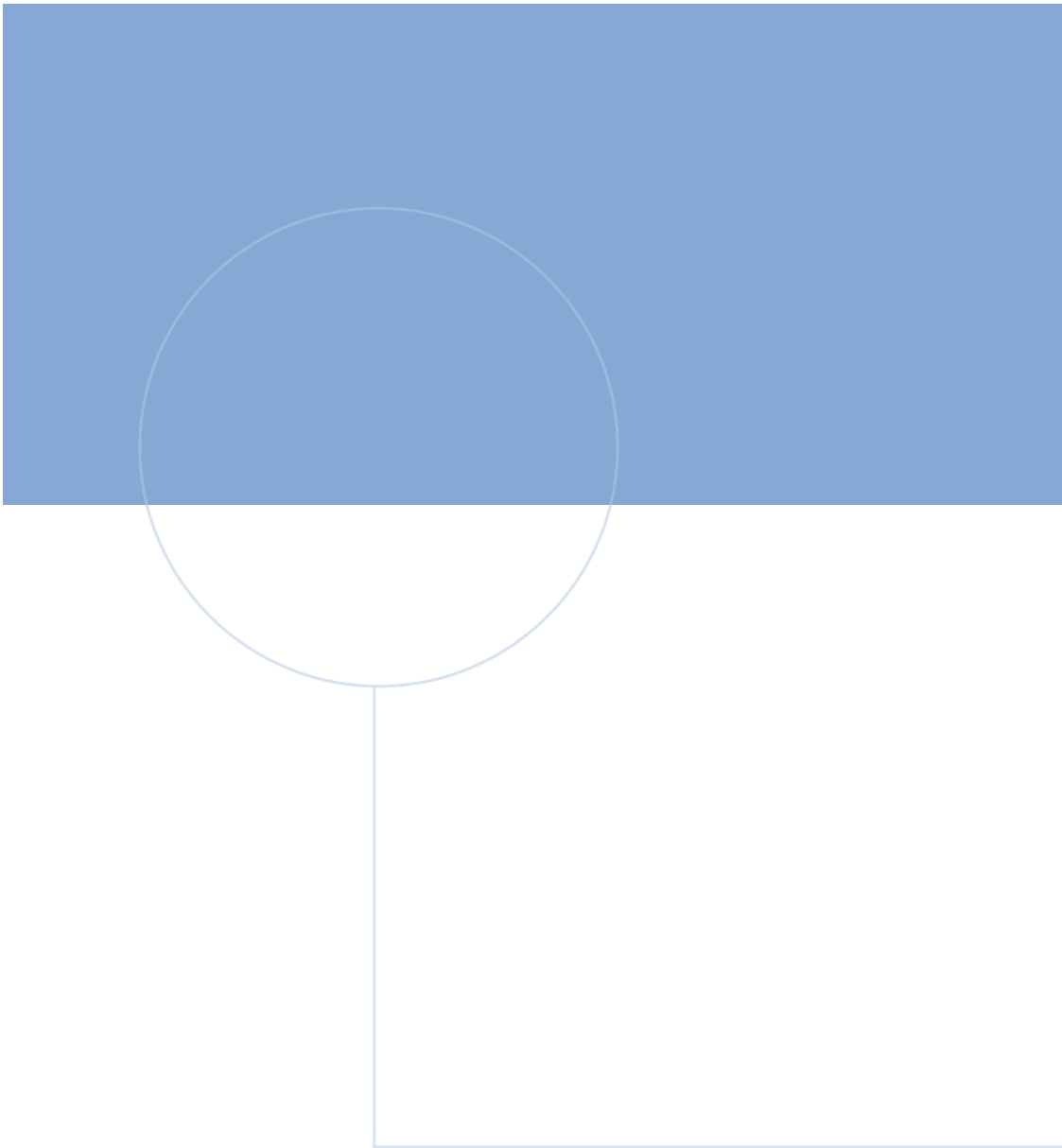

NTNU

Norwegian University of
Science and Technology